

# AS&E

NASA CR-143724

**American Science  
and Engineering, Inc.**  
955 Massachusetts Avenue  
Cambridge, Massachusetts 02139  
617-868-1600

30 SEPTEMBER 1974

ASE-3604

(NASA-CR-143724) , ANS HARD X-RAY EXPERIMENT DEVELOPMENT PROGRAM Final Report, Nov., 1970 - Sep., 1974 (American Science and Engineering, Inc.) : 146 p HC \$5.75 CSCL 03A N75-22247  
Unclas 18626  
G3/89

FINAL REPORT FOR:

## ANS HARD X-RAY EXPERIMENT DEVELOPMENT PROGRAM

30 NOVEMBER 1970 - 30 SEPTEMBER 1974

PREPARED FOR:

NATIONAL AERONAUTICS AND  
SPACE ADMINISTRATION  
GODDARD SPACE FLIGHT CENTER  
GREENBELT, MARYLAND 20771



7

TECHNICAL REPORT STANDARD TITLE PAGE

1. Report No. ASE-3604	2. Government Accession No.	3. Recipient's Catalog No.	
4. Title and Subtitle ANS HARD X-RAY EXPERIMENT DEVELOPMENT PROGRAM		5. Report Date 30 September 1974	
		6. Performing Organization Code	
7. Author(s) *See below		8. Performing Organization Report No. ASE-3604	
9. Performing Organization Name and Address American Science & Engineering, Inc. 955 Massachusetts Avenue Cambridge, Mass. 02139.		10. Work Unit No.	
		11. Contract or Grant No. NAS 5-11350	
		13. Type of Report and Period Covered Final Report for Period November 1970 through September 1974.	
12. Sponsoring Agency Name and Address National Aeronautics & Space Administration Goddard Space Flight Center Greenbelt, Maryland 20771		14. Sponsoring Agency Code	
15. Supplementary Notes			
16. Abstract The Hard X-ray (HXX) Experiment Development Program was initiated at AS&E in November 1970, as part of a cooperative NASA/Dutch scientific program. The HXX experiment is one of three experiments included in the Dutch Astronomical Netherlands Satellite, which was launched into orbit on 30 August 1974. The overall objective of the HXX experiment is the detailed study of the emission from known X-ray sources over the energy range 1.5-30keV. The instrument is capable of the following measurements: a) Spectral content over the full energy range with an energy resolution of ~20% and time resolution down to 4 seconds, b) source time variability down to 4 milliseconds, c) silicon emission lines at 1.86 and 2.00keV, d) source location to a limit of one arc minute in ecliptic latitude, and e) spatial structure with angular resolution of ten (10) arc minutes.  The report is organized into three (3) primary sections: (1) Scientific Aspects of the Experiment; (2) Engineering Design and Implementation of the Experiment, and (3) Program History...			
17. Key Words (Selected by Author(s)) Hard X-rays, Astronomical Netherlands Satellite, Bragg Crystal, Proportional Counter, Stellar X-ray Emission Pulsar		18. Distribution Statement	
19. Security Classif. (of this report) Unclassified	20. Security Classif. (of this page) Unclassified	21. No. of Pages	22. Price*

\*For sale by the Clearinghouse for Federal Scientific and Technical Information, Springfield, Virginia 22151.

\*D. Parsignault, H. Gursky (SAO), R. Frank, K. Kubierschky, G. Austin, R. Paganetti, V. Bawdekar.

ANS HARD X-RAY EXPERIMENT DEVELOPMENT PROGRAM

Prepared by:

American Science & Engineering, Inc.  
955 Massachusetts Avenue  
Cambridge, Massachusetts 02139

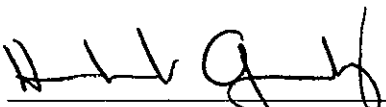
30 September 1974

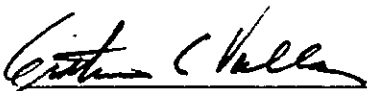
Final Report for Period 30 November 1970 - 30 September 1974

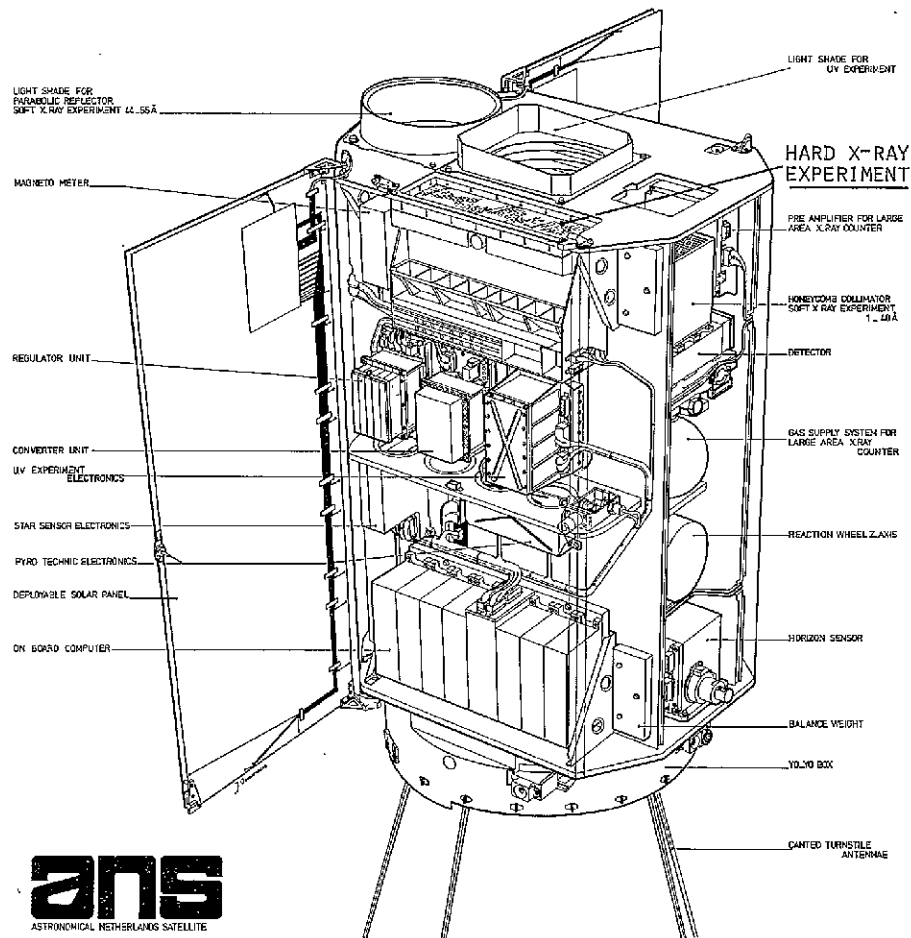
Prepared for:

National Aeronautics and Space Administration  
Goddard Space Flight Center  
Greenbelt, Maryland 20771

Approved:   
Ralph Paganetti  
Program Manager

  
Herbert Gursky, Ph. D.  
Principal Investigator

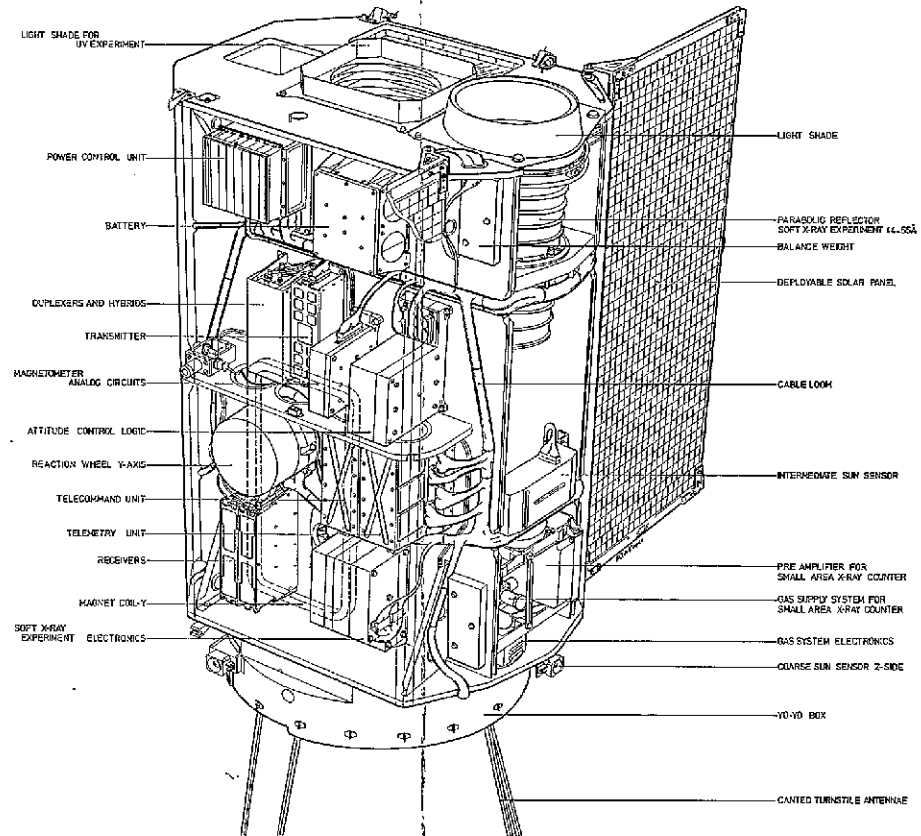
  
Arthur C. Vallas  
Vice President  
Space Division



**ans**  
ASTRONOMICAL NETHERLANDS SATELLITE

FOLDOUT FRAME

1



FOLDOUT FRAME

2

HARD X-RAY EXPERIMENT IN THE ASTRONOMICAL NETHERLANDS SATELLITE

## CONTENTS

<u>Section</u>		<u>Page</u>
FOREWORD		
1.0	SCIENTIFIC ASPECTS OF THE HARD X-RAY EXPERIMENT	1-1
1.1	Research Objectives	1-1
	1.1.1 Source Accessibility	1-1
	1.1.2 Observational Capability	1-5
	1.1.3 Summary	1-9
1.2	Scientific Description of the Experiment	1-10
	1.2.1 The Large Area Detector System	1-10
	1.2.2 The Bragg Spectrometer System	1-12
	1.2.3 The Pulse Shape Discrimination	1-17
	1.2.4 The Collimators	1-17
	1.2.5 The Calibration Sources	1-20
	1.2.6 Data Handling	1-20
	1.2.7 Operating Modes	1-24
2.0	ENGINEERING IMPLEMENTATION OF THE HARD X-RAY EXPERIMENT	2-1
2.1	Electrical Engineering Description	2-3
	2.1.1 HXX Experiment Block Diagram	2-3
	2.1.2 Electronic Packaging	2-28
	2.1.3 Ground Support Equipment	2-29
2.2	Mechanical Engineering Description	2-44
	2.2.1 Mechanical Interface	2-51
	2.2.2 Structural Considerations	2-52
	2.2.3 Thermal Design Considerations	2-56
	2.2.4 Proportional Counters	2-59
	2.2.5 Collimators	2-62
	2.2.6 Bragg Crystal Plate	2-69
2.3	Reliability	2-73
	2.3.1 Parts	2-73
	2.3.2 Materials	2-77
	2.3.3 Failure History	2-78
3.0	PROGRAM HISTORY	3-1
3.1	Structural, Thermal and Electrical Models	3-1
3.2	Ground Support Equipment	3-4
3.3	HXX Protoflight and Flight Units Design Phase	3-4
3.4	HXX Protoflight Unit Fabrication and Test Phase	3-7
3.5	HXX Flight Unit Fabrication and Test Phase	3-10
3.6	HXX Protoflight Unit Refurbishment	3-12
3.7	HXX Flight Unit Refurbishment as a Spare Backup	3-14

CONTENTS (Cont'd)

<u>Section</u>		<u>Page</u>
3.8	Detailed History of HXX Proportional Counters	3-15
3.8.1	Background	3-15
3.8.2	Bragg Proportional Counters #1 and #2	3-17
3.8.3	LAD Proportional Counter #1	3-17
3.8.4	LAD Proportional Counter #2	3-20
3.8.5	Proportional Counter #3	3-21
3.8.6	Additional Procurement of LAD'S #4, 5, 6, and 7	3-22

## ILLUSTRATIONS

<u>Figure</u>		<u>Page</u>
1-1	ANS-SXX X-ray and UV-Sky	1-3
1-2	ANS Hard X-ray Experiment	1-11
1-3	Proportional Counter Efficiencies	1-13
1-4	Crystal and Collimator Alignment	1-15
2-1	Hard X-ray Experiment	2-2
2-2	Block Diagram ANS-HXX Experiment	2-4
2-3	Preamplifier - Amplifier Module	2-5
2-4	Analog Summer Assembly No. 135-2411	2-7
2-5	Detector Identification Threshold Detectors	2-9
2-6	LAD PSD Summer Assembly No. 135-2411	2-12
2-7	Logarithmic Analog to Digital Converter	2-15
2-8	Rack Mounted Unit ANS HXX Experiment (ECE)	2-31
2-9	Input/Output Unit ANS HXX Experiment (ECE)	2-31
2-10	ANS HXX Experiment Checkout Equipment	2-32
2-11	ANS Hard X-ray Experiment	2-45
2-12	Collimator Assemblies	2-46
2-13	X-ray Detectors	2-47
2-14	ANS HXX Main Electronics Assembly	2-48
2-15	HXX Thermal Configuration	2-57
2-16	Collimator Construction Detail	2-64
2-17	Rotomike Assembled on X-Y Table	2-68
2-18	Two-Crystal Spectrometer with Point-Focus X-ray Tube and Alignment Autocollimator	2-71
3-1	ANS-HXX Program History	3-2, 3-2a
3-2	HXX Structural Model	3-3
3-3	HXX Thermal Model	3-3
3-4	HXX Electrical Model	3-5
3-5	HXX Ground Support Equipment	3-6
3-6	Protoflight Test Sequence	3-11
3-7	HXX Flight Unit	3-13
3-8	Proportional Counter Histories	3-16

TABLES

<u>Table</u>		<u>Page</u>
1-1	Characteristics of the Silicon Lines to be Observed	1-4
1-2	Pointing Directions at 19.5° C	1-16
1-3	X-ray Acceptance and Background Rejection of LAD	1-18
1-4	X-ray Acceptance and Background Rejection of BRAGG	1-19
1-5	Energy Channel Boundaries of the PHA	1-21
1-6	HXX Accumulator Contents	1-22
1-7	HXX Data Handling Modes	1-25
2-1	HXX Experiment Parameters	2-1
2-2	Address Word Accumulator Selection	2-21
2-3	Data Blocks Transferred on Key Address Words	2-22
2-4	Command Word Functions	2-24
2-5	Data Read Out Groups	2-34
2-6	HEX - Set Printer Format	2-39
2-7	Weight Breakdown	2-50
2-8	Qualification Vibration Levels	2-53
2-9	Proportional Counter Parameters	2-60
2-10	Protoflight Assemblies and Subassemblies	2-74
2-11	Burn-in Data Analysis	2-75

## FOREWORD

This document constitutes the Final Report for the Astronomical Netherlands Satellite (ANS) Hard X-Ray (HXX) Experiment Development Program. This program was initiated at AS&E in November 1970, as part of a cooperative NASA/Dutch scientific program. The fine program coordination, interfacing and cooperation among AS&E, NASA and the Dutch, resulted in a fully operational scientific payload being launched into orbit in August 1974, as originally scheduled four years earlier. The Hard X-Ray Experiment was first turned on in orbit on September 8, 1974, and has continued to perform to specification as of publication of this report.

This report is organized into three primary sections: 1) Scientific Aspects of the Experiment; 2) Engineering Design and Implementation of the Experiment; and 3) Program History.

## 1.0 SCIENTIFIC ASPECTS OF THE HARD X-RAY EXPERIMENT

### 1.1 Research Objectives

The overall objective of the HXX experiment is the detailed study of the emission from known X-ray sources over the energy range 1.5 - 30 keV. The instrument is capable of recording several distinct attributes of this emission; in particular, we can study:

1. The spectral content over the full energy range with an energy resolution of  $\sim 20\%$  and time resolution down to 4 seconds.
2. Time variability down to 4 msec.
3. The silicon emission lines at 1.86 and 2.00 keV. (Si XIII and Si XIV).
4. Source location to a limit of about 1' arc in ecliptic latitude.
5. Spatial structure with an angular size of 10' arc.

In addition to these well-defined objectives, we will conduct such observations as measurements of X-ray sources simultaneous with ground based studies, a search for transient sources, and other studies of high interest as they occur.

It should be possible to observe any known UHURU sources whose intensity is greater than about 5 UHURU counts/sec. Naturally, the ability to achieve the above objectives is very much a function of source intensity.

#### 1.1.1 Source Accessibility

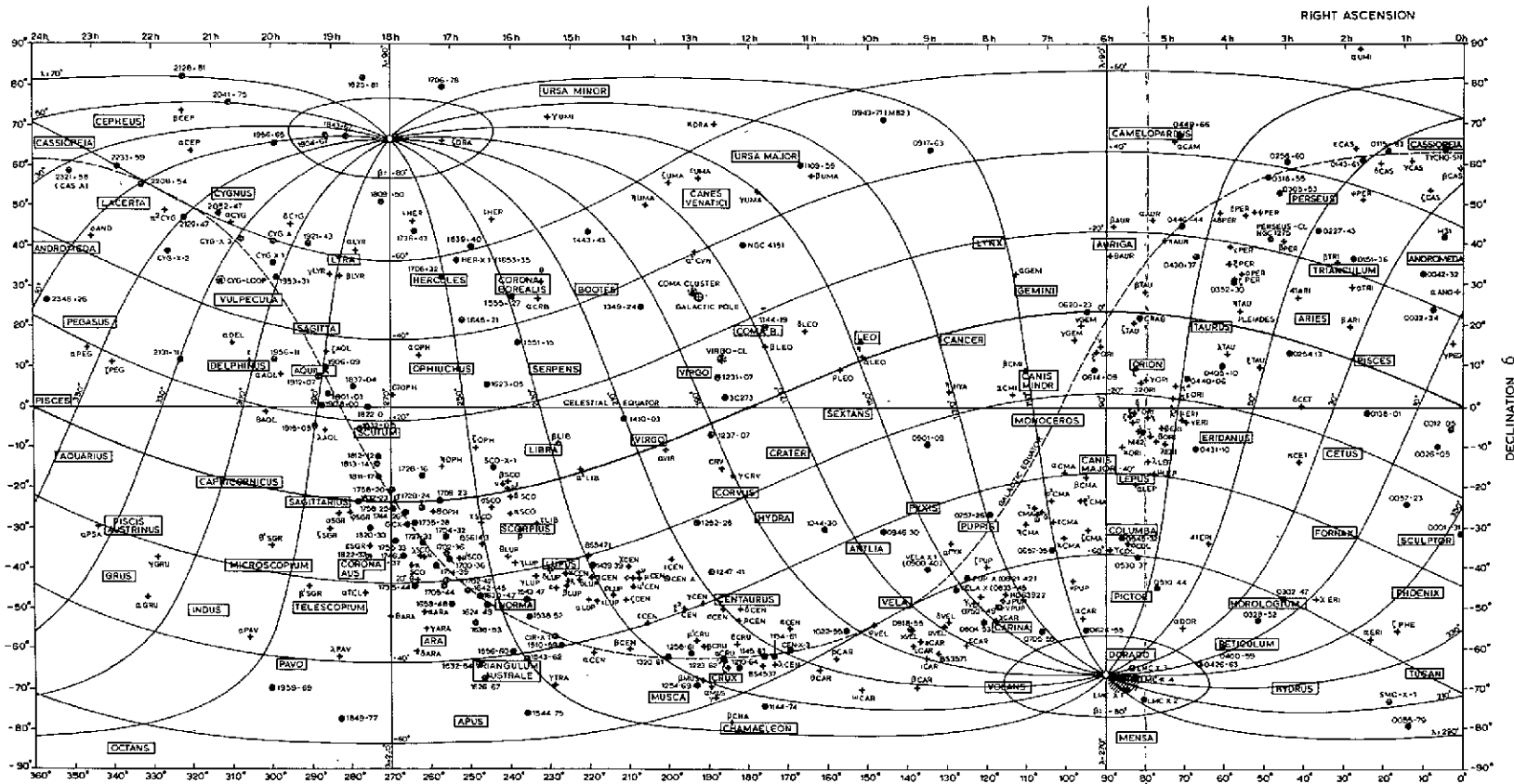
Because of the operational restrictions in orbit, sources can be viewed for only a restricted time twice a year. The reason for this is that the detector axes are constrained to view along a great circle approximately  $90^\circ$  from the Sun. Given the internal offset of  $\sim 1^\circ$  from the Sun normal and the  $3^\circ$  field of view of the

detectors, the actual viewing window is a period of 5 days centered on the date that the source is  $90^\circ$  from the Sun, if the source is on the ecliptic. The duration of the window increases as  $\sec \beta$  ( $\beta$  = ecliptic latitude). Thus, a source within about  $2 - 3^\circ$  of the ecliptic pole can be viewed continuously during the year. Figure 1-1 is a map of the sky in right ascension and declination on which are superimposed ecliptic coordinates. The ecliptic equator is the heavy line which crosses the celestial equator at  $180^\circ$  RA (12 hr.) and  $0^\circ$  RA. The lines of equal ecliptic longitude, normal to the ecliptic equator, are the scan circles defining the region accessible to the detectors on a given day. Plotted on this map are all the 3U sources, plus certain prominent stars which will be observed by the Groningen ultraviolet experiment (UVX). One very important feature of this figure is the great concentration of sources which occur in the constellations Sagittarius and Scorpius. All the sources in this crowded region can be observed only during a 40 day interval. Outside this region the sources are more or less uniformly distributed in longitude. Another interesting feature of this figure is the appearance of the Magellanic Cloud sources very close to the ecliptic pole, where they can be observed virtually without limit.

The information in Figure 1-1 is presented in Table 1-1 which lists the date (in day of the year 1974) for which all the UHURU sources are  $90^\circ$  from the Sun and are thus in the center of the observing window. The second portion of the table lists for each 3U source the day on which it is at center of the window and the duration of the window.

ANS - SXX

X-RAY and UV-SKY



ORIGINAL PAGE IS  
OF POOR QUALITY

FOLDOUT FRAME

$\lambda^{\circ}$	Observation date	
10	190	2 July
30	210	23 Jul
50	230	13 Aug
70	250	31 Aug
90	270	21 March / 20 Sept
110	290	10 April / 10 Oct
130	310	1 May
150	330	21 May
170	350	11 June

● X-RAY SOURCES FROM 3U CATALOGUE  
+ UV - STARS

FOLDOUT FRAME

Figure 1-1. ANS-SXX X-ray and UV-Sky

Table 1-1. Characteristics of the Silicon Lines to be Observed

Ions	Transition	$\lambda$ (Å)	Sin $\theta_B$	$\theta_{\text{Bragg}}$
Si XIV	$1s^2 1S_{\frac{1}{2}} - 2p^2 P_{\frac{1}{2}, \frac{3}{2}}$	6.184	.70739	$45^\circ 01'$
Si XIII	$1s^2 1S_0 - 1s2p^1 P_1$	6.649	.76058	$49^\circ 31'$
Si XIII	$1s^2 1S_0 - 1s2p^3 P_{2,1}$	6.684	.76458	$49^\circ 52'$
Si XIII	$1s^2 1S_0 - 1s2s^3 S_1$	6.739	.77088	$50^\circ 26'$

### 1.1.2 Observational Capability

We can observe any X-ray source during a five day or longer interval. Unfortunately, these 5 days are broken up by system constraints including earth occultation, radiation zones and division of observing time. Between the first two, only between 20 - 30 minutes is available for observing a given source during each orbit. Regarding the latter, the present intent is to alternate orbits between the three on-board experiments. Thus, we will observe only during each third orbit. It is likely, however, that certain observations can be conducted during the orbits allocated to SXX because of common targets. All together, during a five day observing period, between 530 minutes at a minimum and 1600 minutes at a maximum is available for observing a single source. Naturally, if it is desired to view additional sources during this five day interval, the time will be reduced accordingly. In the following sections, we estimate the sensitivity which can be achieved during typical observations.

#### 1.1.2.1 Sensitivity for Source Detection

Each LAD counter has an effective area of about  $40 \text{ cm}^2$  for X-ray detection. The total area for background is about 100 cts/sec. Based on observed UHURU rates, we estimate that the background in orbit (after pulse shape discrimination) will be between 1 and 3 counts/sec in the energy range 2-7 keV. We further estimate that a source seen by UHURU at 5 cts/sec is seen by a single LAD counter at  $\sim 0.25$  cts/sec. Taking 3 cts/sec as the background, the observing time required to achieve a  $4\sigma$  result is,

$$\begin{aligned} t &= 16 (s + 2b)/s^2 \\ &= 16 (.25 \text{ cts/sec} + 2 \times 3 \text{ cts/sec})/ (.25 \text{ cts/sec})^2 \\ &\approx 1600 \text{ sec.} \end{aligned}$$

To make a position determination might require  $\sim 10$  such measurements across the source, or 16,000 sec which is about 270 minutes. This is about  $1/4$  of the observing window and is not unreasonable except during the time when very crowded regions are being observed.

It is difficult to achieve significant spectral results for such weak sources. A  $4\sigma$  result for detection essentially yields only the total flux within the entire observing band. At a minimum,  $10 - 20\sigma$  is required which requires in turn  $\sim 170 - 670$  minutes of observing time plus a comparable amount of time observing only background. Thus, only marginal spectral data can be achieved with such faint sources.

#### 1.1.2.2 Time Variability

Variations in source intensity over a range of sampling time intervals can be measured; namely, 4 ms., 1 sec., 4 sec., 16 sec., and 256 sec. The principal limitation is the source intensity. To see 30% fluctuations from sample to sample, the source intensity has to be given as follows:

<u>Sampling Interval</u>	<u>ANS Count Rate</u>	<u>UHURU Count Rate</u>
1 sec.	10 cts/sec.	200 cts/sec.
4	4	80
16	1.3	26
256	0.3	6

It is probably not reasonable to detect small intensity variations for the weakest sources because of uncertainties in the background; otherwise, the experiment has good capability.

The pulsar mode is a special case. In this case, only 6 counts can be recorded within each 1 second interval. Thus, sources

with counting rates  $\sim 5$  cts/sec (100 UHURU cts/sec) will saturate the registers. For such sources, 1000 seconds of observing will yield 6000 counts with an average separation of 200 msec measured with an accuracy of 4 msec. If these data are binned in 4 msec intervals, the first bin (corresponding to two counts arriving within 4 msec) will contain  $\sim 120$  counts if the counts arrive at random. An excess of  $\sim 40$  counts in this bin would be statistically significant and would indicate that approximately 0.6% of the power was pulsating within a time interval of 4 msec.

The above assumes random variations. Periodic variations are detected by Fourier analysis or folding, preserving phase from second to second. The same 6000 counts, divided into 10 phase bins, will yield  $600 \pm 25$  counts/bin. Assuming a  $10\sigma$  result is required to establish a periodic signal, the limit of sensitivity for detecting such a signal is about 4% of the net intensity. The reason that such a high level of confidence is required is simply that a large number of periods and phases must be sampled if there is no a priori knowledge of a phase or a period.

For a source whose intensity is much less than the background, the accumulated count per 1000 sec is  $\sim 3000$  cts., essentially all background. In this case, each of 10 phase bins contains  $300 \pm 17$  cts and  $10\sigma = 170$  counts. A source of intensity 0.5 cts/sec (10 UHURU cts/sec) will yield 500 cts in this 1000 second interval. Thus, if this source has a periodic component with  $\sim 30\%$  duty cycle (170 out of 500 counts) it will be detected. This is comparable to what is seen in Her X-1 and Cen X-3.

### 1.1.2.3 Spatial Structure

This measure, as the measurement of location described in Section 1.1.2.1, consists of stepping across a source. Thus, for the weakest sources, finite size can be detected in the same 270 minutes required to obtain an accurate location.

To be more specific, we consider measuring the galactic center which is seen by UHURU as a source of about 1 degree in size at an intensity of 40 UHURU cts/sec. The measure would be made in ten steps, each separated by 10' arc. If the surface brightness is uniform, six of these intervals would contain a source of about 7 UHURU cts/sec or 0.35 ANS cts/sec.

To obtain a  $5\sigma$  (0.07 cts/sec) result in each of these intervals requires an observing time of about 12 minutes, or  $\sim 120$  minutes for the whole set of 10 observations. During this time we could measure deviations from smooth surface brightness of 0.14 cts/sec ( $2\sigma$ ) which is about 40% of the average surface brightness. Much larger variations in surface brightness than this are seen in other wavelengths in which the galactic center is seen. In radio at 3GHz, as an example, the variation in surface brightness is about a factor of 5.

### 1.1.2.4 Sensitivity of the Bragg Experiment

The spectral lines of interest in the Bragg experiment are described in Table 1-1. Assuming a background rate of one count per second in the energy interval 1.05 to 4.38 keV, and noting that the relevant silicon lines lie within the energy channel delimited by 1.81 to 2.03 keV, we estimate the Bragg background to be approximately  $.07 \text{ sec}^{-1}$ .

The effective geometric area of either the hydrogen or helium-like

line detector is  $28.7 \text{ cm}^2$  and the overall efficiency is 8%, including the crystal reflectivity (.16), heat shield and window transmission (.62), and PSD efficiency (.8).

A candidate object will be scanned over a  $\pm 5$  arc minute range in Bragg angle in one arc minute steps at one step per orbit. Assuming 20 observing minutes per orbit, and noting that the FWHM of the crystal rocking curve is 2.3 arc minutes, the estimated background per resolution element is about 158 counts. This leads to a minimum detectable flux (MDF) of  $.01 \text{ cm}^{-2} \text{ sec}^{-1}$  at a 99% confidence level.

Uncertainties in the estimated background and source continuum suggest an error in the computed MDF of  $\pm 40\%$ .

### 1.1.3 Summary

The above estimates, which are conservative, indicate that significant measurements can be made for most of the UHURU sources covering a broad range of observational objectives. Many of these, such as the Bragg spectral measurements and the 4 msec intensity variability, will be conducted for the first time.

## 1.2 Scientific Description of the Experiment

The Hard X-ray (HXX) experimental package consists of two instruments: the Large Area Detector System (LAD) and the Bragg Crystal Spectrometer (BG). The Large Area Detector System will measure X-ray emission from selected galactic and extragalactic objects in the energy range of 1.5 - 30 keV\* using narrowly collimated proportional counters. The Bragg Crystal Spectrometer will measure two silicon emission lines in the 1.8 - 2.0 keV energy range using two Bragg Crystals and two collimated proportional counters. The Hard X-ray Experiment configuration is shown in Figure 1-2.

The experiment is contained in a single package and consists of five major elements of hardware in addition to the housing. The important features of each element are mentioned below.

### 1.2.1 The Large Area Detector System

#### 1.2.1.1 The Spectrometer

The LAD consists of two collimated proportional counters each with an area of about  $105 \text{ cm}^2$ . These proportional counters have a common cathode, but independent gas volumes. The area of each counter is reduced to an effective area of  $34 \text{ cm}^2$ , by the losses due to the window structure (0.80 transmission), the fine collimator and coarse collimators (0.50 and 0.80 transmission respectively). Furthermore, the field of views of the two detectors are offset to allow for azimuthal referencing on strong signals. Each detector has  $10' \times 3^\circ$  field-of-view (FWHM), but the center angles are offset by  $4'$  giving a composite  $14' \times 3^\circ$  (FWHM) field,

\*The energy range of the spare unit is 1.5 - 40 keV.

# ANS HARD X-RAY EXPERIMENT

1-11

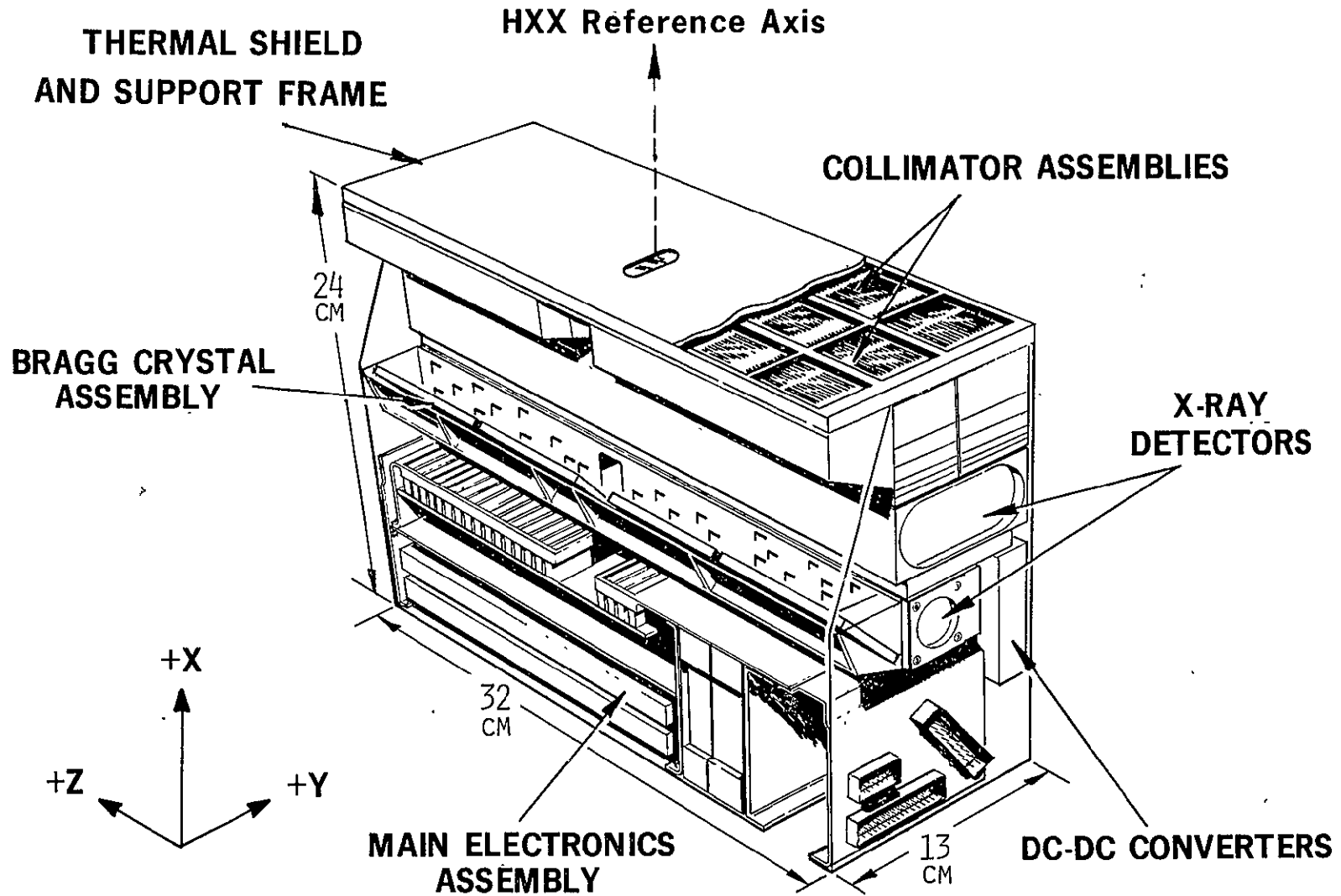


Figure 1-2

and allowing for differences in counting rates to provide the azimuthal reference. As the system is presently configured, the difference in counting rates is obtained by data processing of the output of the high rate LAD accumulators, using the on-board computer. The total effective area of the LAD is therefore  $55 \text{ cm}^2$ .

#### 1.2.1.2 The Proportional Counters

Originally, the proportional counters for the LAD had to maintain a high efficiency over the 1.5 - 40 keV range. For this reason the best choice of fill gas was Xenon at about 2 atmospheres of pressure; however, because of the high sensitivity of this gas to impurities, several attempts at using it in a closed system met with only partial success. The final choice for the fill-gas of the proportional counters for the Flight Unit LAD is Argon-CO<sub>2</sub>-Helium (90%, 9.5%, and 0.5%) at 1.4 atmosphere of pressure.

For the backup unit, the proportional counters of the LAD are filled with Xenon-CO<sub>2</sub>-Helium (90%, 9.5% and 0.5%) at 2 atmospheres of pressure.

The depth of the gas in either case is 3.7 cm, and the window is made of beryllium, 50 $\mu\text{m}$  thick. The efficiencies as a function of energy of the Flight Unit LAD (Ar-CO<sub>2</sub>-He) and backup unit LAD (Xe-CO<sub>2</sub>-He) proportional counters are shown in Figure 1-3; of course, the useful energy range with Argon is reduced to 1.5 - 30 keV, from 1.5 - 40 keV with Xenon.

### 1.2.2 The Bragg Spectrometer System

#### 1.2.2.1 The Spectrometer

The crystal most suitable for the studies of line emission of silicon in the 1.8 - 2.0 keV energy range was found to be PET (C(CH<sub>2</sub>OH)<sub>4</sub>). Each crystal is approximately  $56 \text{ cm}^2$  in area and has a

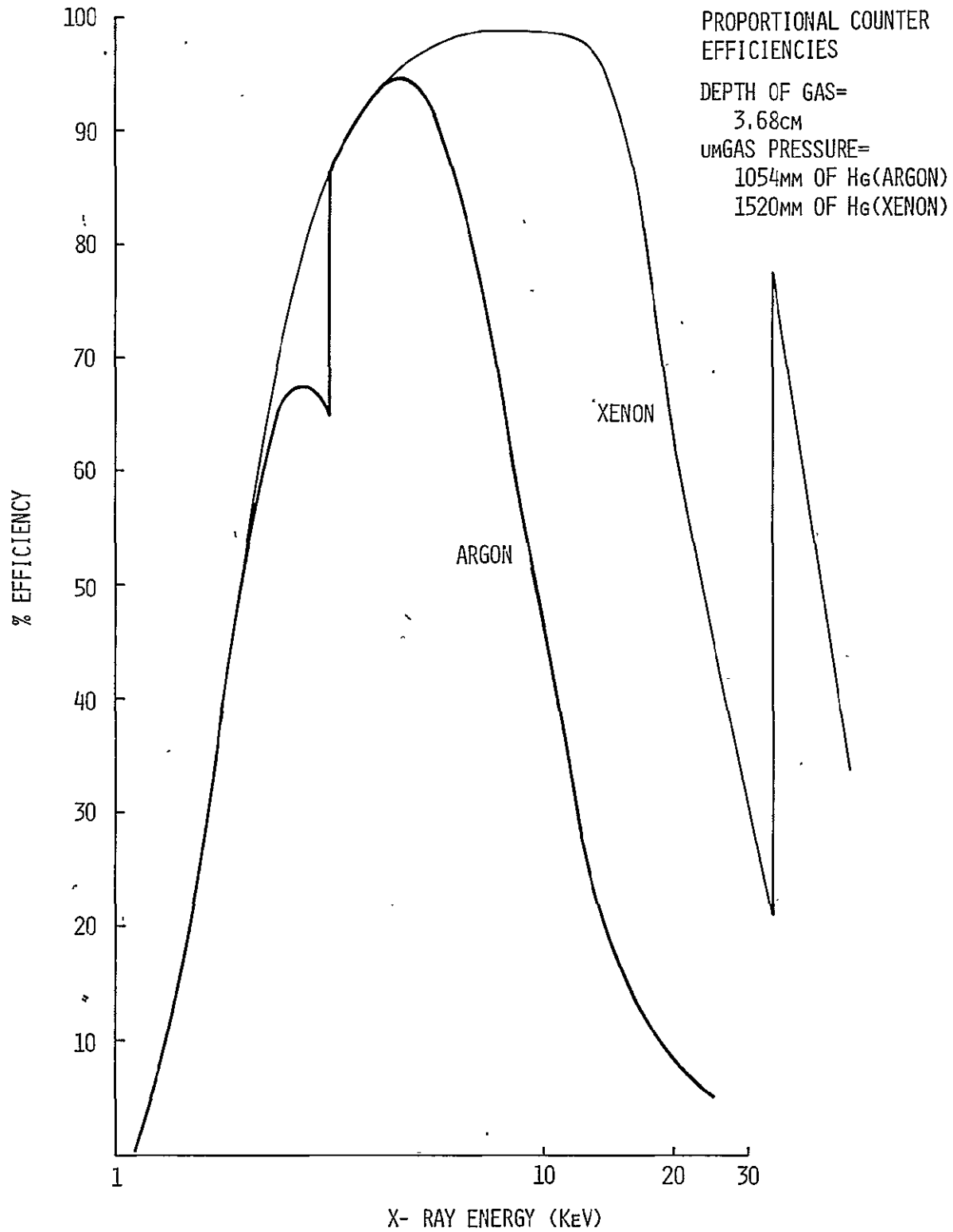


Figure 1-3. Proportional Counter Efficiencies

projected area of about  $40 \text{ cm}^2$ . Two independent proportional counters record the reflected X-rays from each crystal. The two crystals are at such angles relative to the optical axis (X-axis) of the spacecraft and to each other, that when the angle for one of the crystals corresponds to the critical angle for one of the lines, the other angle for second crystal is off the second critical angle (the critical angle corresponding to the second Si line of interest). Thus, this second crystal reflects X-rays corresponding to the X-ray continuum, plus any fluorescence and scattered X-rays from the instrument collimators. Furthermore, since the LAD and one of the two Bragg crystals are coaligned, it is possible to measure the photon intensity of the X-ray continuum simultaneously.

Figure 1-4 shows schematically the alignment of the 2 crystals and of the 2 LAD Proportional Counters around the z-axis relative to the reference HXX mirror. The HXX mirror is itself aligned to better than 0.5 arc minute to the X-axis of the S/C. The angles in the figure are greatly exaggerated for clarity. The angles in the x-y plane increase as the vector rotates around the z-axis from the +x-axis toward the +y-axis.

The values for these different vectors are given in Table 1-2, and are for an experiment temperature of  $19.5^\circ\text{C}$ .

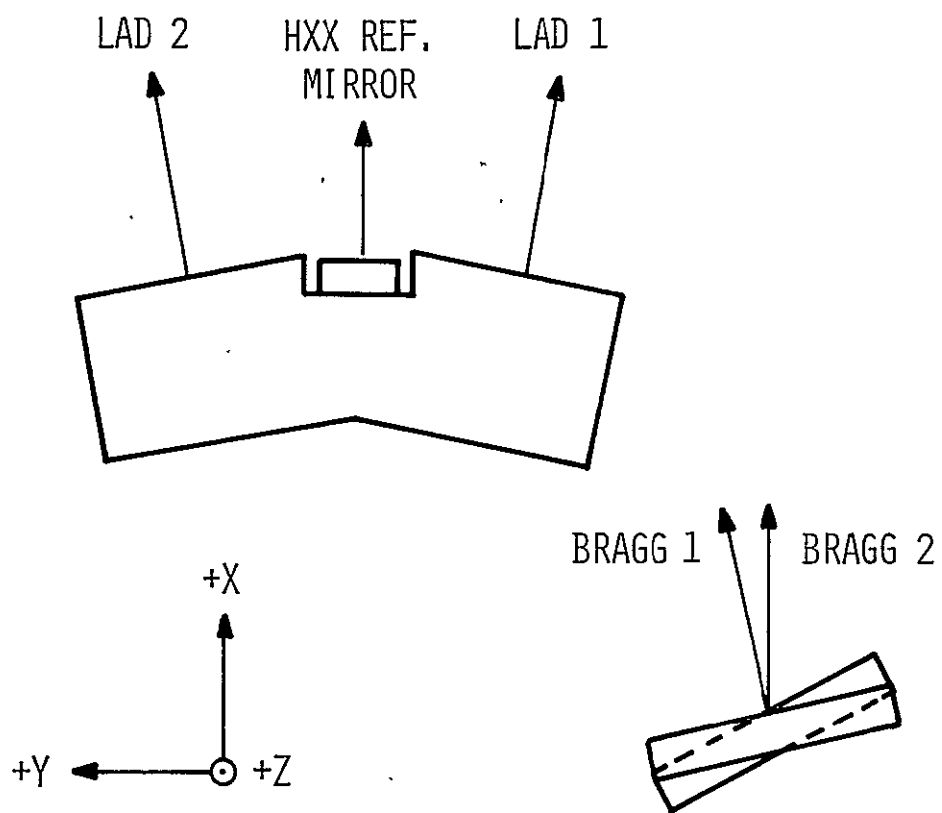


Figure 1-4. Crystal and Collimator Alignment

Table 1-2. Pointing Directions at 19.5°C

HXX Mirror	0.0 arc min.
LAD, Side 1	-2.0 arc min.
LAD, Side 2	+2.0 arc min.
BRAGG 1	
$1_P - 1_S$	+12.6 arc min.
$3_P - 1_S$	+33.9 arc min.
$3_S - 1_S$	+67.6 arc min.
BRAGG -	
$2_P - 1_S$	0.0 arc min.

Note: The Bragg pointing direction will increase toward more positive values, with decreasing temperatures (from LAD 1 toward LAD 2), at the following rates:

BRAGG 1; 0.525 arc min/°C

BRAGG 2; 0.432 arc min/°C

#### 1.2.2.2 The Proportional Counters

The detectors are designed to have a high efficiency near the Si lines (~70%). The gas fill is Argon-CO<sub>2</sub>-Helium (90%, 9.5%, 0.5%) at 1.3 atmosphere. The gas depth is 3 cm and the windows are made of beryllium, 25μm thick.

#### 1.2.3 The Pulse Shape Discrimination

This is a technique of discrimination between real X-ray events and background events charged particles, bremsstrahlung in the proportional counters, by using the fact that the former produce faster rise-time pulses at the anode than the latter.

Tables 1-3 and 1-4 show the X-ray acceptance and background rejection (simulated with  $\gamma$ -rays from a CO<sup>60</sup> source) at different energies for the LAD and the BRAGG detectors systems.

#### 1.2.4 The Collimators

##### 1.2.4.1 The LAD Collimator

A wire grid collimator of six wire planes is mounted in front of the Large Area Detector. This collimator has a slit field of view of 10' FWHM. In addition, the field of view is restricted by a tube-type collimator of 3° FWHM so that the net field of view is 10' x 3°. The collimator wires are made of copper.

##### 1.2.4.2 The BRAGG Collimator

A tube-type collimator is used to provide a 3° FWHM field of view. The optical center lines of the LAD Collimator and the BG Collimator are aligned to within 1 arc-minute.

Table 1-3. X-Ray Acceptance and Background Rejection of LAD

Energy (KeV)	X <sup>A</sup> (%)	BG <sup>R</sup> (%)
1.5	70 ± 3	58 ± 3
2.9	77 ± 2	68 ± 3
4.5	82 ± 2	75 ± 3
5.9	90 ± 2	82 ± 3
8.0	89 ± 2	88 ± 3
10.5	85 ± 2	91 ± 3
13.4	87 ± 2	91 ± 3
22.2	82 ± 2	90 ± 3

Table 1-4. X-Ray Acceptance and Background Rejection of BRAGG

Energy (KeV)	X <sub>A</sub> (%)	BG <sub>R</sub> (%)
1.5	78 ± 3	67 ± 3
1.84	83 ± 3	67 ± 3
4.5	93 ± 2	76 ± 3

### 1.2.5 The Calibration Sources

Radioactive calibration sources are mounted in a fixed position in front of each Bragg detector. The radio element used is Platinum 193 which emits 10 keV X-rays. In the calibration mode, the gain of the summing amplifier is reduced such that the 10 keV line corresponds to about 3 keV of the normal operation mode of the BRAGG Detector System.

### 1.2.6 Data Handling

A Logarithmic pulse high analyzer resolves the outputs from the two large area detectors taken together into 15 energy channels, and outputs from the two Bragg Detectors taken separately into eight energy channels. Table 1-5 shows the energy boundaries of the PHA. The detector identification circuit indicates the source of the pulse and provides control signals to the PHA and Accumulator Input Control to enable the appropriate 15-channel (LAD 1 or 2) or 8-channel (BG 1 or 2) portion of the PHA and to form part of the address which, when combined with the output of the PHA, will increment the appropriate accumulator. In all, the Experiment Scientific Data are contained in 27 16 bits accumulators. The accumulator designations are given in Table 1-6.

Readout of the accumulators is accomplished via spacecraft control. The spacecraft presents the coded address of the desired accumulator and transfer pulse to the instrument readout control. Upon receipt of the transfer pulse, the accumulator contents are strobed into a buffer register whose contents are then readout to the spacecraft in serial bit fashion under control of the spacecraft clock. After the sixteenth bit has been readout, the spacecraft may address another accumulator.

Table 1-5. Energy Channel Boundaries of the PHA

LAD PHA	
Ch. No.	E (keV)
	1.06
1	1.32
2	1.65
3	2.06
4	2.57
5	3.21
6	4.02
7	5.02
8	6.27
9	7.83
10	9.78
11	12.3
12	15.4
13	19.2
14	24.0
15	30.0

BRAGG PHA	
Ch. No.	E (keV)
	1.05
1	1.35
2	1.62
3	1.81
4	2.03
5	2.32
6	2.68
7	3.13
8	4.38

Table 1-6. HXX Accumulator Contents

Acc. Number	Contents	Group	Optional Data Reduction Type	Remarks
0 1	Background Status	- -	- -	
2 3 4 5 6 7 8 9 10	LAD PHA 0 " 1 " 2 " 3 " 4 " 5 " 6 " 7 " 8	PHA 1	T. 9. 16	If in the measurement command PULSAR is ON then the second PHA group is replaced by:  Time 1st pulsar event: " 2nd " " " 3rd " " " 4th " " " 5th " " " 6th " "
11 12 13 14 15 16	" 9 " 10 " 11 " 12 " 13 " 14	PHA 2 PULSAR	T. 9. 16 T. 7. 14	
17 18 19 20 21 22 23 24	BD 1 PHA 0, 1 " " 2, 3 " " 4, 5 " " 6, 7 BD 2 " 0, 1 " " 2, 3 " " 4, 5 " " 6, 7	BRAGG	-	PHA x, y stands for $(\text{PHA } x) \cdot 2^8 + \text{PHA } y$
25 26	Window LAD 1 " LAD 2	LAD	T. 9. 16	Gives attitude reference in the X-ray pointing mode.

The six accumulators used for PULSAR mode represent the high energy end of the LAD spectrum. In the PULSAR mode, the spectral data is not required and is waived in favor of the time of occurrence of each event. Thus, these accumulators switch to counting clock pulses and, as each event occurs, one of the six accumulators is inhibited, thereby storing the time of occurrence of the event. After telemetry readout, once each second, these accumulators are reset and the sequence of counting time is repeated.

Accumulators 25 and 26 register the integral number of counts in the LAD's, in the energy range 1.5 - 7.7 keV. These accumulated counts over a given time interval are used, among other things, to generate an error signal used by the attitude control system in the "X-ray Pointing Mode".

Sixteen different measurement status-words exist which allow different experimental configurations. These commands are listed below:

1. (MSB) LAD Window lower threshold increased
2. Background Accumulator only counts PSD events
3. Alternate address keying used
4. High Voltage ON
5. Bragg Accumulator only selected
6. LAD Accumulator only selected
7. Bragg PHA interchanged
8. L1 Disabled
9. L2 Disabled
10. B1 Disabled
11. B2 Disabled
12. Anticoincidence OFF
13. PSD OFF

14. Bragg Calibrate Mode ON
15. Pulsar Mode ON
16. (LSB) High Voltage Reduced

#### 1.2.7 Operating Modes

Six basic operating modes exist. They are: the normal mode, pulsar mode, high rate mode, calibration mode, and two slow scan modes. Table 1-7 lists these modes, indicating at what rate (in seconds) the accumulators are sampled.

Table 1-7. HXX Data Handling Modes

	Normal	Normal; during Slow Scan	Pulsar	High Rate	Intermediate Rate	Calibration
Background	64	64	64	64	64	64
Status	64	64	64	64	64	64
PHA 1	256	256	256	4*	64*	-
PHA 2/Pulsar	256	256	1*	4*	64*	-
Bragg	256	-	256	-	-	256
LAD	16	16	16	1*	4*	-
Nominal data rate	3.94 bps	3.44 bps	93.56 bps	92.5 bps	12.25 bps	1 bps
Data rate after reduc- tion	-	-	50.56 bps	48.50 bps	6.50 bps	-

\*indicates use of data reduction option.

## 2.0 ENGINEERING IMPLEMENTATION OF THE HARD X-RAY EXPERIMENT

Figure 2-1 is a photograph of a delivered Hard X-ray Experiment with its thermal shield removed. Table 2-1 lists the experiment's parameters of primary interest.

The following sections discuss the experiment's electrical and mechanical engineering implementation along with that of the ground support equipment. A section on the reliability aspects of the experiment is also included.

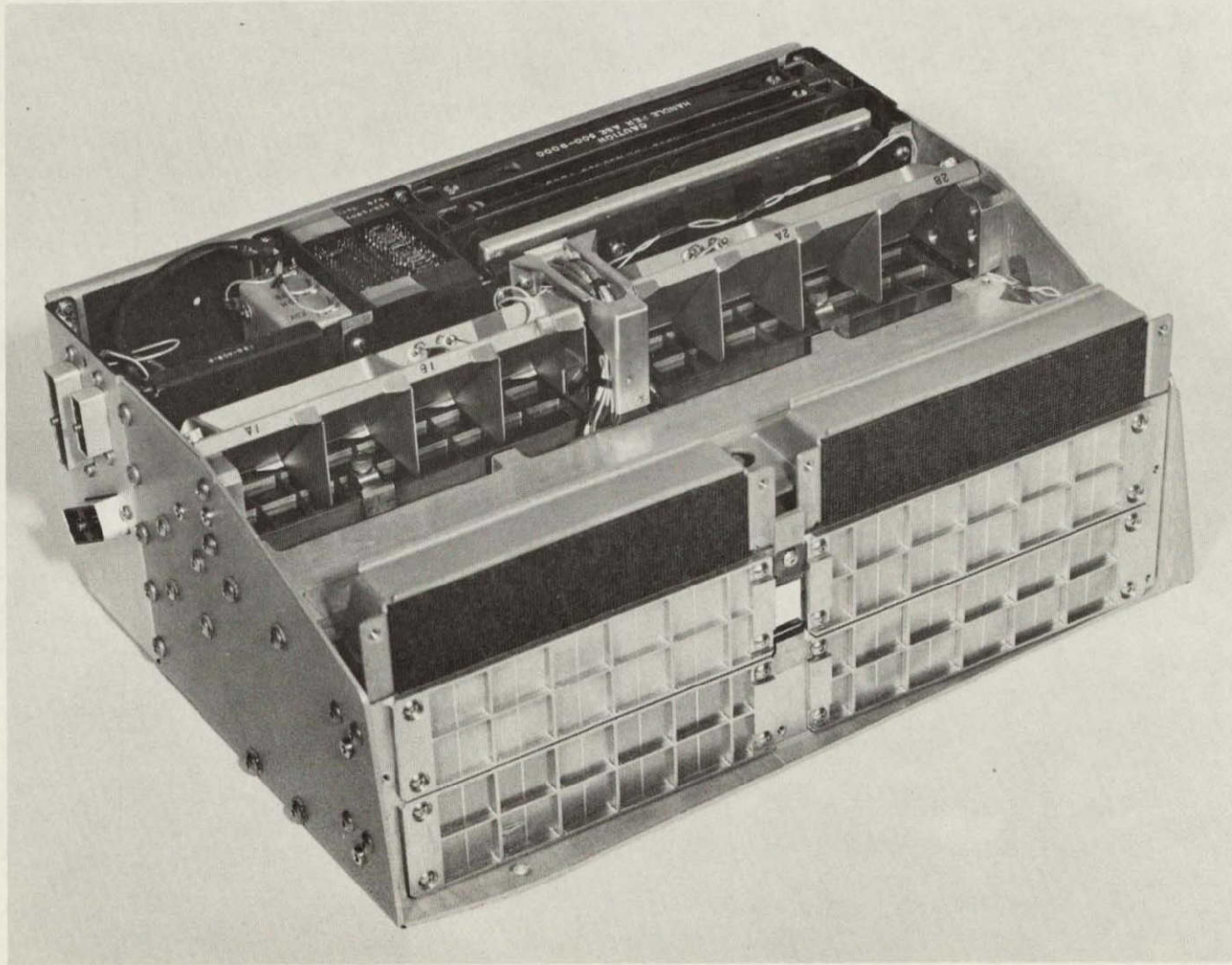
Table 2-1  
HXX Experiment Parameters

Size	24 cm x 32 cm x 13 cm
Weight*	7.8 Kg/8.1 Kg
Specific Gravity	0.8
Power	2 Watts
Data Rate	~ 4 to 100 bits/sec.

\*Protoflight Unit (7.8 Kg) contained Beryllium LAD Proportional Counter, Flight Unit Spare (8.1 Kg) contained Aluminum LAD Proportional Counter.

ORIGINAL PAGE IS  
OF POOR QUALITY

2-2



ES-149

Figure 2-1. Hard X-ray Experiment

## 2.1 Electrical Engineering Description

### 2.1.1 HXX Experiment Block Diagram

The HXX Experiment Block Diagram is given in Figure 2-2. Its operation is as follows.

#### 2.1.1.1 Proportional Counters

Each proportional counter detects X-rays and Gammas by the ionization caused, and provides an electrical pulse proportional to the energy of the event. Rise time of the pulse, on the average, is shorter for X-rays than for other events. The two LAD Proportional Counters, L1 and L2, and the two Bragg Proportional Counters, B1 and B2, are biased by a common high voltage source of approximately 2300 volts. Each counter output is connected to a dedicated preamplifier.

#### 2.1.1.2 Preamplifiers (Figure 2-3)

The preamplifier has a nominal charge gain of 10 volts/picocoulomb, a nominal rise-time of 0.1 $\mu$ sec and a nominal clipping time of 35 $\mu$ sec.

The amplifier consists of a charge sensitive amplifier and a voltage amplifier. The input FET, Q1, is operated at a drain current of .6mA. Voltage gain is provided by a PNP cascade stage (Q2) operating into a bootstrapped output stage (Q4 and Q5) which includes both capacitive and resistive neutralization. This output stage provides a factor of 3 additional closed-loop gain.

The voltage amplifier consists of two transistors (Q6 and Q7) connected in a conventional "Middlebrook" configuration. Provision is made to permit trimming the gain of the amplifier in order to standardize the preamplifier output for the expected range of variations in detector gain.

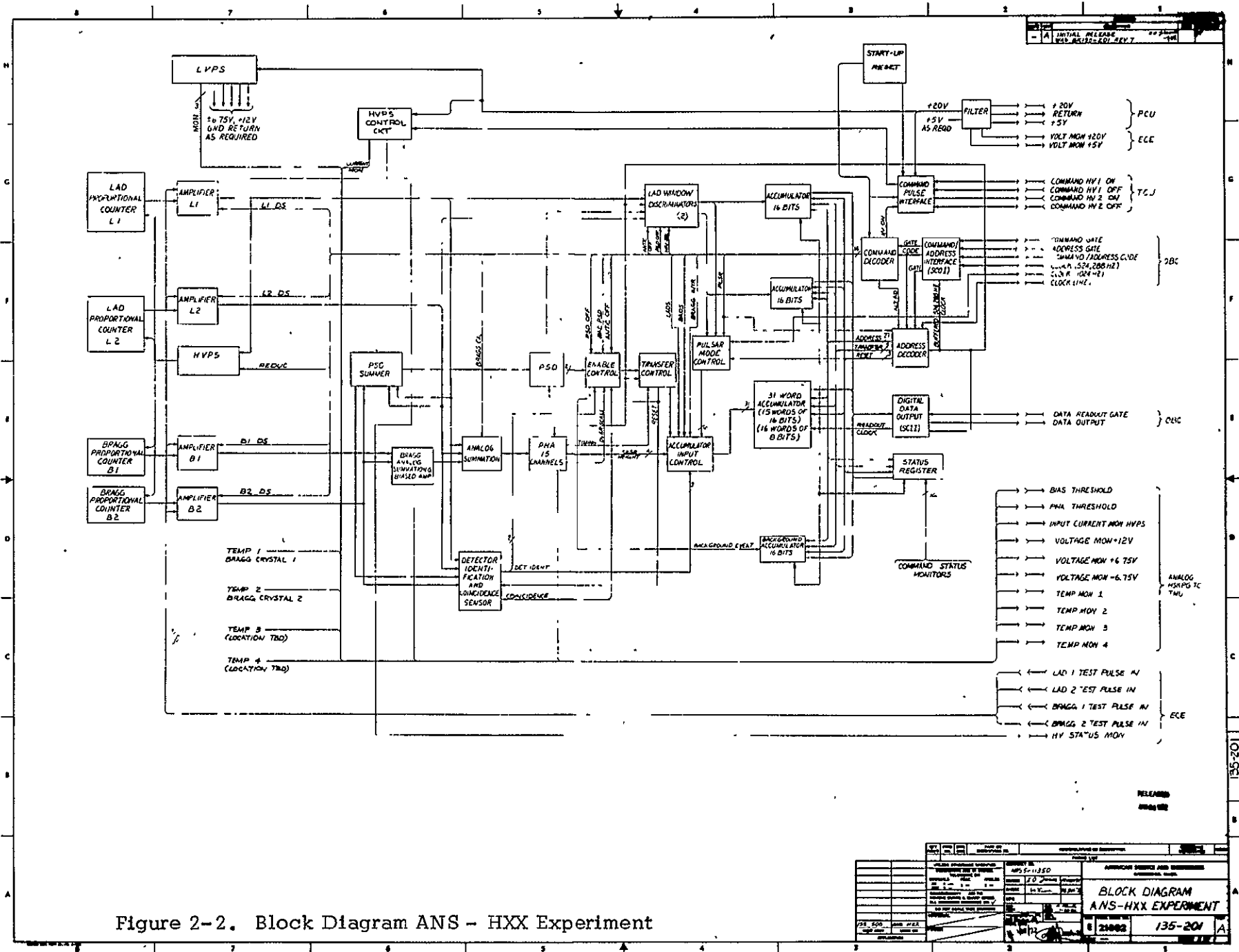


Figure 2-2. Block Diagram ANS - HXX Experiment

PART OF DISPOSITION NO.		APPROVED BY:	
DATE:		DATE:	
BY:		BY:	
TITLE:		TITLE:	
PROJECT:		PROJECT:	
DRAWING NO.		DRAWING NO.	
REVISION:		REVISION:	
28 500		135-201	

**BLOCK DIAGRAM  
ANS-HXX EXPERIMENT**

ORIGINAL PAGE IS  
OF POOR QUALITY

2-5

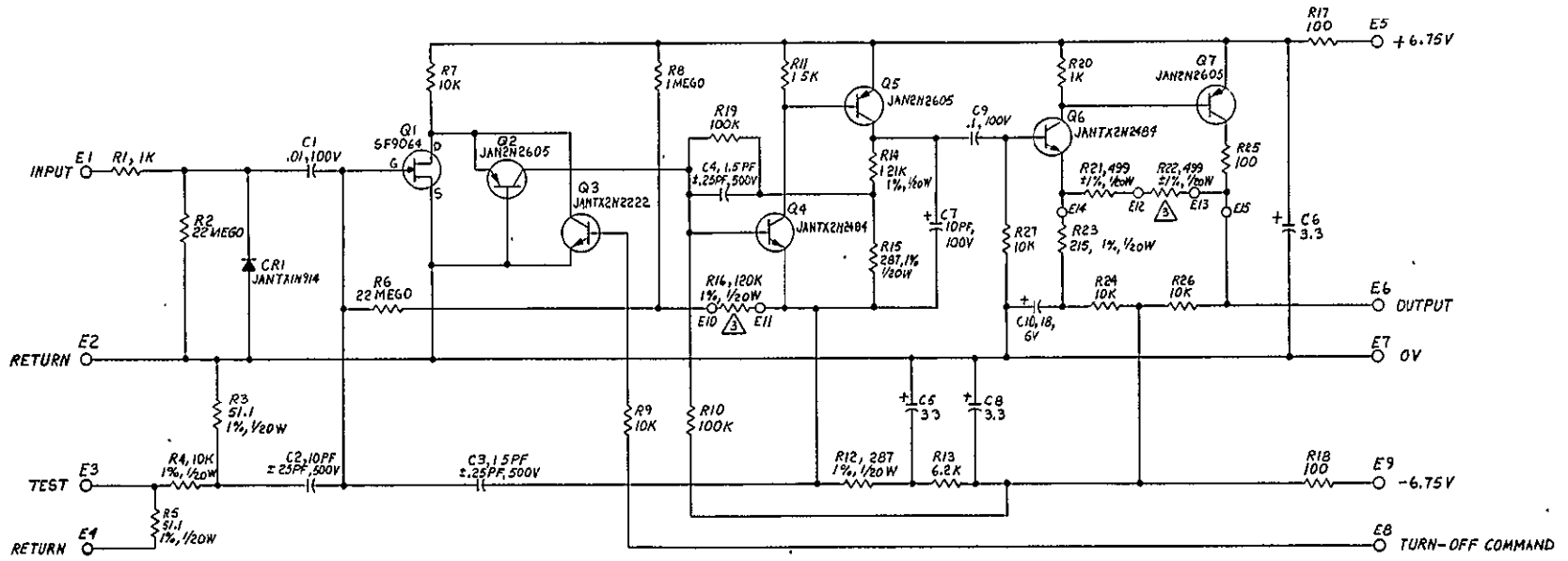


Figure 2-3. Preamplifier - Amplifier Module

A network is provided to inject test pulses into the preamplifier input. This network includes attenuation to reduce noise susceptibility and 50 ohm termination to interface with standard electronic test equipment.

#### 2.1.1.3 Analog Summer (Figure 2-4)

The analog summer combines the signal from the four preamplifiers and assigns to each the appropriate relative weight.

A biased amplifier combines the outputs of the two Bragg preamplifiers. The signal levels from the preamplifiers are matched. Transistors Q1, Q2 and Q3 are matched for base-to-emitter voltage at the operating collector current. Q1 and Q2, each associated with one preamplifier, are normally biased at cut-off. When the input signal exceeds the quiescent bias level at the base of Q3, the appropriate input transistor (Q1 or Q2) in conjunction with Q3, Q4 and Q5, forms a feedback amplifier which is followed by an emitter follower (Q6). The signal at the emitter of Q6 thus is equal to the preamplifier signal exclusive of a bias level determined by R41, and multiplied by a gain factor determined by R10. The bias level at the base of Q3 is amplified and buffered by amplifier U1 and furnished to TM as a diagnostic.

The thus summed Bragg signals are connected to a second amplifier through a one-step attenuator. On command, this attenuator reduces the signal into the second amplifier by a known ratio, thereby increasing the Bragg detector energy range of the instrument so as to include radiation from two on-board calibration sources. This makes it possible to verify the calibration of the instrument in flight.

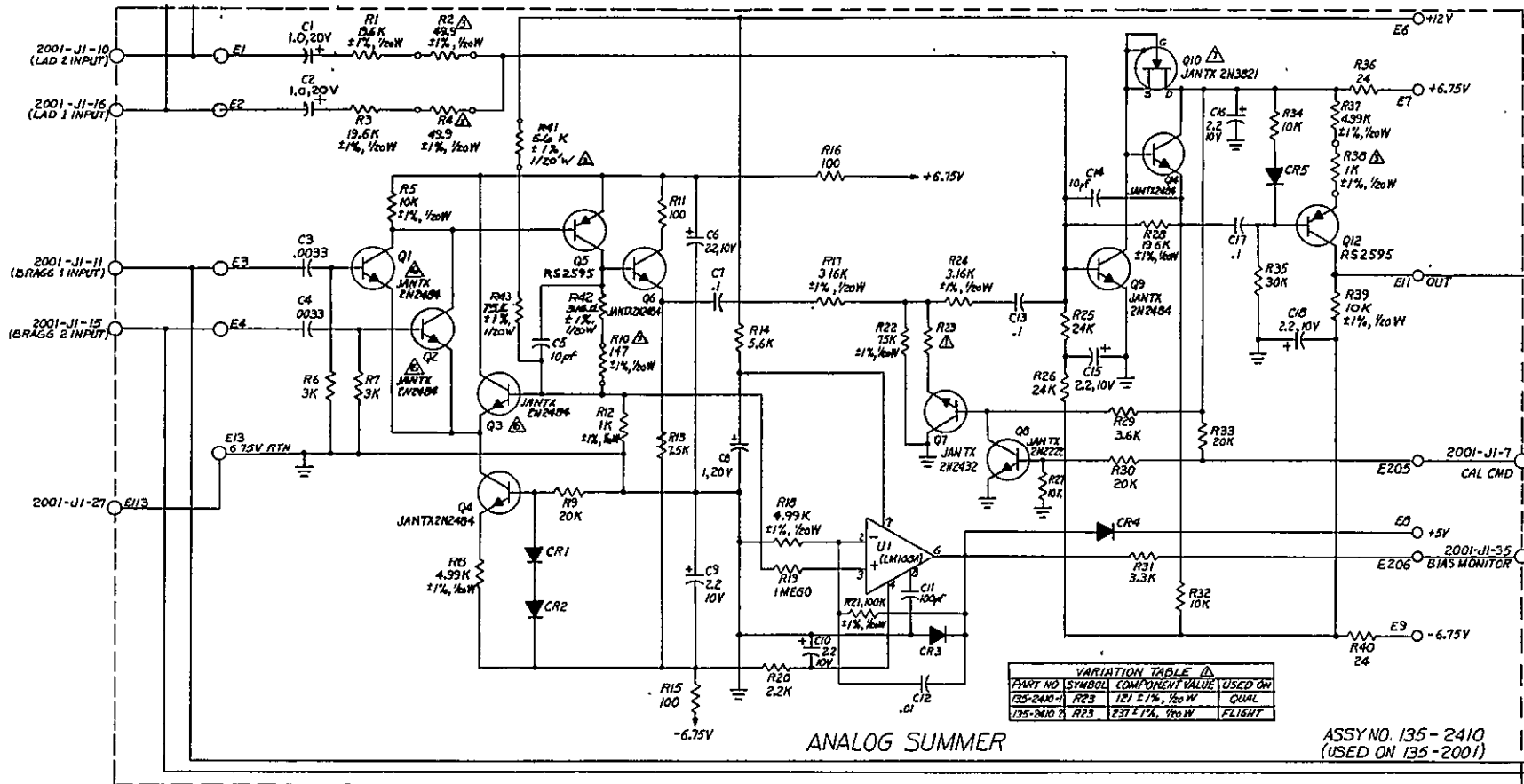


Figure 2-4. Analog Summer Assembly No. 135-2410

In the second amplifier, the combined Bragg signals are summed with the signals from the two Large Area Detector preamplifiers. The summed junction is provided by a single common-emitter stage with feedback. A final stage provides an inversion and an opportunity to trim the overall gain of the combined signal amplifier.

#### 2.1.1.4 Detector Identification (Figure 2-5)

Detectors are identified by a logic level pulse generated by a comparator associated with each detector. The comparator is an ICL8001 monolithic integrated circuit. The input signal to the comparator is coupled through a fast differentiating network to speed up circuit recovery.

#### 2.1.1.5 Detector Identification and Coincidence Logic

This circuit accepts detector identification pulses from the analog Detector Identification threshold detectors and status commands from the Command Register. It provides logic signals to the Enable Control, to permit the generation of an increment pulse, and to the Accumulator input logic for steering the increment pulse to the proper Accumulator. When a LAD 1, LAD 2, Bragg 1, or Bragg 2 event has been detected by a Detector Identification threshold comparator, a corresponding flip-flop in the Detector Identification logic is set. Information is stored until the Enable Control Reset signal from the Enable Control logic is received.

Signals from the Command Register which are used in the Detector Identification logic are:

- (1) LAOS (LAD Only Accumulator Select) which causes all events to be counted in the LAD Accumulators.
- (2) BAOS (Bragg Only Accumulator Select) which causes all events to be counted in Bragg 1 Accumulators.

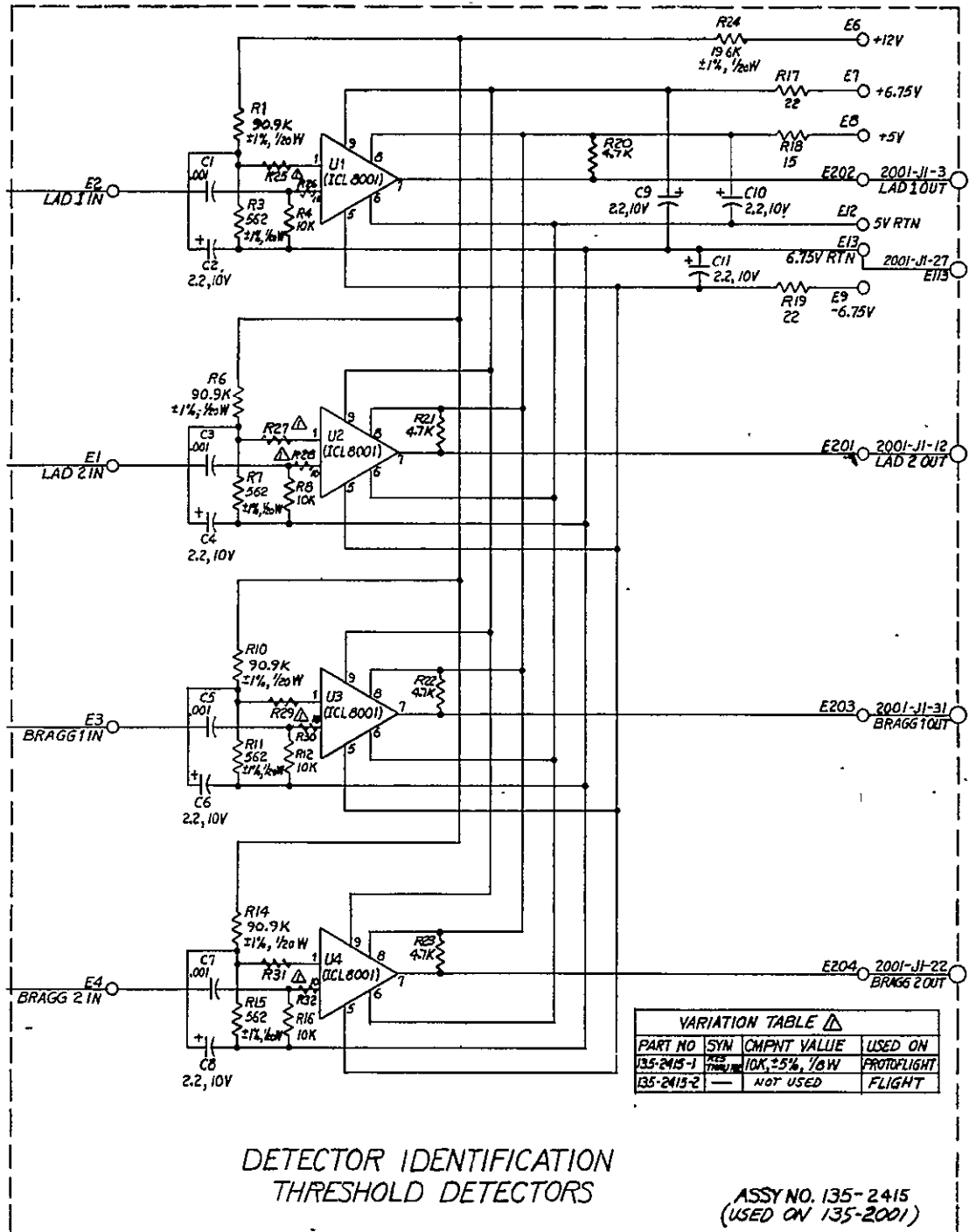


Figure 2-5. Detector Identification Threshold Detectors

- (3) Bragg Interchange which interchanges Bragg 1 and Bragg 2 Accumulator functions.

The LAD ID output signal is used for steering increment pulses to the LAD Accumulators. It is present if BAOS has not been commanded and, (1) If a LAD event was detected or (2) if LAOS has been commanded.

The BD ID output signal is used for steering increment pulses to Bragg 1 Accumulators. It is present if LAOS has not been commanded and, (1) If a Bragg 1 event has been detected, or (2) if BAOS has been commanded. A BD1 ID signal is also generated if Bragg Interchange has been commanded and conditions for a BD2 ID signal exist.

The BD2 ID output signal is used for steering increment pulses to Bragg 2 Accumulators. It is present if a Bragg 2 event has been detected. A BD2 ID signal is also generated if Bragg Interchange has been commanded and conditions for a BD1 ID signal exist.

The LAD ID Enable output signal is used in the Enable Control logic. It is present if a LAD event has been detected or if either LAOS or BAOS has been commanded.

The BRG ID Enable output signal is used in the Enable Control logic. It is present if a Bragg event has been detected or if either LAOS or BAOS has been commanded.

The coincidence output signal is used in the Enable Control logic. It is generated if two or more detector events are sensed during pulse processing time.

The Detector Identification and Coincidence Logic is located in 135-6004 and part of 135-6021  $\mu$ sticks.

#### 2.1.1.6 Pulse Shape Discrimination

For background discrimination, the rise time of pulses is analyzed. Pulses with rise times which fall below a pre-established threshold value are accepted as X-rays. In the analog section of the circuit (Figure 2-6), pulses are shaped by a fast feedback amplifier (Q1 and Q2) with an emitter-coupled input stage, into which the signals from both preamplifiers are summed. The leading edge of the pulse is detected by a so-called "Pulse Detector" (Q6, Q7, and Q8). The peak of the pulse, corresponding to the trailing edge of the differentiated pulse, is detected by a so-called "Zero Cross Detector" (Q3, Q4 and Q5). Both the Pulse Detector and the Zero Cross Detector use DC stabilization to maintain stable threshold levels near zero.

In the digital portion of the Pulse Shape Discriminator, the Pulse Detector signal is used to start a pair of one shots. The first of these disables the circuitry for a suitable processing interval so as to improve the system's noise immunity. The second establishes a time-window within which a zero-crossing must be detected for the corresponding pulse to be accepted as an X-ray. If the zero crossing falls within the allotted time, a pulse is generated which sets a flip-flop for subsequent processing.

#### 2.1.1.7 PSD Logic

PSD Logic consists of two similar circuits; one for Bragg signals and one for LAD signals. Inputs to each section are the PSD Analog Circuit output signals; Pulse Detector and Zero Crossing Detector. The Pulse Detector triggers a Timing One Shot whose output is compared to the Zero Crossing Detector pulse width. If the Zero Crossing Detector signal ends before the One Shot signal, the signal is identified as an X-ray. The Pulse Height Gate sig-

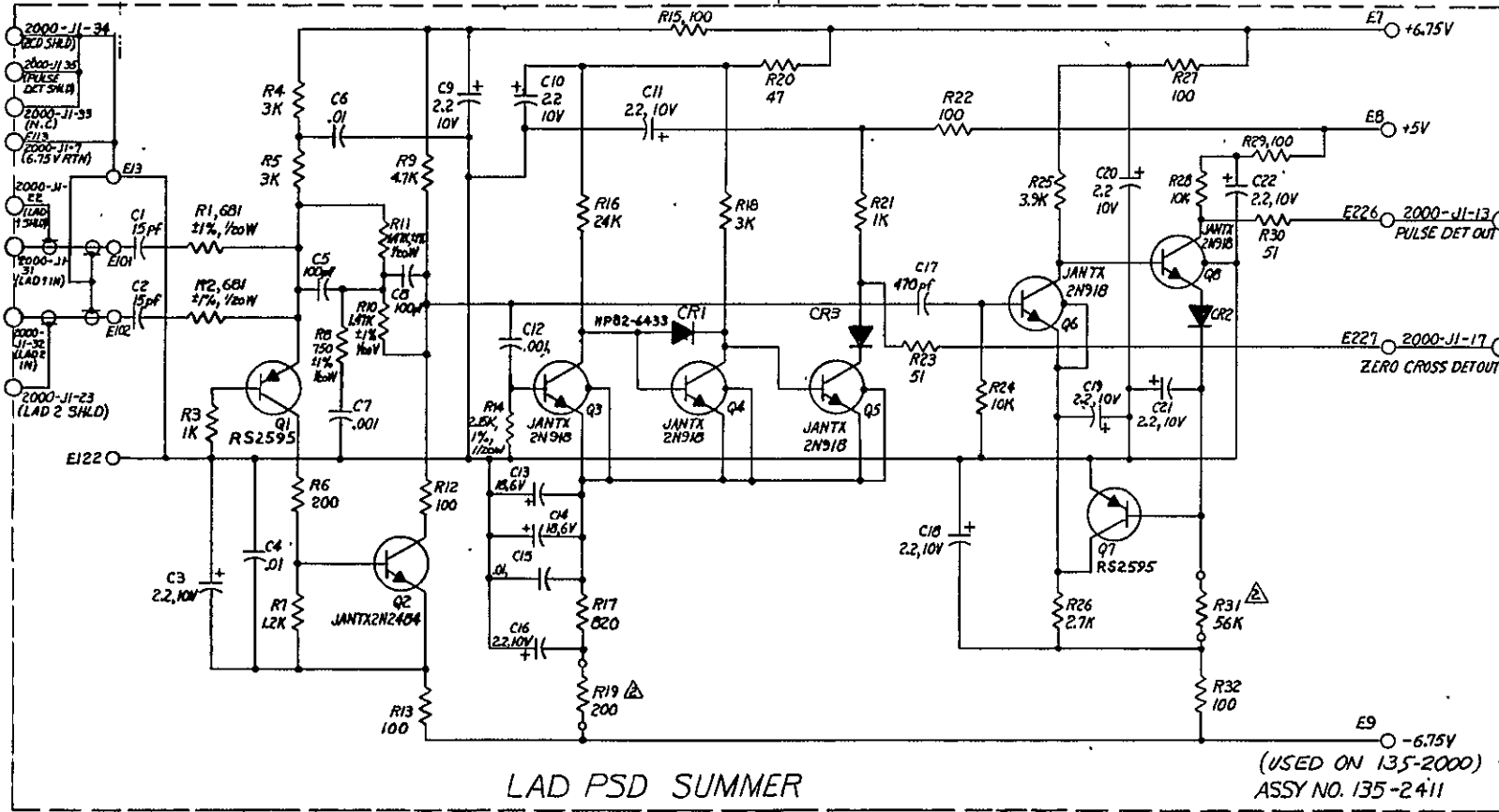


Figure 2-6. LAD PSD Summer Assembly No. 135-2411

nal also triggers a Lockout One Shot which inhibits further triggering of the Timing One Shot for 7  $\mu$ sec. This prevents multiple tries at X-ray identification during pulse processing as may occur if the circuit is triggered by noise. Two cross-coupled Nand gates form a leading edge lockout flip-flop which prevents an X-ray identification from occurring unless a Zero Crossing Detector signal has occurred.

The PSD Logic output signals, Bragg Pulse and LAD Pulse, identify the signal being processed as an X-ray. When either of these signals is present, the PSD Logic Reset Circuit starts its timing cycle. If a Discriminator Gate signal does not occur within 8 $\mu$ sec, the PSD is reset. The Discriminator Gate signal, from the PHA, starts when the detected signal is greater than 1keV and ends when the PHA integration capacitor discharges below the 1keV level. The PSD is therefore reset in two ways. If a noise transient triggers the PSD and is identified as an X-ray, the PSD will be reset as no Discriminator Gate occurs. After the processing of a signal, the Discriminator Gate signal goes to zero and the PSD is reset 8  $\mu$ sec later. This delay time is sufficient to allow normal processing of an accumulator increment pulse which occurs a maximum of 6  $\mu$ sec after the end of the Discriminator Gate.

A PSD lockout prevents any further X-ray identification signals. It is set when the Timing One Shot ends if the Discriminator Gate is present and is reset by the Enable Control Reset which is the normal Enable Logic reset.

The PSD Logic is located in the 135-6002 and part of the 135-6021 logic  $\mu$ sticks.

#### 2.1.1.8 Logarithmic Pulse Height Converter (Figure 2-7)

The logarithmic converter generates a time interval proportional to the logarithm of the pulse height by measuring the time required to discharge a capacitor charged to the peak voltage of the pulse to a prescribed threshold value.

The signal from the summing amplifier is processed in a peak-holding amplifier (Q1 through Q6) which charges capacitor C2 to the peak value of the input pulse. When the threshold level of comparator U1 is exceeded, a level is provided by the logic which opens transistor Q7 and thereby prevents capacitor C2 from discharging. Two to four  $\mu$ sec later Q7 is again closed synchronously with pulses from the spacecraft 524288 Hz clock, thereby initiating an exponential discharge of C2. The time from the initiation of the discharge until the voltage on C2 reaches the threshold voltage of comparator U1 is proportional to the logarithm of the input pulse height. A digital indication of this time is obtained by counting intervening pulses of the spacecraft clock. The U1 threshold level is monitored and amplified by amplifier U2 and transmitted to telemetry for diagnostic purposes.

#### 2.1.1.9 Enable Control

The Enable Control logic generates a Data Advance pulse which is used to increment the count in an Accumulator. The pulse is generated when the following conditions exist:

- (1) PHA count is not overscale.
- (2) No Coincidence signal has been detected or the Command Anti-Coincidence Off has been received.
- (3) The LAD ID Enable signal from the Detector Ident. and a LAD PSD signal have been received.
- (4) The Bragg ID Enable signal from the Detector Ident. and a Bragg PSD signal have been received.

LOGARITHMIC ANALOG TO DIGITAL CONVERTER

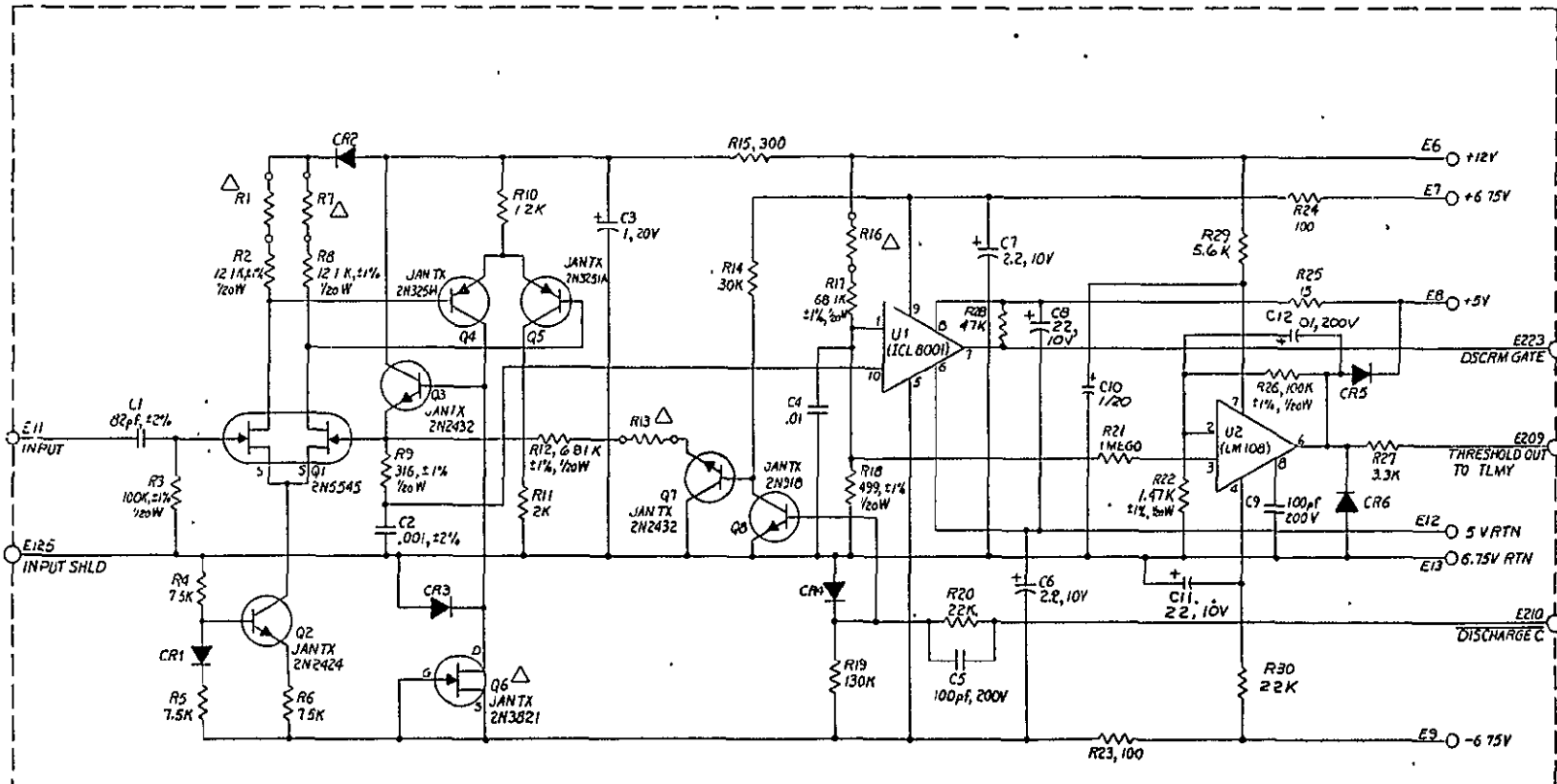


Figure 2-7. Logarithmic Analog to Digital Converter

The LAD PSD signal consists of either a LAD Pulse signal from the PSD logic or a PSD Off command from the Command logic.

When the Discriminator Gate ends, indicating PHA conversion is complete, the Enable timing sequence starts. A 1.9 to 3.8  $\mu\text{sec}$  delay is followed by a 1.9  $\mu\text{sec}$  long Data Advance Pulse. A further delay is then followed by the Enable Control Reset pulse.

An early Enable Control Reset pulse is generated if a LAD ID Enable or Bragg ID Enable signal is received and the PHA has not indicated a count of one or greater within 5.7 to 7.6  $\mu\text{sec}$ . The early reset feature is used to cancel false detector identification signals set by noise. The Enable Control Reset pulse resets the Detector Ident. logic and the Overscale Latch in the Enable Control logic.

The Background pulse which increments the Background Accumulator is generated when one or more of the following conditions exist:

- (1) An Overscale occurs.
- (2) A Coincidence is detected.
- (3) A LAD ID Enable or a BRAGG ID Enable detector ident. signal is generated and a corresponding PSD signal is not generated.

Enable Control logic is located in 135-6007, 135-6008, and 135-6009  $\mu\text{sticks}$ .

#### 2.1.1.10 Accumulators

The Accumulators sum the data pulses and provide the HXX serial data output words to the On Board Computer (OBC). Each output word consists of 16 bits with the LSB shifted out first. Twenty-six data words, obtained from Accumulators, give event counts for LAD PHA, Bragg 1 PHA, Bragg 2 PHA, LAD 1 Window, LAD 2

Window, and Background. Each 16 bit word is a data count except the Bragg PHA words which consist of two 8 bit data counts. The right half is the lower PH channel count and the left half is the next higher PH channel count. The eight Bragg PHA channels are thus compressed into four data words.

Each Accumulator consists of two 16 bit registers. The counter register is usually active counting data pulses. For Bragg Accumulators the counter register is split into two 8 bit registers. When a transfer signal is received, the counting function is inhibited and the count is jam transferred into the shift register. A Reset signal follows the Transfer signal which resets the counter to zero. When a Data Read Out Gate is received, sixteen Clock pulses are gated to the shift register and the register data is shifted out, through an output Or circuit, to the OBC.

Each Accumulator is packaged in a 135-6016  $\mu$ stick. The  $\mu$ sticks are packaged into two Accumulator Bank Plug-In units.

#### 2.1.1.11 Transfer Control and Pulsar Mode

The transfer control logic steers the Data Advance pulse to the Accumulator that is to be incremented. The three groups of PHA Accumulators, LAD, Bragg 1, and Bragg 2, are selected by the LAD ID, BRG 1 ID, and the BRG 2 ID signals respectively from the Detector Ident. logic.

The LAD group consists of 15 Accumulators, one of which is selected by the four amplitude bits from the PHA; each Accumulator representing a PHA amplitude range. Each Bragg group consists of 8 Accumulators, one of which is selected by the four amplitude bits as follows:

<u>PHA Count</u>	<u>LAD Accum.</u>	<u>Bragg Accum.</u>
1	PH 0	PH 0
2	1	
3	2	
4	3	
5	4	
6	5	
7	6	PH 1
8	7	"
9	8	2
10	9	3
11	10	4
12	11	5
13	12	6
14	13	PH 7
15	14	"

The Data Advance pulse increments the PHA Accumulator selected by the detector identification and amplitude data.

In the Pulsar mode LAD Accumulator PH9 to PH14 are used for accumulating until a LAD signal is detected by the LAD Windows. When the first event is detected, PH9 Accumulator count is stopped; when the second is detected, PH10 count is stopped, and so on until the six Pulsar Accumulators have counts in them which gives the time of arrival with a resolution of 1 msec, of six contiguous LAD events. The time reference is the 1 Hz clock which resets the Pulsar Accumulators.

During Pulsar operation, all other Accumulators operate in their normal mode.

Transfer Control logic is located in 135-6012 and 135-6013  $\mu$ sticks.

#### 2.1.1.12 LAD Window Discriminators

The signals from each of the two LAD preamplifiers are buffered in an amplifier which also provides some additional gain and pulse shaping. Two threshold discriminators associated with each

detector determine whether pre-established upper and lower threshold values are exceeded. The crossing of the lower threshold initiates a timing sequence which results in the incrementing of the appropriate accumulator when an event in the window discriminator energy range is detected.

The time constants in the buffer amplifiers and in the coupling networks to the comparators are such as to reduce circuit dead time and improve performance at moderately high count rates.

The lower window threshold may be increased by ground command to twice its normal value in order to improve the system's noise immunity if this should ever become necessary during the mission.

#### 2.1.1.13 LAD Window Logic

The LAD Window logic determines if a LAD event is between 1.5keV and 7.7keV and provides increment signals to the LAD Window Accumulators. Two identical circuits are used; one for LAD 1 and one for LAD 2. LAD Window circuits operate independently of the PHA processing. The signal from a LAD preamp feeds two threshold detectors which determine if the signal exceeds 1.5keV and 7.7keV. These two signals, with the PSD signal, and a LAD Window coincidence signal, determine if an increment pulse shall be sent to a LAD Window Accumulator.

An increment pulse is generated if: (1) The 1.5keV threshold is exceeded, (2) the 7.7keV threshold is not exceeded, (3) the LAD Pulse signal is received from the PSD logic or the PSD Off mode has been commanded, and (4) no coincidence occurs in LAD Window processing or the Anti-Coinc. Off mode has been commanded.

The LAD Window processing detects a coincidence when both LAD 1 1.5keV and LAD 2 1.5keV thresholds are exceeded simultaneously.

LAD Window timing is initiated by the trailing edge of the 1.5keV threshold signal. A transfer pulse is generated, which gates an increment pulse to one of the LAD Accumulators, and is followed by a reset pulse which resets the LAD Window logic. The two output signals are also Ored together to obtain the Pulsar Count signal used in the Pulsar mode.

The window lower threshold may be raised on command from 1.5keV to 3keV by the WINSEL command signal.

LAD Window logic is located in the 135-6010 and part of the 135-6011 logic  $\mu$ sticks.

#### 2.1.1.14 Address Selection and Digital Data Output

The Data Output Word is selected by the Address Word. An Address Word from the Command/Address Word input is read into the Address Buffer when the Address Read In Gate is present. Sixteen 524 KHz clock pulses are gated to the Buffer and serially shift in the Address data. The first 11 bits are shifted through the Buffer as only the last five bits of the Address Word are used. These bits are decoded to select one of 27 output signals as given in Table 2-2. The corresponding Accumulator output is enabled so that the data is shifted out serially by sixteen clock pulses, gated by the Data Read Out Gate.

Each Accumulator output feeds the Digital Data Output logic which is basically an output line driver having 27 OR'd inputs, one from each output shift register and interfaces with the data output line to the OBC. It conforms to the requirements for a Standard Computer Input Interface (SCII). The OBC provides the 524, 288 Hz clock and a readout gate to cause the transfer from any output shift register addressed by the Address Decoder.

Table 2-2  
Address Word Accumulator Selection

<u>Accum. No.</u> <u>(Address Word)</u>	<u>Accumulator</u> <u>Contents</u>
0	Background
1	Status
2	LAD PH 0
3	LAD PH 1
4	LAD PH 2
5	LAD PH 3
6	LAD PH 4
7	LAD PH 5
8	LAD PH 6
9	LAD PH 7
10	LAD PH 8
11	LAD PH 9 or Pulsar
12	LAD PH 10 "
13	LAD PH 11 "
14	LAD PH 12 "
15	LAD PH 13 "
16	LAD PH 14 "
17	BD 1 PH 0 and PH 1
18	BD 1 PH 2 and PH 3
19	BD 1 PH 4 and PH 5
20	BD 1 PH 6 and PH 7
21	BD 2 PH 0 and PH 1
22	BD 2 PH 2 and PH 3
23	BD 2 PH 4 and PH 5
24	BD 2 PH 6 and PH 7
25	LAD 1 Window
26	LAD 2 Window

The 27 Accumulators are divided into 5 blocks of data. For the purpose of later data analysis, it is desirable to transfer the content of all counters associated with a given data block simultaneously to their corresponding output shift registers. For this purpose, there are five addresses (one for each block) termed key addresses. When the Address Decoder receives any one of these

5 key addresses, it generates a transfer signal to all accumulators associated with that block causing the simultaneous transfer of data from the counters to the associated shift registers. Upon completion of transfer, a reset pulse originates at the Address Decoder, clearing the counters for that block. Key address words initiate block transfers as given in Table 2-3. After transfer, the data in each block is sequentially read out to telemetry as their respective Data Read Out Gates occur.

An alternate addressing sequence is implemented when the ALT AD command is activated. Data Transfer occurs following the Address Read In Gate of the Alternate key words as given in Table 2-3. Each of the alternate key addresses is contained in its associated block. This is an alternative mode of operation in the event the normal key addresses cannot be used.

Table 2-3  
Data Blocks Transferred on Key Address Words

Accum. Addresses of Transfer Block	Accum. Block Data	Key Address Words			
		Normal Addressing		Alternate Addressing	
		Norm Mode	Pulsar Mode	Norm Mode	Pulsar Mode
00-01	Bkgrnd, Status	00	00	01	01
02-10	LAD PHA	02	02	16	10
11-16	LAD PHA or Pulsar	02	*	16	16
17-24	Bragg PHA	17	17	24	24
25-26	LAD Windows	25	25	26	26

\*Date is transferred on the negative transition of the 1 Hz clock.

In Pulsar mode, Accumulators 11 to 16 contain Pulsar data rather than LAD PHA data. Their timing is then taken with reference to the 1 Hz clock.

The input buffers for the Data Read Out Gate, Address Read Out Gate, Command/Address Word and clock signals are contained in the 135-6000 and 135-6001  $\mu$ sticks. The address decoding and selection is performed in the 135-6015  $\mu$ stick. Accumulator  $\mu$ sticks, 135-6016 and 135-6017, are contained in two plug-in Accumulator Modules. The Status Register is in 135-6008  $\mu$ stick.

#### 2.1.1.15 Command and Status Words

A 16 bit Command Word is serially shifted into the Experiment from the OBC, on the Command Address Word input by gated 524 kHz clock pulses. This occurs when the Command Read In Gate is present. The Command Word logic consists of two registers; an input shift register, into which the Command Word is shifted, and a storage register into which it is jam transferred after shifting is complete. Each bit represents a specific command as given in Table 2-4.

Table 2-4  
Command Word Functions

Bit No.	Command Name	Function
1	WINSEL	Raises lower level for LAD Windows from 1.5keV to 3keV.
2	BAC PSD	Background Accumulator counts PSD rejects only.
3	ALT AD	Accumulator data transfer keyed on Alternate Addresses.
4	HV ON	Turns HVPS on. Has Priority over HV Command Pulses.
5	BAOS	All PHA pulses are counted in Bragg 1 Accumulators. No data counted in LAD Accumulators. Bragg 2 Accumulator function unchanged.
6	LAOS	All PHA pulses are counted in LAD Accumulators. No data counted in Bragg 1 Accumulators. Bragg 2 Accumulator function unchanged.
7	BRAGG INTER	Bragg 1 and 2 Accumulator functions interchanged.
8	L1 DIS	Disables LAD 1 Preamp.
9	L2 DIS	Disables LAD 2 Preamp.
10	B1 DIS	Disables Bragg 1 Preamp.
11	B2 DIS	Disables Bragg 2 Preamp.
12	ANTI-COINC OFF	Anti-Coincidence function does not affect PHA counts in Accumulators.
13	PSD OFF	PSD function does not affect PHA counts in Accumulators.
14	BRAGG CAL	Bragg Biased Amp gain reduced so that Bragg PHA range includes calibration source energy level.
15	PULSAR	Six LAD PHA Accumulators used for the time tagging six detected X-rays.
16	REDUCE HV	HVPS output reduced to 60% of nominal to protect Proportional Counters in high X-ray flux areas.

A start up reset circuit in the Command Word logic sets the Experiment in a nominal operating mode, consisting of all commands in the off condition, when power is turned on.

The Status Word, which is one of the output data words, monitors the operating status of the Experiment as set by the Command Word. Each bit of the Command Word has a corresponding monitor bit in the Status Word.

Command and Status Word logic is packaged in 135-6005 and 135-6006  $\mu$ sticks.

#### 2.1.1.16 Low Voltage Power Supply

The Low Voltage Power Supply (LVPS) receives its input from the +20 VDC spacecraft power.

It provides +6.75 volt and -6.75 volt operating bias to the analog circuits of the instrument as well as a low current +12 volt reference supply. The three voltages are monitored by analog house-keeping monitor outputs.

The output voltages are generated by rectifying the secondary voltages of a power inverter. Regulation is provided by a duty-cycle regulator in the primary which operates at the same frequency as the power inverter. A regulator amplifier compares the 12 volt reference voltage to an internal zener reference and generates a suitable control signal which is transformer coupled to the series switch.

Current limiting is provided by sensing the current through the output rectifiers and generating a voltage which overrides the control signal from the 12 volt supply if the maximum current for any output is exceeded.

All digital logic circuitry is powered directly from the +5 VDC input from a spacecraft power. The +20 VDC and +5 VDC inputs are under direct control of the PCU and command the experiment on or off.

#### 2.1.1.17 High Voltage Power Supply

The High Voltage Power Supply (HVPS) provides the regulated high voltage of approximately 2300 volts for the proportional counter

anodes. Its input is a 20V DC switched voltage supplied via the High Voltage Power Supply Control Circuit from the +20 VDC spacecraft power. The HVPS can, on command, reduce its output voltage to approximately 60% of the nominal value. This is provided to protect the instrument when passing through regions of intense radiation.

The HV Reduce Command is obtained from the Command Word supplied by the OBC.

High voltage is generated by a voltage-multiplier network from a transformer-coupled oscillator. The high voltage is sensed by a high-resistance divider and compared to a precision Zener reference. The error signal is amplified and chopped, and transformer coupled to an input series regulator.

Additional resistance is introduced in the reference comparator to reduce the output voltage in response to the HV Reduce Command.

#### 2.1.1.18 HVPS Control

The HVPS Control Circuit is a transistor switch and associated logic that provides 20V DC for the HVPS input. The HVPS must be commanded on after the low voltage is applied and will automatically turn off if the low voltage is interrupted.

Redundant HV On and HV Off pulse commands are obtained from the TCU.

In the event that the TCU cannot turn it on due to a malfunction, it may be turned on by the HV On command in the Command Word from the OBC. However, it then can be turned off only by the TCU command or by turning off input power to the experiment.

The HVPS input current is monitored by the housekeeping monitor. The high voltage is not directly monitored to minimize the risk of system failure.

EMI filtering is built into both the LVPS and HVPS. In addition, a separate EMI filter is provided for the spacecraft power to control the rise time of any transients on the +20 VDC and +5 VDC input lines.

#### 2.1.1.19 Input Filter

The input filter attenuates interference on the spacecraft power line and prevents it from entering the instrument. It also prevents interference generated within the instrument from getting onto the spacecraft power lines and reduces turn-on surge currents drawn from the 5 volt bus. It further provides the instrument from damage in case of accidental polarity reversal of the power buses.

Interference filtering is accomplished by means of LC filters. Polarity protection for the 20 volt bias is accomplished by means of a redundant series diode. Polarity protection and surge current limiting for the 5-volt bus is provided by a redundant switching transistor. A large capacitor from base to emitter of this transistor limits the current provided by the transistor during turn-on. This capacitor is installed so that it is slightly back-biased during normal operation in order to prevent it from being damaged if the supply voltage polarity is reversed.

#### 2.1.1.20 Analog Monitors

A set of supply voltage monitors are provided as diagnostics. Monitors for the +6.75 volts, -6.75 volts, and +12.00 volt power supplies are buffered to provide voltages within the spacecraft telemetry range and are clamped to the spacecraft 5 volt bus by diodes to prevent exceeding the input voltage limits of the telemetry converters. The spacecraft 5 volt and 20 volt buses are monitored through the ground support equipment interface. These

outputs are decoupled with 10K resistors to prevent damage from accidental short circuits.

### 2.1.2 Electronic Packaging

The packaging concept relies heavily on welded circuit construction. Analog circuitry is packaged in miniature welded cordwood modules. Digital circuits are packaged in welded Microsticks<sup>TM</sup>.

#### 2.1.2.1 Preamplifiers

Preamplifiers are packaged in an assembly that mounts directly to the Large Area Detectors. This takes full advantage of the shielding provided by the body of the proportional counter and minimizes the input cable length. The preamplifiers are molded welded cordwood modules with threaded inserts resulting in simplified installation.

#### 2.1.2.2 Upright Modules

Except for the power line filter, the power supplies and the preamplifiers, all analog circuits are packaged in two molded welded circuit modules, each consisting of a number of welded cordwood assemblies interconnected by a welded matrix. Each of these "Upright Modules" (so designated because of their orientation in the instrument) is provided with a Mini-Wasp<sup>TM</sup> connector through which it interfaces with the instrument. The module which contains the sensitive Pulse Shape Discriminator circuits also is shielded by an outer laminated Mylar-backed copper foil.

#### 2.1.2.3 Accumulator Banks

The accumulators and the associated output gating are packaged in two miniature "drawers" which plug into the instrument main frame. Electrical connections are provided by an in-line Mini-

Wasp<sup>TM</sup> connector. The drawers are mechanically secured by guide pins and captive screws.

Each drawer is assembled from a number of Microsticks<sup>TM</sup> and a suitable printed wiring motherboard.

#### 2.1.2.4 Logic Assembly

The remainder of the instrument logic circuits are packaged in Microsticks<sup>TM</sup> which are installed on a printed wiring motherboard. Terminals on this motherboard are wired directly to other parts of the instrument.

#### 2.1.2.5 Power Supplies

Power supplies are subcontracted modular units. Construction is along conventional lines using printed wiring techniques. Power dissipating components are secured to the module frame with suitable hardware. High voltage is fully contained in totally encapsulated modules with an electroplated grounded external shield proprietary to the vendor. High voltage terminations are made in a well which is potted with an approved silicon rubber. Low voltage interface connections are made with Mini-Wasp<sup>TM</sup> connectors.

#### 2.1.2.6 Power Line Filter

The power line filter is packaged on a circuit board which is installed in a shielding enclosure near the input connector.

### 2.1.3 Ground Support Equipment

#### 2.1.3.1 General Description

The Experiment Checkout Equipment (ECE) is a portable set of test equipment consisting of a HEX Set, which is a rack mounted unit, an Input-Output Unit (IOU), general purpose test equipment, and

radioactive sources. The IOU interfaces directly with the Experiment, the HEX Set, and may be interfaced with the Spacecraft. Photos of the rack mounted unit and IOU are shown in Figures 2-8 and 2-9.

The HEX Set monitors the Experiment operation and may provide power and control signals to the Experiment.

The IOU senses the Experiment's input and output signals, buffers them, and sends them to the HEX Set. It also provides switching so the Experiment may obtain its power and control signals either from the HEX Set or the spacecraft.

The ECE has two basic modes of operation. In the ECE Control Mode, it supports the operation and test of the instrument without the requirement of support from any of the other spacecraft subsystems. In this mode, it simulates the functions of the Power Control Unit, Onboard Computer, Telecommand Unit and Telemetry Unit. Primary power, commands, clock signals and timing gates are provided by the ECE.

In the OBC Control Mode, the experiment is interfaced with and operates under the control of the other spacecraft subsystems. The ECE synchronizes its data acquisition with the spacecraft subsystems and monitors experiment operation directly without interfering with the spacecraft system operation. Figure 2-10 is a block diagram of the ECE.

#### 2.1.3.2 Experiment Controls

The HEX Set provides clock signals, data control signals, and power to the Experiment as follows.

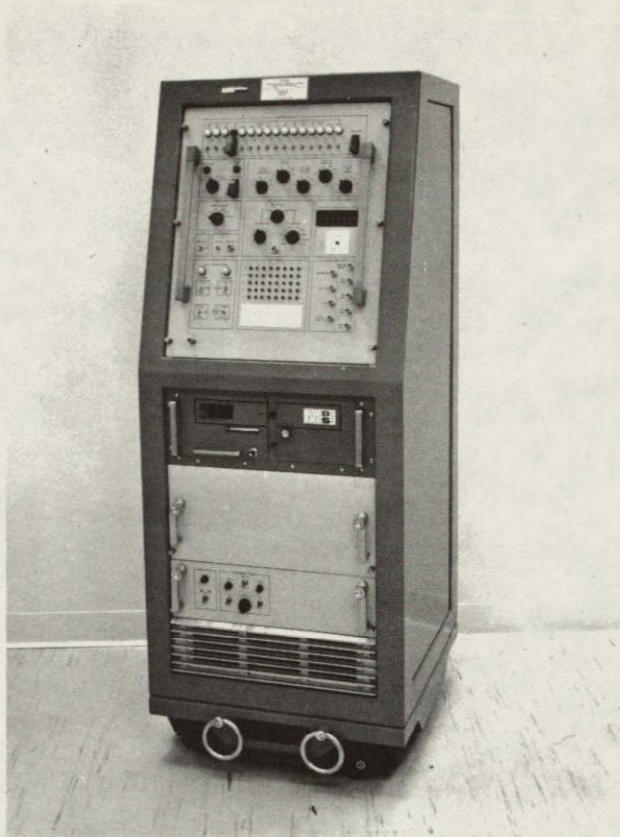


Figure 2-8  
Rack Mounted Unit  
ANS HXX Experiment  
Experiment Checkout  
Equipment (ECE)

ES-042



ES-028

Figure 2-9 Input/Output (IOU)  
ANS HXX Experiment  
Experiment Checkout Equipment (ECE)

ORIGINAL PAGE IS  
OF POOR QUALITY

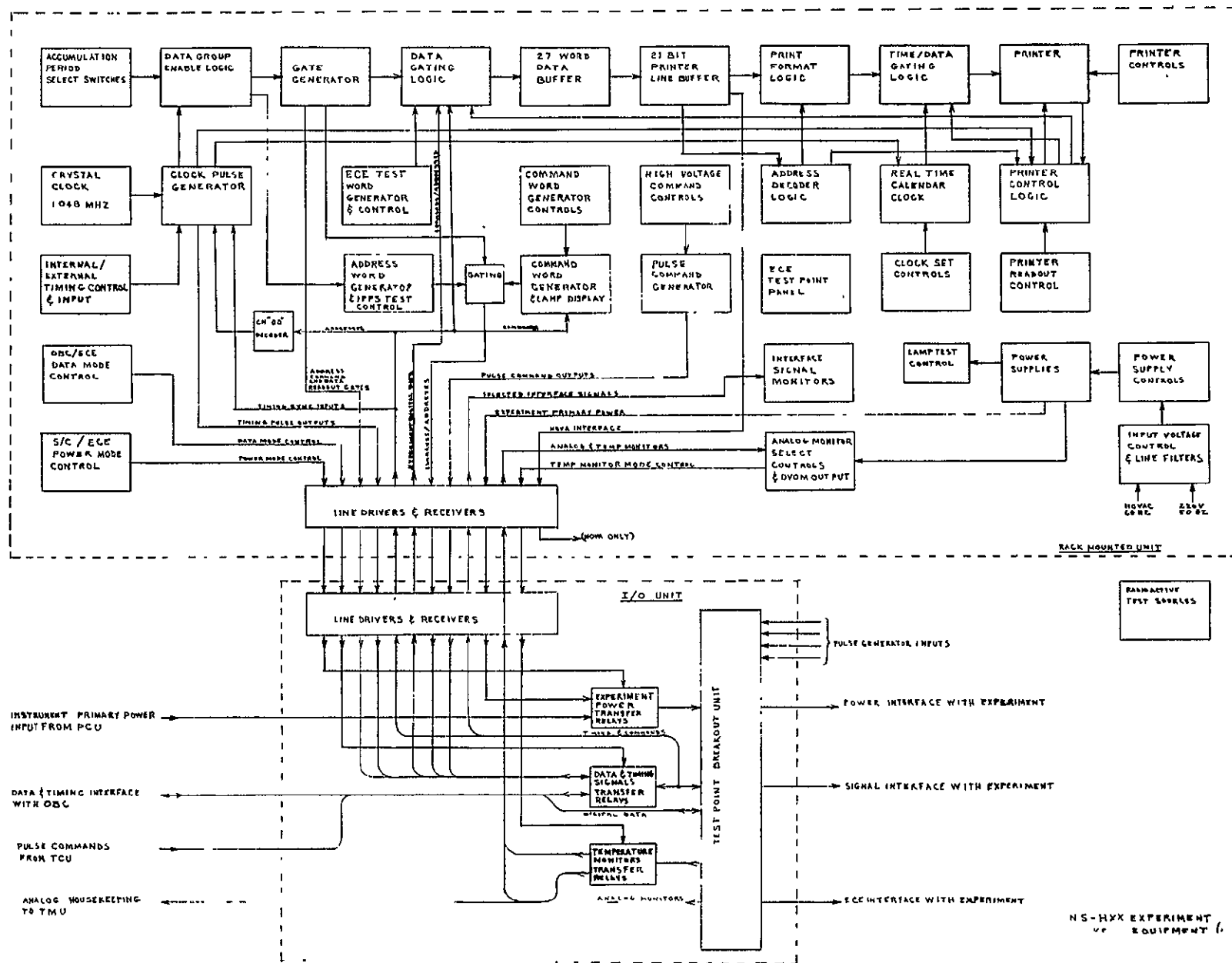


Figure 2-10 ANS HXX Experiment Checkout Equipment

#### 2.1.3.2.1 Timing

The Experiment requires spacecraft clock signals of 524,288 Hz, 1024 Hz, and 1 Hz. These signals must be aligned in phase. They are obtained from the Clock Pulse Generator which consists of a Crystal Clock operating at 1.048 MHz and a synchronous counter.

This Clock Pulse Generator provides simulated spacecraft clocks and readout gates when the experiment is operated in the ECE Control Mode. It also provides the timing for all ECE circuitry, and is synchronized to the CH "00" Address Decoder to assure proper phasing of data acquisition.

The Clock Pulse Generator may be synchronized to any one of three different clock sources. In the ECE control mode, a front panel control, Internal/External Timing, permits the selection of either the internal Crystal Clock or an external clock as the master time reference. When the Experiment is being controlled by the OBC, the Clock Pulse Generator is synchronized to the OBC timing by monitoring it in the IOU.

#### 2.1.3.2.2 Digital Data Output Control

The Experiment requires an Address input on the Command/Address input line which is gated by an Address Read In Gate and followed by a Data Read Out Gate. The first signal enables a data channel and the read out gate allows the data to be gated out serially by the 524,288 Hz clock. Digital output data from the Experiment is divided into five groups, as listed in Table 2-5.

All data channels from a given group are interrogated in a fixed sequence within one second, but each group may be read out at different periodic intervals equal to or greater than one second.

Table 2-5  
Data Read Out Groups

Group Number	Address Word	Data
1	0 1	Background Status
2	2 3 4 5 6 7 8 9 10	LAD PH 0 LAD PH 1 LAD PH 2 LAD PH 3 LAD PH 4 LAD PH 5 LAD PH 6 LAD PH 7 LAD PH 8
3	11 12 13 14 15 16	LAD PH 9 or Pulsar LAD PH 10   " LAD PH 11   " LAD PH 12   " LAD PH 13   " LAD PH 14   "
4	17 18 19 20 21 22 23 24	BD 1 PH 0 and PH 1 BD 1 PH 2 and PH 3 BD 1 PH 4 and PH 5 BD 1 PH 6 and PH 7 BD 2 PH 0 and PH 1 BD 2 PH 2 and PH 3 BD 2 PH 4 and PH 5 BD 2 PH 6 and PH 7
5	25 26	LAD 1 Window LAD 2 Window

The sampling interval for each data group may be manually selected by the Accumulation Period Select Switches. One switch is available for each data group and the following sampling intervals are available: Off, 4, 16, 128, 256 or 512 seconds.

When the Address Word switch is in the 1 PPS test position, each group is read out once a second. As a convenience in testing, a read out of all experiment digital data channels may be initiated by depressing the Enter/Reset Cycle switch located on the Real Time Calendar Clock to the Reset Cycle position. A complete data read out will then occur within four seconds and the read out cycle timing will be reset to zero. In the OBC control mode, these switches are non-functional. Timing is under OBC control.

The Gate Generator produces data transfer gates from the Clock Pulse Generator timing. The period of the 8 kHz clock signal is divided into four intervals. The first 31.25  $\mu$ sec interval is Address RIG or Command RIG time. No operations occur during the second interval. The third interval is Data ROG time. An Address register is incremented after each Address RIG time and reset by the 1 Hz clock signal. If the Group Enable signal is present, as selected by the Period Selection Switches and the data output timing, the Address and Address RIG are gated to the Experiment followed by the Data ROG.

#### 2.1.3.2.3 Command Word and Monitor

The 16 bit command word as given in Table 2-4 may be sent to the Experiment by setting the Command Word switches on the HEX Set front panel and operating the Send Command Switch. Command transmission time occurs once a second after the Address Register has sequenced through the 27 Addresses. If the Send Command Switch has been operated, a Command Read In Gate in synchronism

with the Command Word on the Command/Address line will be sent to the Experiment.

The Command Word is sensed in the IOU and sent to the HEX Set where it is shifted into a register and displayed by the Command Word display lamps. This occurs if the Command Word originated in the HEX-Set, when the Experiment is under ECE control, or if the Command Word originated in the OBC, when the Experiment is under Spacecraft control.

#### 2.1.3.2.4 HV Commands

The two HV On and two HV Off pulse commands may be sent from the HEX-Set by setting the HV Command Selector Switch to the desired command and operating the Send Command switch. The HV Command Monitor lamp shall light when a HV On command is sent and go off when a HV Off command is sent. The HV Monitor lamp is controlled by a feedback signal from the Experiment and lights when the Experiment logic has sensed a HV on signal.

#### 2.1.3.2.5 Power Controls

HEX-Set power controls consist of a 220V, 50 Hz/110V, 60 Hz switch on the back panel and a Main Power On/Off switch on the front power panel. The first switch permits use of the ECE in either Europe or the United States and must be set properly before turning power on.

The switch accommodates the difference in voltage by changing taps on an input autotransformer. Primary power line filters are provided to minimize the effect of electromagnetic interference with other equipment. Two primary power connecting cables are provided: One fitted with a U.S. line plug and the other fitted with a European line plug.

The Main Power switch turns power on to all of the HEX Set but not the Experiment. Experiment power is controlled by a Power On/Power Off switch, which applies power to the Experiment, a Lo/Norm/Hi switch, which selects the voltage level as 3% low, nominal, or 3% high, and two resettable circuit breakers. The circuit breakers should not be switched off. Separate power supplies are provided for ECE equipment and for the experiment. The power supplies are regulated and have short-circuit protection.

#### 2.1.3.2.6 Spacecraft/ECE Power Control

The power input to the Experiment may originate either from the HEX-Set or from the Spacecraft PCU as selected by the S/C Power Mode switch. When the switch is in the S/C position, a transfer relay in the IOU connects the Experiment power input lines to the IOU S/C power connector. In the ECE position, the input lines are connected to the HEX-Set.

#### 2.1.3.2.7 Spacecraft/ECE Signal Control

The commands, read out gates, and timing to the Experiment may originate either from the HEX-Set or from the Spacecraft as selected by the OBC Control switch. When the switch is in the OBC position, a transfer relay in the IOU connects the Experiment signal inputs to the IOU S/C signal connector. In the ECE position, the input lines are connected to the HEX-Set. However, in either mode the ECE is able to monitor experiment data outputs without interfering with system operation. Synchronizing signals are monitored at the interface to permit data acquisition from the experiment by the ECE in synchronism with the control and timing signals.

### 2.1.3.3 Experiment Monitors

#### 2.1.3.3.1 Line Printer

The Experiment digital data output is recorded in the HEX-Set on a high speed printer. The printer is a Mohawk Data Sciences Corp. type 2016 drum type digital printer. It has 10 print columns and accepts binary encoded input data. The full printer format is shown in Table 2-6. The data is that produced for the ECE test mode.

Printer controls include a paper Advance Switch, Print Test Switch and Operate/Inhibit Switch. The printer logic requires commands to control printing and data advance, and data to be printed. A Print Pulse and an External Paper Feed signal are generated in the HEX Set logic. The Lockout signal from the Printer indicates when it is busy. Data input consists of ten 3-bit binary or 4 bit BCD inputs.

The Address of the data to be printed is decoded and sensed so that for Bragg channels the data will be treated as two 8-bit binary data words rather than on 16 bit binary data word.

The Printer Readout Period selector switch on the HEX Set front panel provides for selection of a readout interval of 4, 16, 128, 256, or 512 seconds or printer operation may be inhibited by setting the switch at Simulate. If the Printer readout time is less than the Data readout time, only the Clock time will be printed out when no data is available. If the Printer readout time is greater than Data readout time (including 1 PPS Test mode), data will be lost by being read out of the Experiment but not printed.

ECE Test Standard Printout

32	125252	LAD 2 Window Data (Octal)
31	125252	LAD 1 Window Data (Octal)
30	252 252	BD2 PH7 BD2 PH6 Data (Octal)
27	252 252	BD2 PH5 BD2 PH4 Data (Octal)
26	252 252	BD2 PH3 BD2 PH2 Data (Octal)
25	252 252	BD2 PH1 BD2 PH0 Data (Octal)
24	252 252	BD1 PH7 BD1 PH6 Data (Octal)
23	252 252	BD1 PH5 BD1 PH4 Data (Octal)
22	252 252	BD1 PH3 BD1 PH2 Data (Octal)
21	252 252	BD1 PH1 BD1 PH0 Data (Octal)
20	125252	LAD PH14/PUL6 Data (Octal)
17	125252	LAD PH13/PUL5 Data (Octal)
16	125252	LAD PH12/PUL4 Data (Octal)
15	125252	LAD PH11/PUL3 Data (Octal)
14	125252	LAD PH10/PUL2 Data (Octal)
13	125252	LAD PH9/PUL1 Data (Octal)
12	125252	LAD PH8 Data (Octal)
11	125252	LAD PH7 Data (Octal)
10	125252	LAD PH6 Data (Octal)
07	125252	LAD PH5 Data (Octal)
06	125252	LAD PH4 Data (Octal)
05	125252	LAD PH3 Data (Octal)
04	125252	LAD PH2 Data (Octal)
03	125252	LAD PH1 Data (Octal)
02	125252	LAD PH0 Data (Octal)
01	125252	Background Data (Octal)
00	125252	Status Data (Octal)
078	090641	Date Time Code (Decimal)

Table 2-6

HEX-Set Printer Format

#### 2.1.3.3.2 Digital Data Output Processing

The Experiment digital data, as it is gated out by the Data Read Out Gate, is shifted into a serial shift register in the HEX-Set. The 27 Word Data Buffer serial shift register accepts input data alternately from the Address Word Generator and the Experiment data output so that in a one second period the addresses and associated data from all 27 experiment data channels may be stored. The data is read out to the printer during the following 3 second period through Printer Line Buffer which is the last stage of the 27 Word Data Buffer. Preceding digital data readout, the Real Time Calendar Clock data is printed. All information is printed in octal except the Clock data which is printed in decimal.

#### 2.1.3.3.3 ECE Test

An ECE Test Word Generator provides an internal test capability for the ECE. The test generator, under front panel control, permits the loading of each of the registers in the 27 Word Data Buffer with a fixed predetermined binary number which is then printed out as if the data had originated in the experiment. The ECE Test printer output is as given in Table 2-6.

#### 2.1.3.3.4 Real Time Calendar Clock

The Real Time Calendar Clock provides a BCD encoded data to the Printer. The data consists of the calendar day (3 digits), hour (2 digits), minute (2 digits) and second (2 digits). The clock is initially set from a group of Digiswitches on the control panel. The day, hour and minute are entered manually and when the Enter/Reset Cycle switch is set to the Enter position, the data is loaded into the Calendar Clock Counter. Seconds are reset to zero. The clock runs continuously as long as the ECE power is left on.

#### 2.1.3.3.5 Analog Monitors

Monitoring of the Analog Housekeeping outputs of the experiment is provided by three switch controls located on the ECE control panel. The switches transfer individual monitor lines to a connector on the control panel, electrically isolated from chassis, for monitoring by means of a standard Digital Voltohmmeter. Voltages and currents are represented as voltages, and temperatures are represented as resistances at the connector.

The Experiment analog telemetry signals monitored are +12V, +6.75V, -6.75V, PHA, Bias and HVPS 1. In addition, the Experiment +20V and +5V are monitored via the Experiment ECE connector. Signals from the HEX-Set monitored are the +5V and -12V used in the ECE and the +20VI and +5VI which are the current levels supplied to the Experiment from the Experiment Power Supplies in the ECE. Four Experiment temperature monitors may be measured. When this is being done, a transfer relay in the IOU isolates the monitors from the IOU spacecraft connector to prevent interferences from the TMU, when operating in the Spacecraft controlled mode.

#### 2.1.3.3.6 Experiment Signal Monitors

A group of BNC Signal Monitors is located on the control panel of the HEX-Set for monitoring critical timing signals as sensed in the IOU. Monitored signals are 524, 288 Hz, 1024 Hz, 1 Hz, Ch 00 Sync, Command/Address Word, Command Read Out Gate, Address Read Out Gate, Data Read Out Gate, and Data Out.

#### 2.1.3.3.7 ECE Test Point Panel

A test point panel is provided on the HEX-Set control panel to permit monitoring of critical signals within the ECE and to aid in fault isolation and ECE testing.

#### 2.1.3.4 Input/Output Unit

##### 2.1.3.4.1 Line Drivers and Receivers

The IOU and HEX-Set are interconnected by means of cables, 18 meters in length, to permit remote monitoring of the Experiment operation with the least amount of physical interference between ECE and the spacecraft units. Both the IOU and HEX-Set are provided with line drivers and line receivers for interface signals between the two units. This permits the spacecraft subsystems, the experiment and the IOU to be located in a controlled environment room while the HEX Set is operated and controlled from the adjacent test equipment room.

##### 2.1.3.4.2 Experiment Interface

All connections from the two Experiment connectors are brought to the Test Point Breakout Unit. This unit contains a group of printed circuit cards provided with test points and jumper plugs which may be used to monitor or open any one or more of the interface connections to the experiment.

##### 2.1.3.4.3 Spacecraft Interface

Connectors are provided on the IOU that are identical to the Experiment connectors so the Spacecraft harness plugs may be connected to the IOU. Thus, the IOU may be inserted directly between the Spacecraft and the Experiment. Each wire is connected from Spacecraft connector through transfer relays and test point breakout cards to the Experiment connector. Experiment timing and control signals are monitored by signal buffers which feed the HEX-Set. When the relays are de-energized, the Spacecraft controls the Experiment. When energized, the HEX-Set controls the Experiment.

#### 2.1.3.4.4 Test Signal Injection Interface

The experiment has provisions in its ECE connector for the injection of electronic test signals into the detector preamplifiers. The IOU provides four inputs for connecting these injection points to pulse generators. Isolation resistors are provided in these lines (internal to the experiment) as a safety precaution. Outputs from the pulse generators may be used to inject test signals directly into the Experiment.

## 2.2 Mechanical Engineering Description

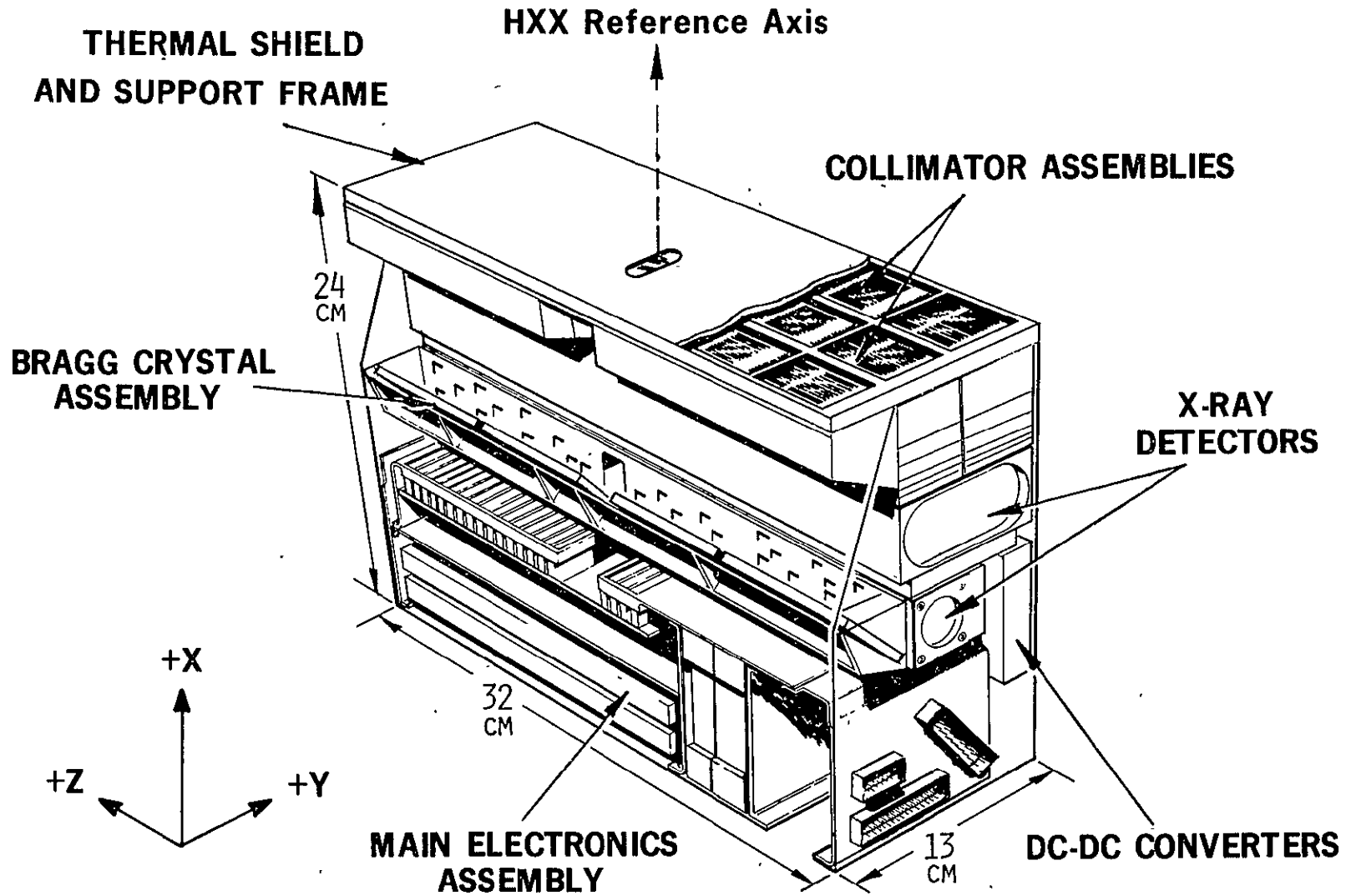
The HXX Instrument consists of two X-ray detector systems with their associated analog and digital processing electronics contained in a wrap-around sheet metal structure. A photograph of the instrument with the thermal shield removed was shown in Figure 2-1. Figure 2-11 is a pictorial view of the instrument with the major components identified.

Each X-ray detector system consists of a device to define the X-ray field of view and an X-ray detector. For the Large Area Detector (LAD), the field of view is defined by two high angular resolution (10 arc-min x 3 degrees FWHM) collimators and a two chamber, sealed, gas filled proportional counter is used for the detector. Each of the chambers of the counter is associated with one-half of the collimator and the collimator halves are offset pointed to permit X-ray pointing of the satellite.

The Bragg detector field of view is defined by a coarse collimator (3 degrees x 3 degrees FWHM) and a Bragg crystal assembly which further defines the angular field of view and the energy range coupled again with a two-chambered, sealed, gas-filled proportional counter. Figures 2-12 and 2-13 show the general configuration of the collimator and detector assemblies.

The analog and digital processing electronics (with the exception of the preamplifiers) are packaged together below the X-ray detector systems. This concept provides a separable assembly as shown in Figure 2-14 which allows assembly and test operations to proceed in parallel with the X-ray detector systems as well as providing ease of repair during system level fault isolation and repair.

# ANS HARD X-RAY EXPERIMENT



2-45

ORIGINAL PAGE IS  
OF POOR QUALITY

Figure 2-11

ORIGINAL PAGE IS  
OF POOR QUALITY

2-46

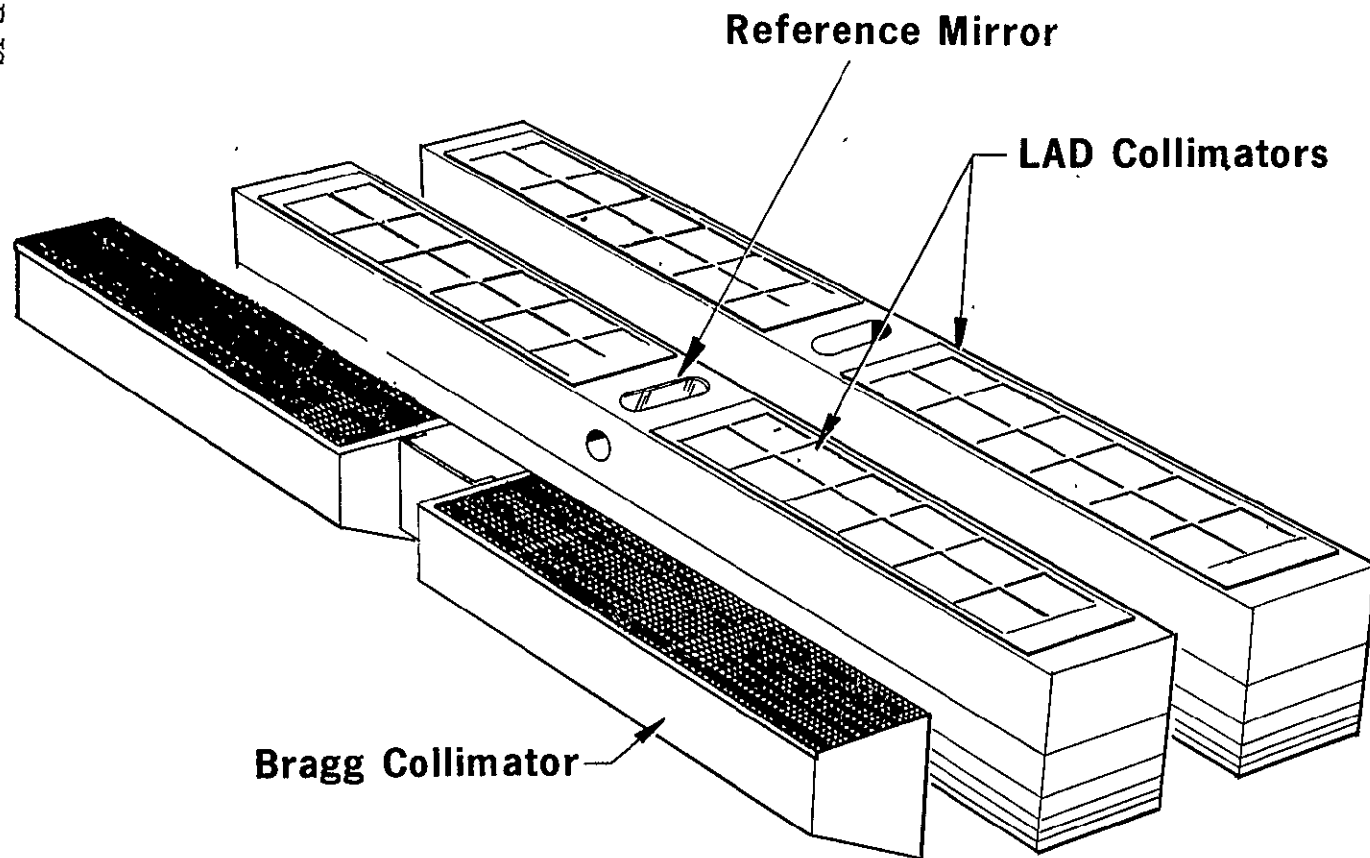


Figure 2-12. Collimator Assemblies

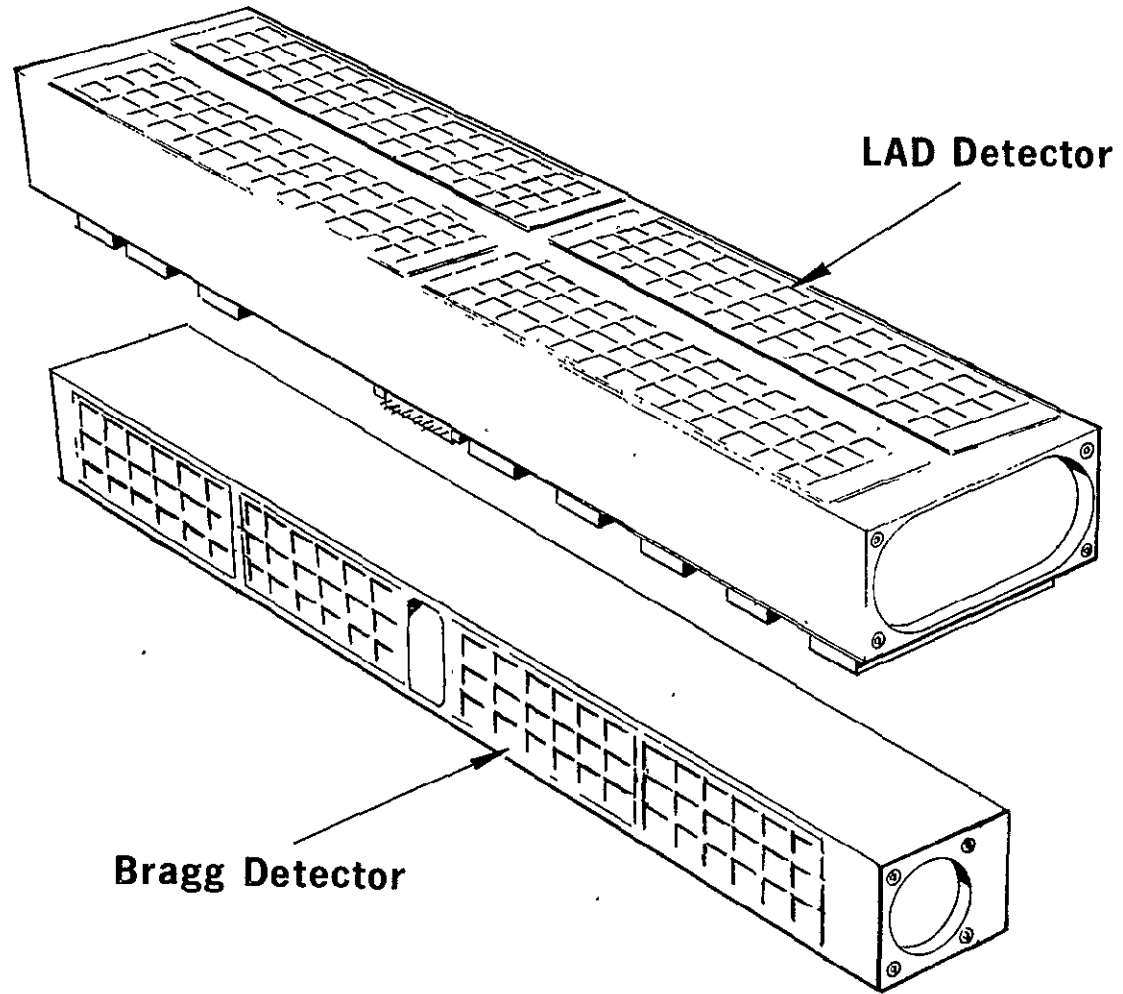


Figure 2-13. X-ray Detectors

ORIGINAL PAGE IS  
OF POOR QUALITY

2-48

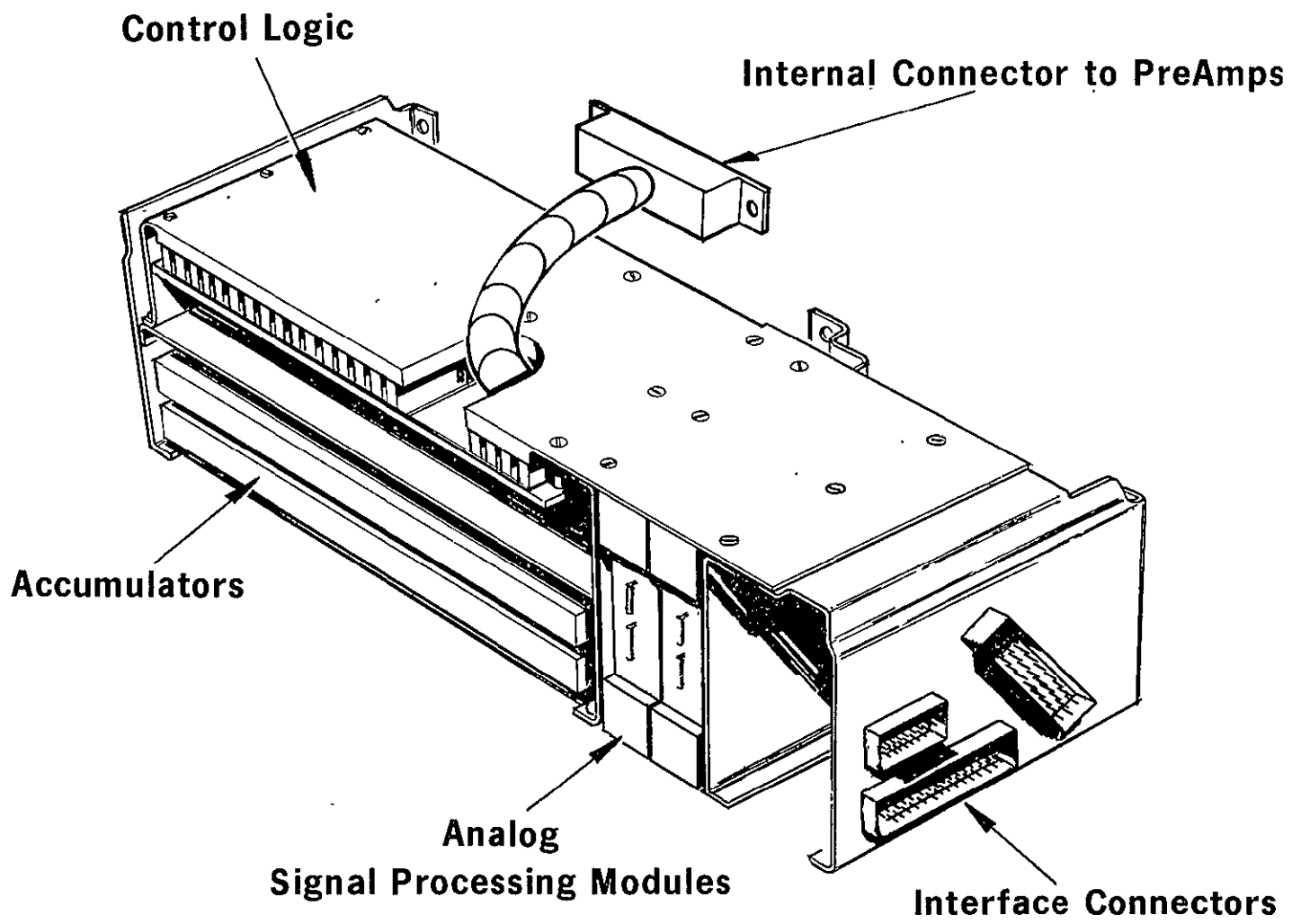


Figure 2-14. ANS - HXX Main Electronics Assembly

The entire upper surface of the HXX Instrument is covered with a 2 micron thick Kapton film upon which has been deposited a 660A layer of aluminum on the inside surface. This film acts as a thermal radiation shield to prevent excessive heat loss from the experiment.

The basic size of the HXX is 24cm x 32cm x 13cm and weighs approximately 8Kg (see Table 2-7). The principal mechanical design features are as follows:

- (1) The HXX Instrument has a high package density (specific gravity of  $\sim .8$ ).
- (2) The instrument can survive the high vibration levels which occur during ascent and maintain internal alignment without significant structural weight by designing the components to be self-supporting.
- (3) The instrument can operate in a thermal vacuum environment over a temperature range of  $-15^{\circ}$  to  $+50^{\circ}\text{C}$ , and a pressure range of 1 atmosphere to perfect vacuum including operation in the corona region.
- (4) The Bragg Crystal Assembly is maintained in a nearly iso-thermal condition by designing for minimum heat loss to space and maximum conduction within the instrument and maximum coupling with the spacecraft.

Table 2-7  
ANS Hard X-Ray Experiment  
Weight Breakdown<sup>1</sup>

	<u>Original Estimate</u>	<u>P/F Unit Refurb.</u>	<u>FLT Unit Refurb.</u>
Main Structure	1039	953	953
LAD Collimator Assembly	2109	1715	1715
Bragg Crystal Assembly	299	308	308
Bragg Collimator Assembly	150 <sup>3</sup>	286	286
LAD & Bragg Detector Assembly (includes HVPS and Preamp Plate Assembly)	1340	1679 <sup>2</sup>	2036 <sup>2</sup>
Electronics Assembly	2151 <sup>4</sup>	2309	2309
Low Voltage Power Supply	226	223	223
Thermal Shield	68	73	73
Screws, Bushings, Shims, Retainers, Spacers, and Dowel Pins	100	221	221
TOTAL	7482	7767	8124

- (1) All weights are in grams.
- (2) The P/F Unit contained a Beryllium LAD and the FLT Unit an Aluminum LAD.
- (3) The original estimate assumed Aluminum tubes instead of the Copper ones actually used.
- (4) The original estimate did not reflect the extensive use of Co-Axial Cable.

### 2.2.1 Mechanical Interface

The mechanical interface is relatively simple. The HXX is mounted to the honeycomb structure of the spacecraft on four coplanar pads, one in approximately each corner of the instrument. It is held on by a #10 bolt through each pad into the spacecraft structure. The four holes in the pads were drilled with a template provided by Fokker to eliminate any possibility of mismatch at integration. Since the fourth pad over constrains the mounting and because the honeycomb structure was not machined in the pad mounting areas, a procedure was developed for shimming one corner of the HXX to correct for non-coplanarity. In practice, however, no shims were required, the measured gap being less than .001 inches.

The alignment of the HXX to other on-board instruments is also straight forward. The alignment with respect to the star sensor is not critical (approximately centered in the star sensor field of view is sufficient) however, the stability of that alignment once measured is critical. The alignment tolerance between the HXX and the Soft X-ray Experiment (SXX) of 3 arc-min around the Y and Z axes is met by an adjustment of the SXX. The HXX/SXX alignment tolerance around the X axis of 40 arc-min would be met by shimming two HXX mounting pads, however, in practice, this was not required since the "as assembled" alignment was within tolerance.

Since the HXX X-ray axes are difficult to work with (requiring X-ray sources or generators, etc.), a reference mirror for detecting the Y and Z axis rotation and a scribe line for detecting X axis rotation was included. The X-ray axes offsets with respect to these optical references were measured at MIT during the Bragg to LAD alignment testing and were provided to the Dutch for use during integration so that all alignment could be performed optically.

The installation of the thermal shield was completed after installation of the HXX on the spacecraft because the shield obscures one of the four mounting bolts. It was originally intended that the thermal shield be installed with the Satellite aperture plate or top panel removed to provide complete access to the top of the HXX. Subsequently, it was learned that the top panel was not to be removed for HXX installation, so special protective covers were designed to protect the thermal shield during installation from the side via a torturous route and yet be removable through the aperture in the top panel after installation.

#### 2.2.2 Structural Considerations

The primary factors influencing the structural design concept were as follows:

- ... High sinusoidal vibration inputs
- ... Stringent alignment stability between X-ray optical system components
- ... Minimum weight
- ... Maximum thermal conductivity
- ... Access to instrument components for fault isolation and repair

The sinusoidal vibration levels were those for typical scout payloads. All other dynamic loads, random vibration and steady state acceleration were relatively benign. Because of the extreme position of the HXX on the satellite with respect to the EH section attachment flange, the HXX receives the largest inputs of any package on the spacecraft. The qualification level vibration inputs to the HXX are given in Table 2-8.

The principal internal alignment requirement was between the Bragg Crystal Assembly and the LAD Collimator as this determines

Table 2-8  
ANS-HXX  
Qualification Vibration Levels

1.0 Thrust Axis (X-X) Sinusoidal Sweep

<u>Freq. (Hz)</u>	<u>Level<sub>1</sub>(g's)</u>
5-50	12 inches/sec
50-100	$\pm 10.5$
100-200	$\pm 21$
200-2000	$\pm 1.5$

Sweep Rate: 2 octaves/minute

2.0 Lateral Axes (Y-Y & Z-Z) Sinusoidal Sweep

<u>Freq. (Hz)</u>	<u>Level (g's)</u>
5-10	5.0 inches/sec
10-20	0.8 inches peak to peak
20-30	$\pm 16$
30-50	$\pm 10$
50-80	$\pm 3$
80-200	$\pm 5$
200-2000	$\pm 1.5$

Sweep Rate: 2 octaves/minute

3.0 Random Vibration - All Axes

<u>Freq. (Hz)</u>	<u>PSD Level (<math>g^2/Hz</math>)</u>
200-500	+ 5 db/octave
500-2000	0.045

Overall Level: 8.7 grams

Duration: 4 minutes/axis

the viewing direction for each part of the instrument. Alignment stability of the order of 0.5 arc-minutes was required. The Bragg Collimator alignment is less critical due to its course. Shifts on the order of several arc-minutes when compared to the 3 degree FWHM field of view produce negligible changes in total Bragg system transmission and no change in viewing direction.

The primary external alignment requirement was that the LAD Collimator/Bragg Crystal System remain fixed with respect to the four mounting pads so that the alignment with respect to the SXX at the spacecraft level is not changed as a result of dynamic loads. Although no tolerance for such shifts was ever developed with the Dutch, test results from both the structural model spacecraft and the Flight model spacecraft show the shifts to be less than 1 arc-minute.

The requirements for minimum weight and accessibility are self-explanatory and the requirement for minimum thermal conductivity will be discussed in a later section of this report.

The high vibration levels were met by designing the collimators, proportional counters and Bragg Crystal plate, (which are all inherently beam elements), to have a first resonance above the frequency of the peak input. In the case of the beryllium proportional counters, this was trivial because of the hollow tube construction and the high specific stiffness of beryllium resulted in a natural frequency of approximately 2000 Hertz. The Bragg Crystal plate, however, was more difficult and required ribbing on the back of the plate to achieve a first resonance of approximately 250 Hertz.

Since the most severe vibration axis, the thrust axis, X-X, and one of the lateral axes, Y-Y, are both perpendicular to the length

of the beams, the only remaining problem was to prevent a "rocking" of the HXX in the Z-Z axis which is parallel to the length of the beams. This was accomplished by providing in effect three stiffening beams, one each at the top, middle and bottom of the instrument. The top deck was affected by providing shear ties between the LAD Collimator and the back wall of the wrap-around structure. The middle deck was provided by the top cover of the removable electronics assembly and the bottom deck by the wrap-around structure itself.

The alignment requirements were met by fastening the ends of the LAD Collimator and Bragg Crystal Plate to the same piece of metal using light press fit dowel pins. Without any intervening screwed connections to shift, the only way internal misalignment could occur, would be by distortion of the metal in the area of the pins, which was prevented by providing adequate bearing area, or by permanent distortion of the LAD Collimator or Bragg Crystal plate.

The latter was prevented by the stiff design of the collimator and crystal plate resulting in stress levels well below the yield point. In addition, for external alignment stability, the four mounting pads were well gusseted and integrally attached to the structure by dip-brazing.

The requirements of minimum weight and maximum thermal conductivity were met by the use of .090 inches thick aluminum for the wrap-around structure. Accessibility was achieved by having the top and front sides of the structure open and by design of a removable electronics package with its own structure which becomes an integral part of the instrument structure when installed in the instrument.

It is interesting to note that because of the design approach

selected, the structure has no real rigidity by itself. Only when all the beam elements and the electronics package are installed does the entire package develop any rigidity. Because the metal ends of the electronics package must become an integral part of the wrap-around structure, screws were selected as the fasteners holding the electronics package. The screws had an unthreaded shank which when installed in close toleranced holes, achieved a joint as close as possible to a pinned connection while still maintaining a good accessibility.

### 2.2.3 Thermal Design Considerations

The principal features of the HXX Thermal design, illustrated in Figure 2-15, are:

- (1) An aluminum structure of high thermal conductance.
- (2) Close fastener spacing and high bolting pressure at bolt lines to ensure high interface thermal conductance.
- (3) Low power dissipation, widely distributed.
- (4) Low-emittance surfaces facing neighboring assemblies to minimize radiation heat gain.
- (5) High-emittance surface facing the satellite structure and high interface conductance at the four mounting pads.
- (6) A thermal radiation shield covering the viewing aperture.
- (7) A mounting plate of high thermal conductance supporting the temperature sensitive Bragg crystals.
- (8) Four thermistor temperature monitors.
- (9) An aluminized plastic collar covering the gap between the HXX and the satellite top panel around the HXX viewing aperture.

The lower power dissipation and high thermal conductance of the structure ensure that temperature gradients are not large enough

ORIGINAL PAGE IS  
OF POOR QUALITY

2-57

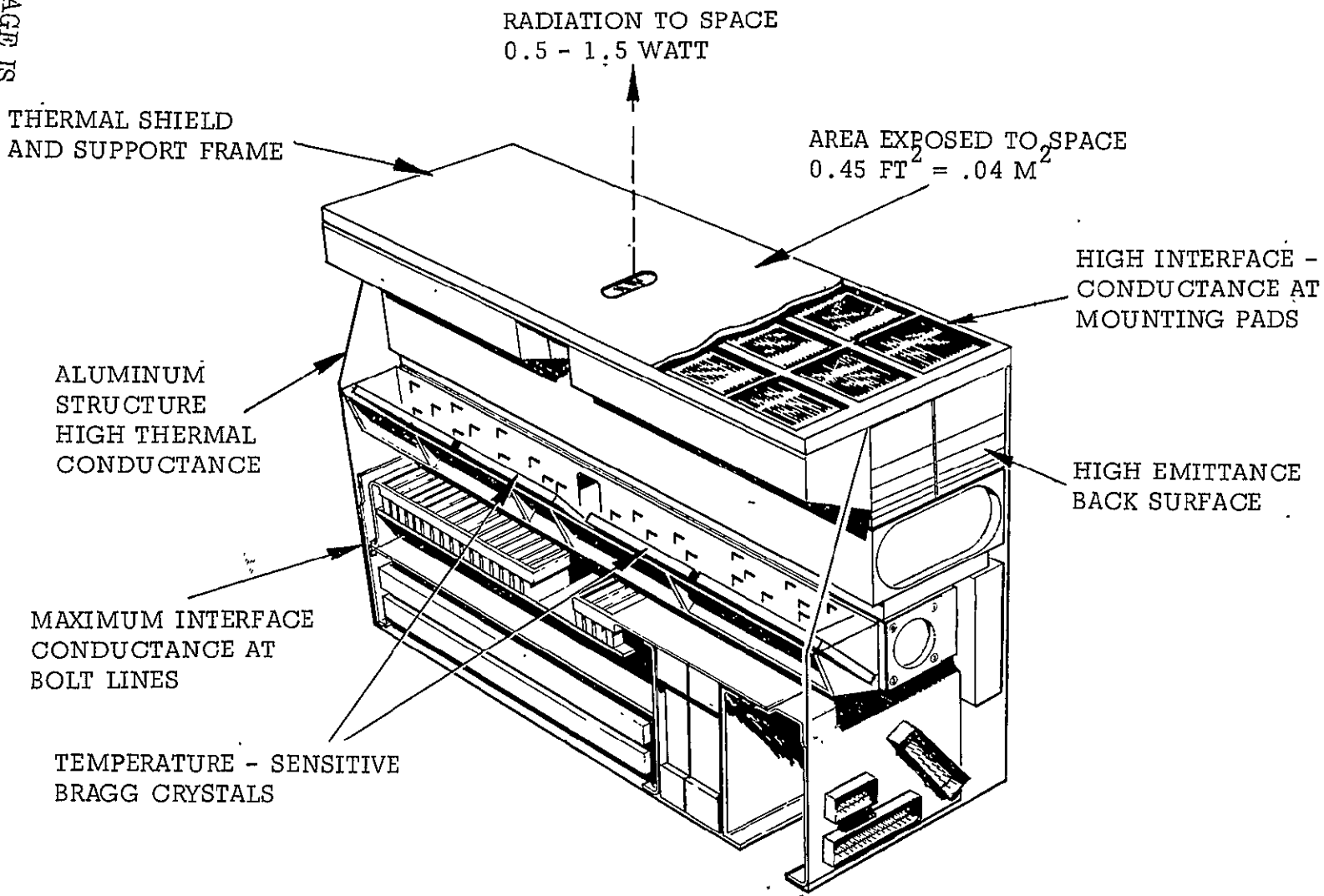


Figure 2-15. HXX Thermal Configuration

to cause alignment difficulties. Measurements during thermal-vacuum tests indicate all temperatures to be within 3°C of each other. The LAD collimator is the subassembly most sensitive to thermal gradients, a temperature difference of 20°C producing a 10% loss of resolution. The actual temperature distribution is more than an order of magnitude within this limit.

The viewing direction of the Bragg Crystal plate is sensitive to absolute temperature, and the crystals themselves to temperature gradients. The crystal mounting ensures that gradients are minimized, and all test data indicates the plate to be isothermal to within about 0.1°C. Two of the four instrument temperature sensors (RT 1 and RT 2) are mounted on the crystal support plate to provide redundant temperature indication for data reduction purposes. The Bragg Crystal plate and the LAD Collimator are aligned for coincident viewing of the satellite.

The two remaining temperature monitors are located as follows:

RT 3 is cemented to the structure in the -X, +Y, +Z, inside corner.

RT 4 is cemented to the structure adjacent to the +X, +Z mounting pad.

All temperature monitors are thermistors, type number RTH06BS472F.

Based on thermal-vacuum test calibration, temperature data may be correlated by the relationship,

$$R/R_0 = \exp \left[ B (1/T - 1/T_0) \right]$$

where R is the resistance at temperature T,  $R_0 = 5720$  ohms,  $T_0 = 293.8^\circ\text{K}$  and  $B = 3950^\circ\text{K}$ . The error in correlation is less than 0.4°K at 263°K and at 313°K, and less than 0.1°K at 293.8°K.

The thermal shield covering the viewing aperture is polyamide of thickness 2 - 2.5 microns, with a deposition of 660Å of aluminum

on the inner surface. The  $\alpha/\epsilon$  of the outer surface is approximately  $0.25/0.31 = 0.8$ . Total radiation loss from the aperture is approximately 2 watts at a nominal temperature of  $18^{\circ}\text{C}$ . Thermal radiation from the viewing aperture matches the internal HXX power dissipation very closely; therefore the HXX operating temperature will closely track the main satellite structural panel temperature because of the high mounting conductance.

The gap between the thermal shield and the satellite top panel around the HXX viewing aperture is covered by a Kapton collar cemented to the periphery of the thermal shield support frame. This collar is slit at intervals to permit bending during launch venting. The outside surface is aluminized to minimize thermal radiation from the gap during normal operation.

#### 2.2.4 Proportional Counters

The HXX Proportional Counters are similar in design to those used successfully in the SAS-A and Apollo Programs. They are thin-window, doubled chambered, epoxy sealed detectors with independent gas volumes and a single central anode wire in each chamber. The anode wires in spring tensioned to prevent wire sag or overstressing at temperature extremes. Figure 2-13 illustrates the general configuration of the detectors and Table 2-9 provides a summary of detector parameters.

The Bragg detector has a one-piece cathode with the two chambers situated end to end with provision on the back for encapsulation of the high voltage connection and the filter network. The windows are pieces of foil sandwiched between an inner and outer grid structure epoxy bonded onto the cathode. The cathode is beryllium to avoid a coefficient of thermal expansion mismatch with the window material which could overstress the thin windows or epoxy

Table 2-9  
Proportional Counter Parameters

	<u>Beryllium Cathode LAD Detector</u>	<u>Aluminum Cathode LAD Detector</u>	<u>Bragg Detector</u>
Window Material	Beryllium	Beryllium	Beryllium
Window Thickness, inches	.002	.002	.001
Anode Wire Material	Tungsten	Tungsten	Tungsten
Anode Wire Diameter, inches	.003	.001	.003
Gas Mixture	90% Argon 9.5% CO <sub>2</sub> 0.5% Helium	90% Xenon 9.5% CO <sub>2</sub> 0.5% Helium	90% Argon 9.5% CO <sub>2</sub> 0.5% Helium
Gas Pressure, atmos.	1.4	2	1.4
Window Size, inches	.322 x .420	.322 x .420	.565 x .576
No. of Windows per Gas Volume	96	96	96
Gas Volume Dimensions, inches	1.450 Deep 1.438 Wide 11.534 Long	1.350 Deep 1.438 Wide 11.534 Long	1.180 Deep 1.180 Wide 5.050 Long
No. of Gas Volumes	2	2	2
Inner Window Support Structure	Yes	No	Yes

joints as the temperature of the detector varies.

The LAD detector also has a one-piece cathode, but the two chambers are parallel to each other with a well on each end for high voltage connection and filter networks. The original design of the LAD detector called for a beryllium cathode and a sandwiched .001 inch thick window construction like the Bragg detector. It was to be filled, however, with 2.0 atmospheres of a Xenon gas mixture instead of the 1.4 atmosphere at the Argon mixture used in the Bragg.

Early in the program, it was discovered that due to the shallow depth into the Xenon gas where the photon interactions occur, the field distortions caused by the inner grid of the window sandwich resulted in poor detector performance. Therefore, the inner grid was eliminated. This could be accomplished because of process controls and equipment at the detector manufacturers which prevent any inward acting pressure differentials on the detector windows.

The three LAD detectors built to this design all suffered failures of undetermined cause (discussed elsewhere in this report), requiring replacement detectors. At this time, the temperature limits of the HXX were sufficiently defined and the resulting range small enough that the high cost and long delivery of the beryllium cathode detector could be surmounted by changing to an aluminum cathode.

The only design change required was to increase the thickness of the window faceplate to compensate for the reduced stiffness of aluminum. However, the window thickness was increased to .002 inches in the event that the failures were due to diffusion leaks through the windows. Also, process controls at the manufacturer's facility were further tightened to reduce possible internal contamination in the detectors in the event that was the source of the

failures. Three detectors of this design were purchased, one of which was ultimately successful and is now installed in the Flight Spare HXX.

At the time of purchase of the three aluminum cathode detectors, a decision was made to procure a beryllium cathode detector filled with an argon gas mixture because of the possibility that the failures were inherent in the use of Xenon. Because of the use of argon, an inner window grid was installed without affecting performance and while it should not have any predictable benefit, nevertheless, all previous successful detectors were built with an inner grid. The window was again changed to .002 inches thickness. One counter of this design was purchased and is the counter installed in the HXX Flight Instrument (PFU HXX).

#### 2.2.5 Collimators

The collimator requirement for the LAD portion of the instrument is 10 arc-minutes x 3 degrees FWHM. This requirement is met by combining a modulation collimator and a tube type collimator. The modulation collimator has 6 geometrically spaced grid layers which result in a central response peak of 10 arc-minutes FWHM with the nearest side lobes approximately 5 degrees either side of the center peak. The side lobes are eliminated and the collimation in the elevation direction is established by inserting a 3 degrees x 3 degrees FWHM tube type collimator in between the first and second grid layers of the modulation collimator.

The collimators for each half of the LAD detector are required to be offset from each other by 5 arc-min. By doing so, the signal obtained by dividing the sum of the two LAD channels into the difference, has a zero crossing when the average of the two collimators is pointing at an X-ray source, thereby allowing X-ray

pointing by the satellite altitude control system.

The general configuration of the LAD collimator was shown in Figure 2-12, and the details of construction in Figure 2-16. The modulation collimator wire planes are not wire wound but are etched metal grids. The two inch depth of the collimator requires a .006 inch wide slot to obtain the required 10 arc-min FWHM collimation. The solid bars between the slots are correspondingly .006 inches wide. Copper was selected for ease on etching, close thermal coefficient of expansion match with aluminum and high density for X-ray attenuation. The thickness of copper grid planes required to produce satisfactory collimation at the higher energy levels is .006 inches also. Because of problems with undercutting during etching, it was not possible to maintain adequate tolerances with that thickness so as a result, each grid plane is actually two etched grids each .003 inches thick sandwiched, but not bonded, together. Each grid has four holes, one in each corner etched in at the same time as the slots for proper registration. The grid layers are held in alignment by dowel pins through the corner holes and spaced apart by a series of aluminum spacers of appropriate thickness which also contain the hole pattern for the dowel pins.

The thickest spacer, the one inch thick spacer between the first and second grid layers, is common to each half of the LAD collimator and has the 5 arc-min offset angle machined into it for stability of that parameter. The remaining spacers are independent, for each half of the collimator. Because of physical size limitations on the etching of the grids, a grid layer is not long enough to span the length of the collimator, so there are two sets of grid layers in each half of the collimator for a total of four quadrants.

ORIGINAL PAGE IS  
OF POOR QUALITY

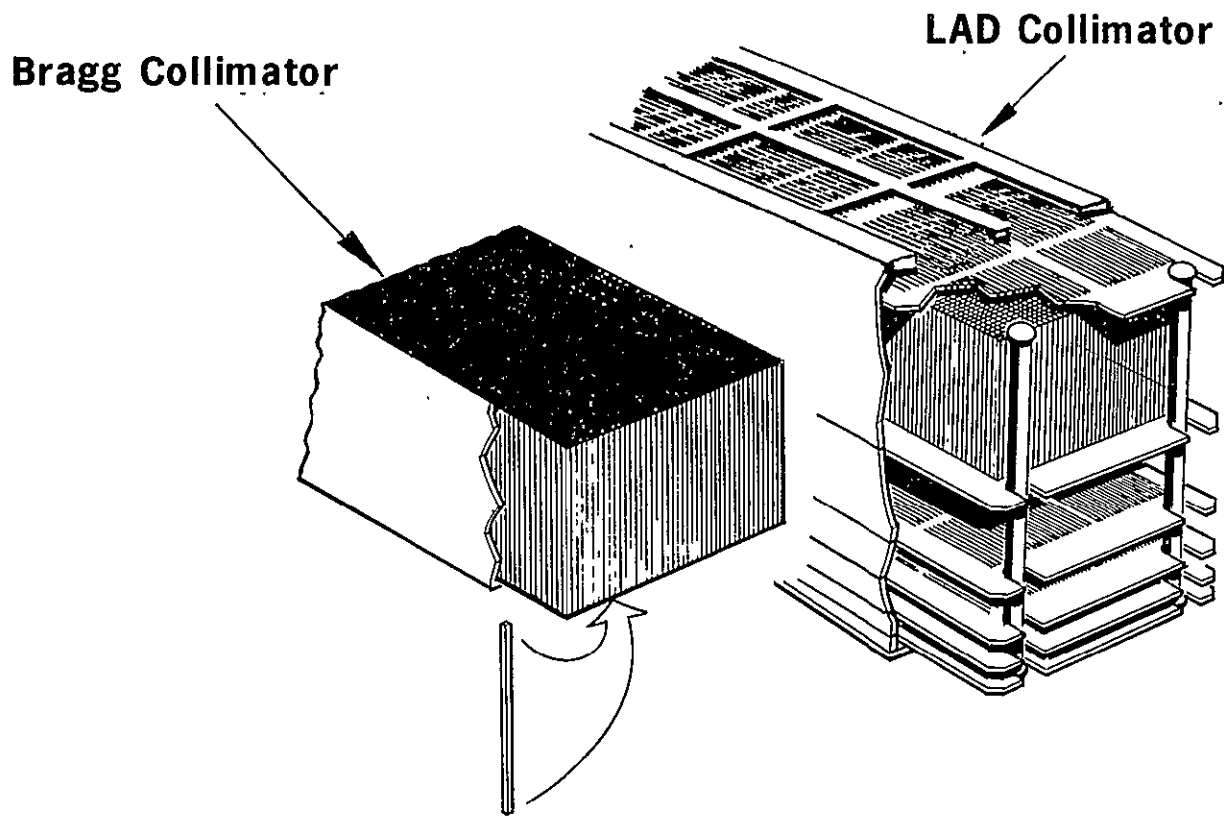


Figure 2-16. Collimator Construction Details

The coarse slit collimator is simply constructed by epoxy bonding .050 inch square x .950 inch long x .002 inch thick wall copper tubes one to another in small bundles. The bundles are bonded together in larger bundles, etc. until a single block of tubes of the desired size is obtained. Each block contains approximately 2700 tubes and four such blocks were built, one for each quadrant of the collimator. The blocks were bonded into openings in the one inch thick spacer between the first and second grid layers. That spacer also contains the HXX Reference Mirror, mounted on three machined pads and held down by spring clips. The mirror is held laterally by silicon rubber.

The collimation requirements for the Bragg portion of the instrument are less stringent because the fine collimation is actually performed by the Bragg crystals themselves. Thus, only a coarse 3 degree x 3 degree FWHM collimator is needed for limiting background and scattered radiation effects. The general configuration and construction details were illustrated in Figures 2-12 and 2-16 respectively. The collimator is built in two sections, one for each crystal set, and the two are nominally parallel in viewing direction. Each section is comprised of a block of square tubes identical to the tubes used in the LAD coarse collimator. It was intended to use aluminum tubes of the same dimension because of the reduced energy range to be collimated, but difficulties were experienced in the packing, shipping and handling of the more delicate aluminum tubes so copper was substituted after ascertaining that sufficient weight margin existed to permit such a choice.

No internal alignment features were designed into the LAD collimator. It was intended to be aligned upon assembly by holding tight tolerances on the component parts. However, piece part tolerances

consistent with reasonable cost and delivery proved to be inadequate to produce a collimator assembly which was in proper alignment. Proper alignment, that is the two quadrants in each half of the collimator pointing in the same direction and the two pairs offset by 5 arc-min, was achieved by loosening the screw on the dowel pins and skewing the grid stack laterally to change the viewing direction. The alignment process was not completely straightforward because of the fact that the grid plane spacers on either half of the collimator are common to both quadrants on that half and thus prevent independent adjustment of each quadrant. This led to a compromise between alignment of the quadrant average viewing directions and collimator "twist" (change in viewing direction at different points along the length of the collimator). The effect of this on collimator response was to round the peaks on the individual response curves and round the corners on the combined response curve. However, the amount of rounding is within acceptable limits. A detailed response curve for the entire collimator was not obtained because of time and equipment limitations, but sufficient spot mapping was completed to insure that a response curve obtained in orbit by scanning across a strong X-ray source will be acceptable.

The actual alignment was accomplished using optical techniques at AS&E, and the results verified in X-rays using equipment at MIT. The optical set-up consisted of a 16 inch diameter parallel light beam (obtained by placing a point light source at the focus of a 16 inch diameter parabolic mirror) illuminating the entire collimator which was mounted on a rotary table to scan across the beam. By placing an aperture in front of the collimator and a photometric telescope behind the collimator, individual areas at the collimator were mapped. This information was used to determine

the extent and direction of movement of the grid stacks required to produce correct alignment.

The X-ray verification was performed at MIT using equipment designed and built by MIT for use in checking crystal to crystal alignment on the Bragg crystal plate. This equipment consists of two main sections, an X-ray generating system which produces a fan-shaped X-ray beam and a translation/rotation table which can translate in the two horizontal axes and rotate about the vertical axis.

The X-ray system takes the output of an X-ray generator tube and collimates it with a pair of slits to produce a fan-shaped beam approximately 1.3 arc-min wide in the narrow dimensions. The system is equipped with a laser which can be introduced onto the X-ray path by use of a beam splitting prism and which is used for X-ray/optical alignment measurements. The target in the X-ray tube is changed to produce X-rays of the desired energy depending upon whether collimator mapping or Bragg crystal testing is desired.

The translation/rotation table is shown in Figure 2-17 and is an open loop computer driven system so that all positional data from the table and X-ray data taken from detectors can be correlated and plotted automatically. Although the system is open-loop, the repeatability and accuracy have been verified by independent measurements with autocollimators. Autocollimator measurements are taken during the course of actual testing for substantiation of the computer data.

X-ray mapping of the collimator was accomplished by placing the collimator on the rotary table with the slits in the collimator parallel to the rotation axis. The table was held at a constant angle and the collimator was stepped across the beam by one of the

ORIGINAL PAGE IS  
OF POOR QUALITY

2-68

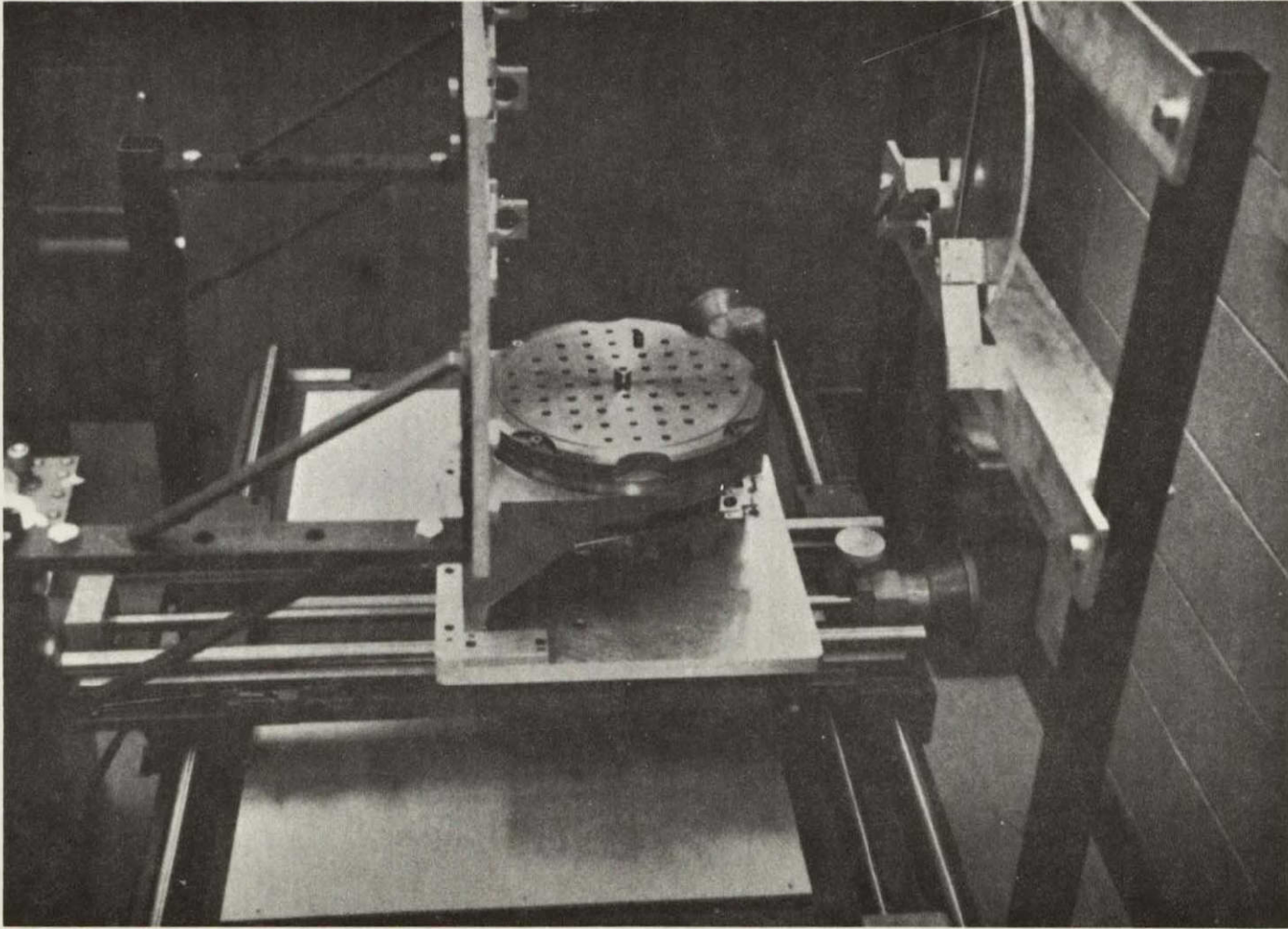


Figure 2-17. Rotomike Assembled on X-Y Table

ES-026

translation stages. Data was collected at each step by an X-ray detector behind the collimator. The data for each half of the collimator were integrated over the entire scan and each value plotted as one point on the corresponding response curve for the halves of the collimator. X-ray beam intensity fluctuations were detected with a monitor counter which measured the intensity before and after each scan. The two integrated values for each scan were normalized prior to plotting using the monitor counter data. The rotary table was then incremented and another stepping scan was taken. This sequence was continued until the entire angular response width was mapped. By selective placement of apertures and the use of two detectors, two areas of arbitrary size could be mapped simultaneously.

#### 2.2.6 Bragg Crystal Plate

The Bragg Crystal Plate consists of an aluminum beam on which four Bragg crystals are mounted by imbedment in a room temperature cured silicone rubber (Dow Corning Sylgard 184). The crystals are arranged in two pairs, the pairs intended to observe X-rays of different wavelengths and hence different Bragg angles. It was necessary to use a pair of crystals for each Bragg angle because of limitations on size of commercially available crystals and indeed limits in the crystal growing process itself. The crystals in each pair are mounted to within 1 arc-min alignment to each other and the two pairs are offset by  $4^{\circ} 14'$  nominal which is approximately 18 arc-min less than the difference between the Bragg angles. This allows measuring a line with one crystal pair and simultaneously measuring the background with the other pair. Then by rotating the satellite by 18 arc-min, the same measurements can be performed for the X-ray line without having to have the guide star go out of the star tracker field of view. Eighteen

triangular vanes are mounted between the crystal plate and the Bragg counter to collimate scattered radiation off the crystals.

The choice of crystal material was made after an extensive test program at MIT. The program was initiated with the design and fabrication of an X-ray generating system (previously discussed in the collimator section of this report) as well as a one-crystal and a two-crystal spectrometer both designed for use in vacuum (see Figure 2-18). This equipment was used to determine the rocking width and reflection coefficient of three candidate materials including the effects on these parameters of various surface treatments. The three materials investigated were Ammonium Dihydrogen Phosphate (ADP), Ethylene Diamine Tartrate (EDDT) and Pentaerythritol (PET). PET with surface etching was selected as the material best suited to the HXX requirements. The crystals were purchased from Quartz and Silice in Paris, France.

After mounting on the plate crystal to crystal, alignment was checked with the same equipment used for the collimator mapping to determine the exact offset from crystal to crystal as well as the extent of any twist in the assembly in the free state.

Following integration into the HXX assembly, the crystal plate was aligned to the LAD collimator using the collimator mapping and crystal to crystal alignment testing equipment. The alignment process started with scanning the LAD collimators in X-rays and locating the peaks. The peak locations were then determined with respect to both the HXX reference mirror and a second reference mirror on the HXX mounting fixture by using the laser and an auto-collimator focused on a third reference mirror. The angular position of the crystal plate was then measured with respect to the second reference mirror and the reading corrected for, 1) change in Bragg angle for higher energy X-rays used to permit testing in

ORIGINAL PAGE IS  
OF POOR QUALITY

2-71

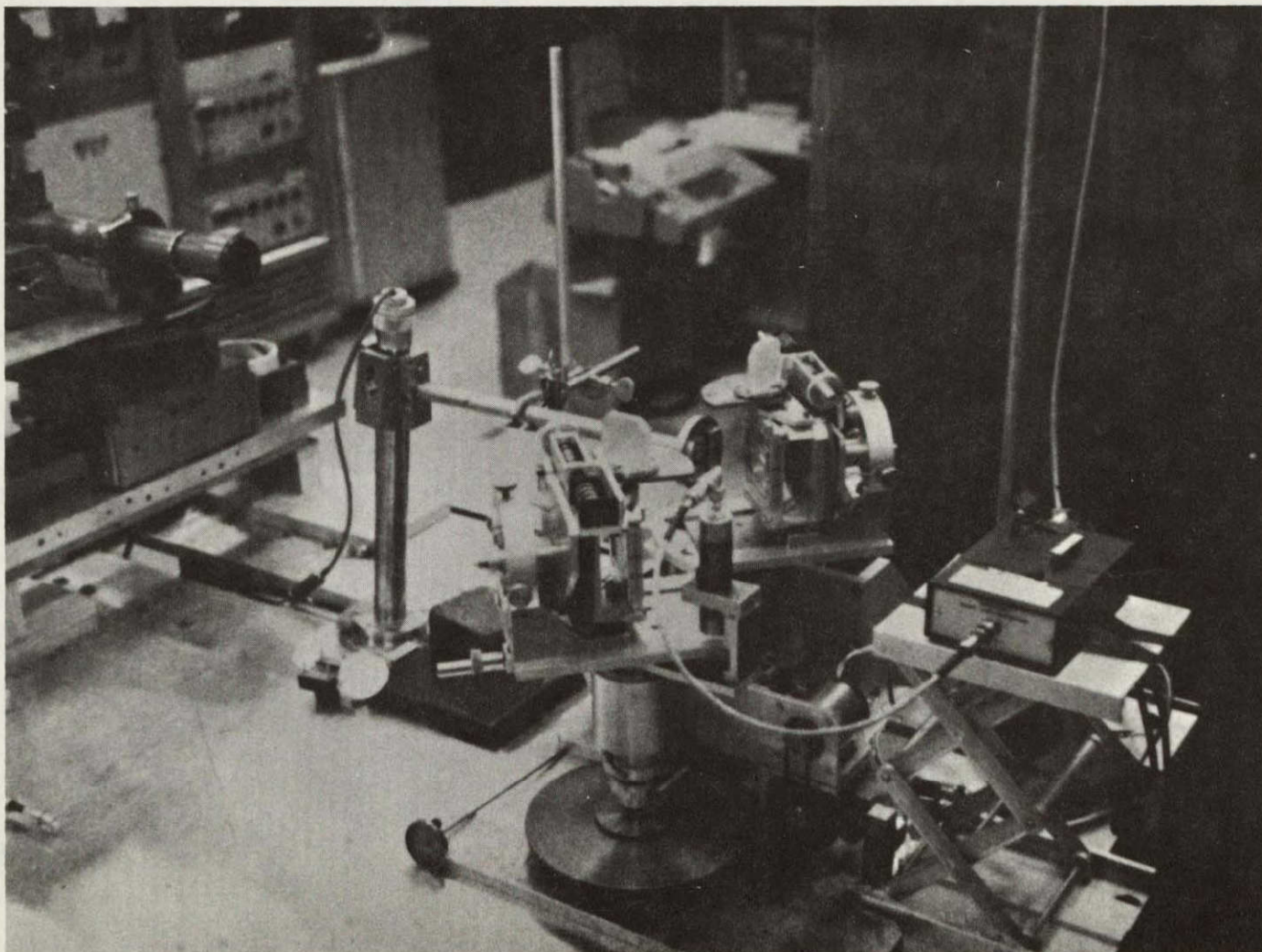


Figure 2-18. Two-Crystal Spectrometer With Point-Focus X-ray Tube  
and Alignment Autocollimator

ES-022

air, 2) change in Bragg angle due to the test temperature being different than the expected orbital temperature of the HXX (Bragg angle sensitivity is approximately  $1/2$  arc-min/ $^{\circ}$ C), and 3) the offset between the LAD peaks and the second reference mirror. For proper Bragg/LAD alignment, the resulting value should be zero and any difference indicates the magnitude and sense of the correction needed to produce proper alignment. Adjustment was accomplished by loosening the crystal plate mounting screws and tapping the plate while monitoring the rotation of the plate with an autocollimator viewing reference mirrors temporarily attached to the plate. At this time the free state twist in the plate was removed.

Following adjustment, the alignment checking process was repeated to verify that adjustment was correct which the Bragg crystal plate was pinned. The LAD collimator was pinned in place at initial assembly into the HXX. After pinning, the alignment was checked once again to insure that no movement occurred during pinning.

## 2.3 Reliability

As a part of the reliability effort, a preliminary Failure Mode Effects Analysis (FMEA) was presented at the Critical Design Review (CDR) on March 23 and 24, 1972. The analysis showed that there were no criticality I failures. A criticality I failure results in a loss of life or of the spacecraft. The analysis also indicated that there were twelve (12) major subassemblies with a total of seventeen (17) modes of failure in criticality II. A criticality II failure results in a failure to attain system performance. As of the publication of this report, the HXX experiment has been successfully launched into orbit and has continued to operate to specification.

### 2.3.1 Parts

#### 2.3.1.1 Selection Criteria

The parts used in engineering protoflight and flight models of the ANS-HXX experiment were classified into codes as follows:

Code A - These parts were:

Parts included in the GSFC PPL-11

Military established reliability (ER) parts

Parts screened to AS&E screening specifications

Code C - These were the "OFF the SHELF" parts and were used only in the engineering model of the experiment.

In addition to above requirements, the Code A parts were obtained with weldable leads (per MIL-STD-1276). Code A parts with weldable leads were primarily used in protoflight and flight models.

2.3.1.2 Deviations to Approved Parts

During the fabrication of the protoflight model, it was necessary to deviate from the selection criteria described above (2.3.1.1) because of the unacceptable long delivery times on some of the Code A parts. Assemblies and subassemblies of the protoflight and protoflight (refurb) in which parts outside the Code A classification were used, are shown in Table 2-10. There were no such deviations for the flight unit.

Table 2-10

<u>Item #</u>	<u>Ass'y/Subass'y</u>	<u>Part Used</u>	<u>Model Affected</u>
1	135-6016-1, 135-6016-2	CD4029AK/1	Protoflight ↓
2	135-6012, 135-6013, 135-6015	CD4028AK/1	
3	135-6005	CD4018AK/1	
4	135-2007	CY10	
5	135-6000, 135-6001	RC05	
6	135-6002	RNC50H4642F	
7	135-2418	RNC50H2870F	
8	135-2416	RNC50H6812F	
9	135-2018	RNC50H1203F	
10	135-2410	RNC50H1623F	
11	135-2410	RNC50H1003F	
12	135-2412	RNC50H1003F	
13	135-2413	RNC50H1003F	
14	135-2416	RNC50H1003F	
15	135-2417	RNC50H1003F	
16	135-2410, 135-2417, 135-2418	M39014/05-1091 (Tinned OFHC Cu leads)	
17	135-2415	M39014/05-2837 (Tinned OFHC Cu leads)	Protoflight (Refurb) ↓
18	135-2415	RNC50H9092	
19	135-2418	RNC50H5620	
20	135-2410-2	RNC50H1962F	
21	135-2410-2	RNC50H4991F	
22	135-2410-2	RNC50H2370F	

2.3.1.3 Effect on Reliability of the Deviations to Approved Parts

CD40XXAK/1 (Items 1, 2 and 3) - The difference between these devices and the parts they replaced (CD40XXAK/1 + SEM) was the scanning electron microscope (SEM) inspection of the latter devices. Otherwise the high reliability screening levels of both these devices were identical. Analysis of the burn-in data was performed (Table 2-11):

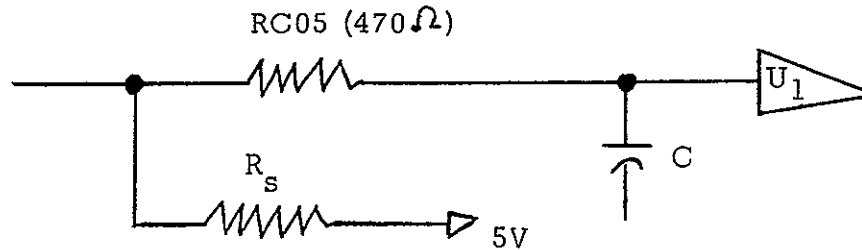
Table 2-11

<u>Device</u>	<u>No. of Devices</u>	<u>No. of Rejects</u>	<u>% Rejects</u>
CD40XXAK/1	277	11	4.06
CD40XXAK/1 with SEM	1222	64	5.24

The data indicated that the performance of both these devices was identical. In addition, to the data analysis, construction analyses were performed on each type of CD40XXAK/1 device used in ANS-HXX protoflight. The analyses indicated that the use of CD40XXAK/1 did not compromise the reliability of the ANS-HXX experiment.

Capacitor CY10 (Item #4) - These are glass dielectric capacitors made in accordance with specification MIL-C-11272/1. The military standard capacitors are rated at 500V (dc) maximum voltage at 125<sup>o</sup>C and are derated to 50%. The logic voltage level on the board 135-2007 was 5.0V. The capacitors CY10 would not ever be subjected to voltages >>5.0V. Therefore, the reliability of the experiment was unaffected by the use of the CY10 capacitors.

Resistors RC05 (Item #5) - Resistors RC05 were used in each microstick assembly 135-6000 and 135-6001 as series input resistors (as shown below). (Ref. Microstick Assembly Logic Diagram #135-203).



C = 220 pf to 2200 pf  
 $R_s$  = 3.0 kΩ to 10 kΩ  
 $U_1$  = SM54L04F1

Under the circuit conditions shown above, the currents through RC05 would be:

Steady State Current	0.1mA
Transient Current	10.0mA (max)
Duration of the Transient Current	0.1-1.0μsec

The resistor RC05 is rated at 1/8 watt (125mw) with a maximum continuous working voltage of 150V and is derated at 30%. The current/voltage conditions present in the circuit indicate that the resistor RC05 ratings would not be exceeded; so the reliability of the ANS-HXX experiment was not compromised with the use of RC05 resistors in place of RCR05 resistors.

Resistor RNC50H (Items #6 to 15, 18, 19, 20 to 22) - The resistors RNC50H were used in place of RNN50H resistors because of the extremely long delivery times on RNN50H resistors. Both

RNN50H and RNC50H resistors have identical reliability characteristics, and failure rates. The only difference between the two resistors is the lead materials - RNN50H has gold plated nickel leads while RNC50H has tinned OFHC copper leads. Different lead materials require different weld schedules. The weld schedule was adjusted to suit the tinned OFHC copper leads of the RNC50H resistors. The new weld schedule was approved and produced repeatable, good quality (and strength) welds.

Capacitors M39014/05-XXXX (Items #16 & 17) - These capacitors have tinned OFHC copper leads, otherwise they have identical reliability characteristics as the original capacitors (M39014/05-XXXX) with gold plated nickel leads. The weld schedule was therefore adjusted to suit the copper leads. The new weld schedule was approved and produced repeatable, good quality (and strength) welds.

General - It is interesting to note that during the development of the ANS-HXX Program, no failures were caused by defective components which indicated that the selection criteria for parts were basically sound and, as a consequence, good reliable performance was achieved.

### 2.3.2 Materials

The materials used in the ANS-HXX experiment were selected on the basis of the following criteria:

Organic Materials - Document X-764-71-314 "A Compilation of Low Outgassing Polymeric Materials normally recommended for GSFC cognizant spacecraft" Fisher & Mermelstein, was used as the primary guideline.

Metals - Cadmium was not used anywhere in the experiment. Tin was permitted only on small exposed areas or on surfaces which

were subsequently soldered.

General - Only fungus-inert materials were used. Organic materials containing sulfides or sulfur were not used.

### 2.3.3 Failure History

The significant failures that occurred during the development of ANS-HXX protoflight and flight modules are described below.

#### 2.3.3.1 Power Supplies

A major problem on the power supplies was the presence of corona during their development at Matrix Corporation.

High voltage Power Supply #1 (Matrix #5598/01 - Corona appeared at the output #3 at a pressure of  $8 \times 10^{-6}$  Torr. No corona was present at sea level (Ref. GSFC Malfunction Report #N0C02992).

High Voltage Power Supply #2 (Matrix #5598/02) - Corona around output #3 at a pressure of  $8 \times 10^{-6}$  Torr. No corona observed at sea level (Ref. GSFC Malfunction Report #N0C02997).

The corona was caused by a lack of adhesion between the potting compound and the spot bonding applied to the HV cable. The terminal wells were depotted and repotted. The repotted assemblies were subjected to functional and thermal vacuum tests. The repotted high voltage power supply #1 was, however, used for qualification purposes only, as it was subjected previously to out-of-spec vibration levels (Ref. GSFC Malfunction Report #N0C02989). The repotted high voltage power supply #2 showed fifteen (15) isolated instances of corona, during thermal vacuum tests. (Ref. GSFC Malfunction Report #N0C02996). The location

of the corona was traced to the high voltage module (Matrix #5608/2) of the high voltage power supply. In view of the history of corona on the power supply #2, the high voltage module (Matrix #5608/2) was replaced by a new module (Matrix #5608/3). The new module was fabricated and potted in accordance with the modified potting procedure (Matrix Procedure #A5682) and a close surveillance was maintained by AS&E QC personnel throughout the fabrication of the module. The power supply #2 with the new high voltage module functioned satisfactorily without corona during thermal vacuum tests.

All the power supplies, high voltage and low voltage, performed satisfactorily without corona at the system level.

#### 2.3.3.2 LAD Proportional Counters

The Xenon carbon dioxide LAD Proportional Counters showed unstable operation during the ANS-HXX Program. The instability showed as degraded resolution and/or gain (Ref. AS&E FR #N028, N037, N060). The degraded performance was attributed to the following causes:

- (1) Leak
- (2) Defective Anode Wire
- (3) Presence of halogen contamination, such as fluorine
- (4) Appropriateness of the quench gas

Extensive tests did not validate the assumption of a leak. The anode wires from two counters showed erosion along their lengths. No further tests, however, were performed to establish the validity of the anode erosion as the possible factor for the shifts in the gain and resolution of the counters. It was considered that the presence of fluorine in the gas volume, resulting from the FREON

cleaning of the beryllium cathode, may have caused the instability of the counter. To establish the validity of this factor and to eliminate the possibility of fluorine contamination of the gas mixture, later counters were meticulously cleaned with non-halogenated solvents, such as acetone and alcohol. However, these counters were also unstable. It was also considered that the beryllium cathode may also have been contributing to the instability of the counter, so following the example of MIT counters, counters were made from aluminum. These counters showed similar unstable performance. Finally, the quench action of carbon dioxide in a Xenon proportional counter was analyzed. The analysis indicated that the carbon dioxide was not a suitable quench gas for use with Xenon, so the counter would perform as a non-quenching type with the inherent instability of such a counter.

Based on the evaluation study of the Xenon counters described above, and the known stable performance of argon/carbon dioxide Bragg counters, it was decided to change the gas mixture in the LAD counter in the Protoflight (Refurb) to argon/carbon dioxide. The performance of this counter has been very stable.

#### 2.3.3.3 Missing Counts

During the testing of the Protoflight model, the following malfunctions occurred:

- (1) A loss of counts between LAD window accumulator and corresponding PHA channels. PHA lost 20-25% for X-rays. (AS &E FR #N031).
- (2) Discrepant counts between LAD Address Only Select (LAOS) and normal modes. (Normal lost 5% for X-rays) (AS &E FR #N033).

Both these malfunctions were caused by the early reset DETECT identification by PSD generated reset signals. To avoid the recurrence of this malfunction, microsticks 135-6021, and 135-6022 were modified per AS & E ECO #7651. This malfunction did not occur in the flight model using the modified microsticks.

#### 2.3.3.4 Corona Discharge in BRAGG 1 Counter Assembly

During the acceptance tests of the flight model in thermal vacuum, excessive background counts were recorded in BRAGG 1 (AS & E FR #N049). The malfunction was traced to the presence of a corona discharge on BRAGG 1 (AS & E FR #N050). The corona was caused by a lack of adhesion between the high voltage capacitors and the potting compound. The high voltage capacitors were not properly primed prior to potting. The high voltage cavity of the BRAGG 1 counter and the high voltage capacitors were properly primed using GE #4004 primer prior to repotting. A procedure was established to ensure that in all future potting operations, parts would be properly coated with undegraded primer.

#### 2.3.3.5 Soft Mounting of the Alignment Mirror

During the qualification test on the ANS-HXX protoflight, alignment data taken at MIT before and after vibration tests could not be correlated (Ref. AS & E FR #N032). The lack of correlation was found to have been caused by a shift of several arc minutes from its original position, after the vibration test. The shift was caused by the soft or flexible mounting of the mirror. The adhesive used had seeped into the space behind the mirror.

The soft mounting was made more rigid by using the method of mounting described in AS & E procedure for the disassembly rework and assembly of the ANS-HXX alignment mirror (P135-038). A mock-up mount made in accordance with P135-038 was tested

2/28/75

# PRE DUP ATS INPUT FORM

CORPORATE SOURCE

Tyco Labs, Inc.  
Waltham Mass

@ . . .	1 TEMPORARY NUMBER				2 PUBLICATION DATE			3 PRIMARY CORPORATE SOURCE CODE					DOCUMENT RELEASE FORM												
	DAY	MONTH	YEAR										<input checked="" type="checkbox"/> ATTACHED	<input type="checkbox"/> REQUESTED	<input type="checkbox"/> NOT NEEDED										
	1	7	2	3	7	0	0	0	8	7	4	1	9	7	9	5	0	2	5		<input checked="" type="checkbox"/>	<input type="checkbox"/>	<input type="checkbox"/>		
@ rpn	RPN	C-227																							
@ cnt	CNTI	CITINAST-RB/PR																							
@ aut	AMTI	RUBIN, EDWARD J.																							
@ utl	UTL	NICKEL-CADMIUM CELLS																							

1 copy.

under vibration and was found to be satisfactory. Flight mirror was mounted according to this method.

#### 2.3.3.6 Intersil Comparator (ICL8001MTZ)

During the alignment test at AS&E on ANS-HXX flight model per TP135-500 LAD 1 and LAD 2 were found cross-coupling into BRAGG 1 (Ref. GSFC Malfunction Report #N0D 5414). The trouble-shooting procedure to determine the cause for cross-coupling required assembly and disassembly operations and the use of an extender cable. Electrical test after the assembly/disassembly operations for the trouble-shooting procedure showed that the data from BRAGG 1 and 2 always appeared in BRAGG 1 and LAD's (Ref. AS&E FR #N052). Analysis of the circuit diagram indicated the possibility of damage to Intersil Comparators (ICL8001MTZ) in the Upright Module (135-2001-2/3883). Failure analysis of the ICL8001MTZ showed that the devices were damaged by the application of >15.0V transients to the inputs #1 and #10 of three comparators ( $U_1$ ,  $U_3$  and  $U_4$ ). Investigations for the existence of such a transient led to the discovery of broken wires in the extender cable. The cable and the upright module were repaired. However, during later electrical tests, it was found that the data was accumulated in both BRAGG's and LAD simultaneously when any one detector was enabled (Ref. AS&E FR #N056). Analysis indicated that the comparators ICL8001MTZ in the upright module (135-2001-2/3883) were possibly damaged. Failure analysis of the comparators ( $U_1$ ,  $U_3$  and  $U_4$ ) showed that they had been damaged by the application of >15.0V transients to the inputs of these devices. The failure mode was exactly similar to the one reported earlier (Ref. AS&E FR #N052). In both cases the quality of workmanship in the devices was very good and the failures

occurred after some assembly/disassembly operations.

In both these cases it was concluded that the devices were inherently of good quality and the failures were caused by the application of transients  $> 15.0V$  to the inputs of these devices. The source of the transients was never positively identified, however, it is generally accepted that the assembly/disassembly operations along with the broken wires in the extender cable would cause such a failure. In order to avoid the possibility of recurrence of this type of failures, current limiting resistors were added in series with the comparators ( $U_1$ ,  $U_2$ ,  $U_3$  and  $U_4$ ) in the upright module (135-2001-2/3883).

### 3.0 PROGRAM HISTORY

Figure 3-1 illustrates the history of the ANS program from contract start, 30 November 1970, through launch, 30 August 1974. This history is given by deliverable model with significant events effecting each model also indicated. In addition, a history of the proportional counters procured on this contract is also given to provide further insight into the sequence of program events. The discussion which follows is a synopsis of the program monthly progress reports.

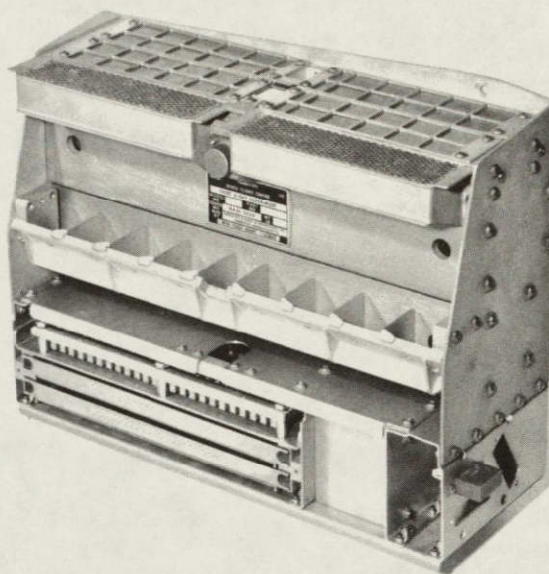
#### 3.1 Structural, Thermal & Electrical Models

During the first six months of the program, effort was concentrated on the design of the structural, thermal and electrical models. The structural model completed fabrication and was delivered in July 1971. The thermal model, followed closely with an August 1971 delivery. Pictures of these models are shown in Figures 3-2 and 3-3. These models were subsequently tested in the Dutch spacecraft structural and thermal models with good results.

The electrical model design started in December 1970. Early in the program, AS&E recommended building a full-up electrical model, however, in August 1971, the electrical model was redefined to the less elaborate contractual concept due to cost and schedule constraints. This concept included no collimators and used analog and digital breadboards for the bulk of the electronics, along with non-flight design power supplies and counters. The electrical model completed fabrication in early March 1972. Integration testing and checkout with GSE #1 was completed in mid-April, at which time the electrical model and GSE #1 were delivered to the Dutch. The electrical model was integrated into the Dutch electrical model test bench by the end of May 1972 without any

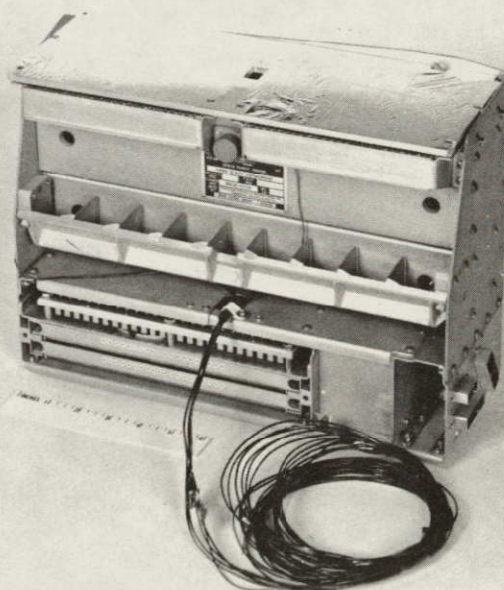






ES-016

Figure 3-2. HXX Structural Model



ES-020

Figure 3-3. HXX Thermal Model

ORIGINAL PAGE IS  
OF POOR QUALITY

major problems. A photograph of the electrical model is shown in Figure 3-4.

### 3.2 Ground Support Equipment (GSE)

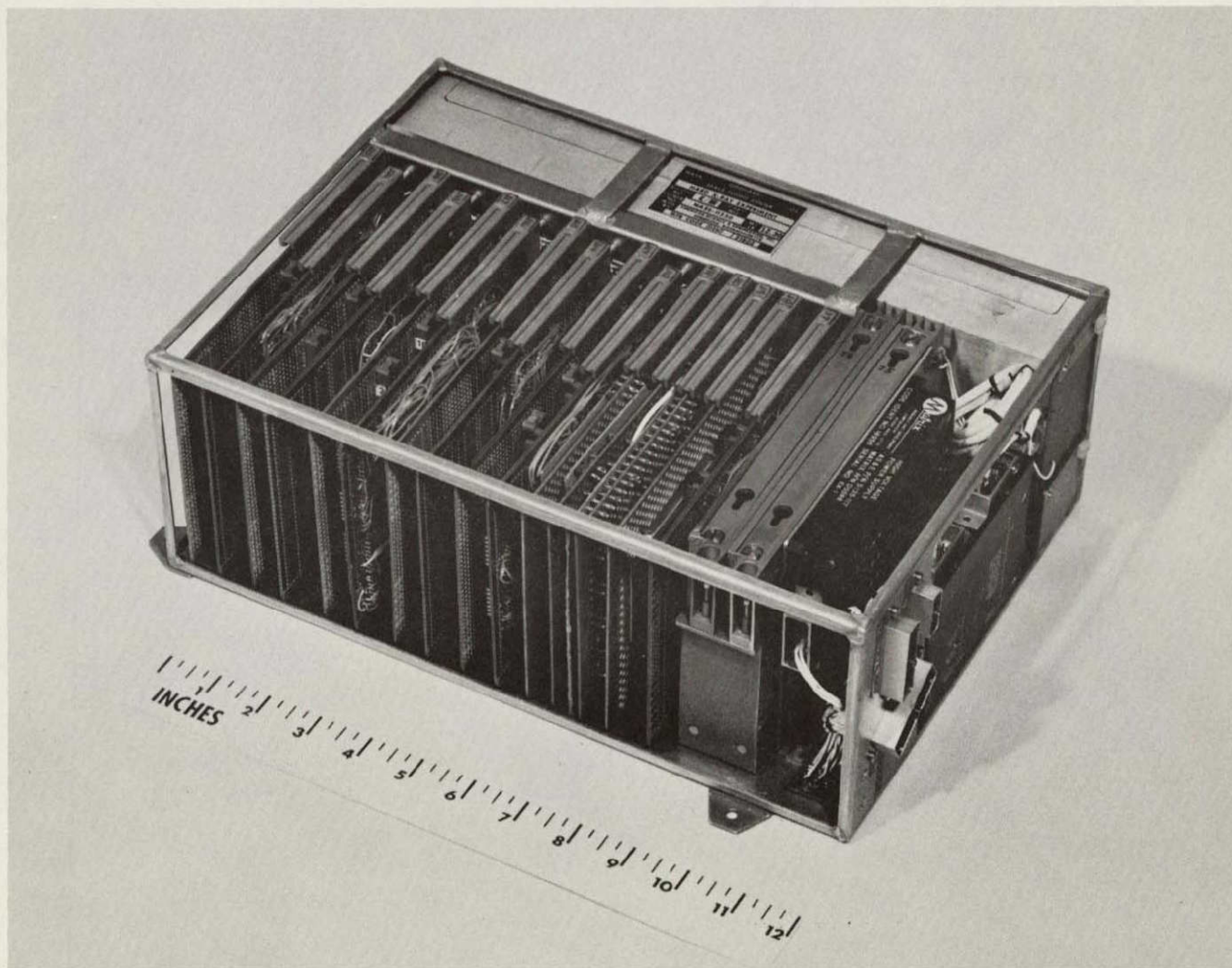
Two sets of GSE were provided under the contract. The GSE design effort was started in August 1971, after the HXX design was well along. The first set of GSE was completed and available for integration with the electrical model in February 1971. This unit was shipped with the electrical model to the Netherlands in mid-April 1972. The second set of GSE was completed and available for checkout of the protoflight unit in November 1974. This unit incorporated interface timing changes required by SCP's #125 and #126. This GSE was subsequently delivered to the Dutch in early July with the protoflight unit. The first set of GSE was returned to AS&E in mid-May 1973 for refurbishment of the interface timing changes and for use in checkout of the HXX flight unit. This refurbishment was completed in early June 1973. A photograph of the GSE is shown in Figure 3-5.

### 3.3 HXX Protoflight and Flight Units Design Phase

The design for the flight units also started in December 1970, and proceeded in parallel with the designs for the structural, thermal and electrical models. In April 1971, a decision was reached to use the COS/MOS digital logic family due to: 1) Inherent low propagation delays, 2) availability of multiple qualified vendors, and 3) reasonable price and delivery quotations. During September/October 1974, the definition of the HXX experiment was reviewed to insure that optimal scientific experiments could be performed, and to eliminate all non-vital features of the instrument not part of the original negotiated proposal effort. As a result, two accumulators, one high voltage power supply and the LAD calibration source were eliminated, providing savings in weight

ORIGINAL PAGE IS  
OF POOR QUALITY

3-5



ES-058

Figure 3-4. HXX Electrical Model



ES-042

a. Rack Mounted Unit



ES-028

b. Input/Output Unit (IOU)

ORIGINAL PAGE IS  
OF POOR QUALITY

Figure 3-5. HXX Ground Support Equipment

and power, in addition to reducing costs to the original level.

In September 1971, a purchase order was placed with Ragen Semiconductor for the design and fabrication of the COS/MOS monolithic circuitry. In November 1971, AS&E had first indications of a delivery problem, which became severe in December 1971, and resulted in AS&E cancellation of the Ragen subcontract. As a further result, it was necessary for AS&E to repackage that portion of the electronics using discrete devices.

During this time frame, it became clear that available program funding for FY 72, would not meet program needs, hence, NASA/AS&E agreed to a plan to stretchout the program to minimize FY 72 expenditures. The plan consisted of deferring all manufacturing activity and short lead time procurement until July 1972, however, the flight design would be carried through CDR in March 1972. AS&E agreed to support with AS&E funds, the long lead procurements and preparation of protoflight and flight model drawings through the balance of FY 72 in order to minimize the overall schedule and cost impact. All other program activity was suspended.

In May 1972, AS&E received four design change requests from the Dutch; two of which SCP #125 and SCP #126 were finally implemented in July through September.

#### 3.4 HXX Protoflight Unit Fabrication and Test Phase

The fabrication of the protoflight unit was well underway by the end of August 1972 and was essentially completed in mid-February 1973. Additional manufacturing effort was expended into May 1973, due to incorporation of modifications and reworks resulting from the integration and evaluation testing. One of the most significant modifications was the additional of coaxial cables to minimize coupling

and cross talk problems. The HXX, being already a high density package, became more so. In addition, handling during assembly and disassembly operations frequently resulted in open, shorted, or intermittent connections. These difficulties were resolved by development of special connection techniques and rework of all coaxial cable connections. Success was clearly demonstrated when the HXX successfully completed protoflight testing without the occurrence of one cabling problem.

Significant events effecting this phase included the following:

- 1) RCA 4000 series COS/MOS deliveries with SEM inspection per GSFC S-311-P12A were well behind original schedule for several key integrated circuits. Waivers were finally granted by NASA to use the RCA MIL-STD equivalent. These parts were given additional screening and have been successful from a reliability viewpoint.
- 2) Delays in delivery of the high voltage power supplies occurred due to several corona problems. Corona was observed in mid-July on High Voltage Power Supplies SN #1 and SN #2 was found to be a result of improper application of staking compound in the potting wells. The staking compound is used to fix the four high voltage exit cables to the potting well wall. As a result, the entire potting well procedure was reviewed and improved before both units were repotted. Upon retest of the repotted units, SN #2 exhibited infrequent corona-like transients, not at all similar to that previously observed. The fault was finally isolated to be in the fiberglass back wall of the potting well or just beneath the surface. The unit was subsequently restructured and the problem did not reappear. However, due to the amount of rework

performed at the back surface and below the potting well in order to find the fault and in order to assure highest reliability, AS&E instructed Matrix, the power supply section contractor, to replace the high voltage module and potting well. This effort was accomplished and the supplies have performed without fault since delivery.

- 3) The deliveries of the proportional counters were also late due to a) the beryllium supplier (KBI) being flooded by Hurricane Agnes, and b) rejection by LND of machined beryllium main housings which were not acceptable for use. Additional detail on proportional counter history is given in Section 3.8.
- 4) During the protoflight unit integration testing, one chamber of the LAD #2 proportional counter was found to be degrading. Due to the Dutch need for a full-up HXX for bench integration testing of all the spacecraft systems, and due to the fact that no replacement LAD counter was available (see Section 3.8), a decision was made with NASA concurrence to deliver this unit. The intent was not to delay the Dutch in their bench integration, and to refurbish this unit after delivery of the flight unit.

The protoflight unit started a two month protoflight test sequence in early May 1973. This test sequence is shown in Figure 3-6. The test sequence was completed with no major problems encountered. An acceptance review was held with NASA at the end of June, and the unit was shipped to the Netherlands during the first week in July. The HXX protoflight unit was successfully integrated into the Dutch test setup by the end of July. All interfaces were tested and no problems were found. The unit subsequently performed without malfunction during its entire stay in the Netherlands. It was returned to AS & E for refurbishment in early March 1974. (See 3.6).

### 3.5 HXX Flight Unit Fabrication and Test Phase

Fabrication was initiated for flight unit microsticks, cordwoods, modules, etc. after the corresponding protoflight components had been fabricated and tested. In this manner, most protoflight component ECO's were incorporated into the flight unit manufacturing drawings before manufacture. In general, the flight unit fabrication and test was a smooth operation. The main source of difficulty for the flight unit was a sequence of LAD proportional counter degradations.

Degradation of LAD #1 was first observed near the conclusion of integration testing in late July 1973. At this time, no spare counter was available. AS & E had placed an order in April 1973 for one counter (LAD #3 for use in future refurbishment of the protoflight unit). This counter was not expected for delivery until mid-August, and then required an extensive two week acceptance test. A decision was made, with NASA concurrence, in early August to replace LAD #1 with LAD #3 when available. LAD #3 passed its acceptance test and was installed into the flight unit in early September 1973. Some degradation in LAD #3 was

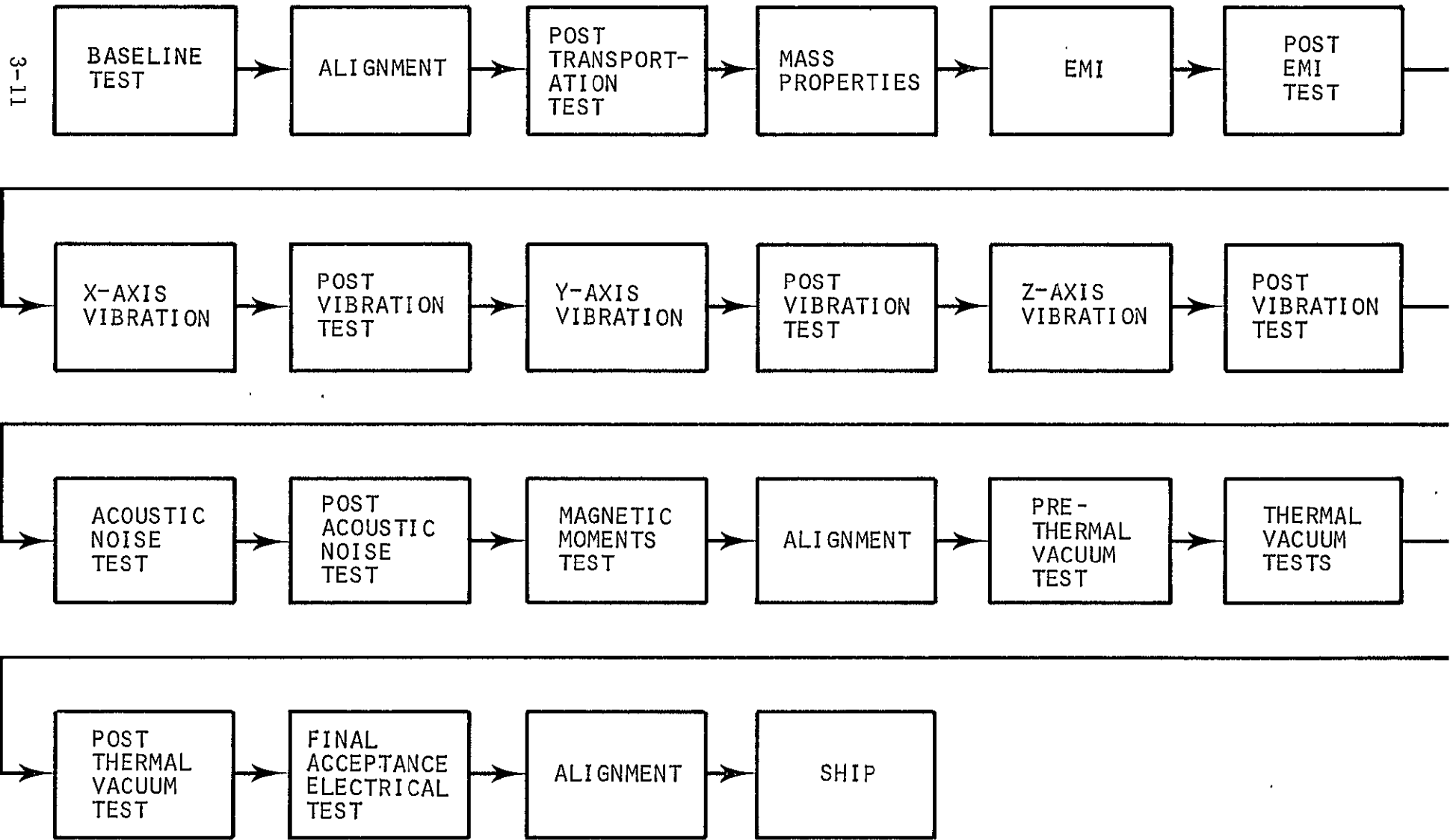


Figure 3-6. Protoflight Test Sequence

observed shortly after installation. No spare counters were available, and a decision was made with NASA concurrence to use LAD #3 as is, due to the existing schedule constraint. In October, after several discussions with LND and based upon the latest Dutch schedule information, AS&E proposed to procure four LAD proportional counters on a crash program. Three of the LAD's would have an aluminum body and use Xenon gas, the fourth would have a beryllium body and use argon gas. From these four counters, it was expected that at least one sound counter would be found. The test program using LAD #3 continued through acceptance test, where several failures had occurred including: 1) Corona in Bragg potting well, and 2) accumulator bank failure. Two of the aluminum counters were received in mid-December and both successfully completed the most severe acceptance test in the first week of January 1974. Both counters were judged equally acceptable. LAD #4 was selected for replacement of LAD #3. The flight unit failures were reworked and LAD #4 was installed. The flight unit successfully completed integration and an abbreviated acceptance test was conducted. At the conclusion of the acceptance test a slight degradation in LAD #4 was observed. However, due to the schedule constraints, a decision was made with NASA concurrence, to deliver this unit for flight as it was superior to the protoflight unit.

The HXX flight unit was delivered in mid-February, and successfully completed integration into the spacecraft by the end of February. A picture of this unit is given in Figure 3-7.

### 3.6 HXX Protoflight Unit Refurbishment

The protoflight unit was returned to AS&E in early March 1974 for refurbishment. A decision was made to abandon the Xenon Counters and refurbish with LAD #7, the backup counter procured with Argon

ORIGINAL PAGE IS  
OF POOR QUALITY

3-13

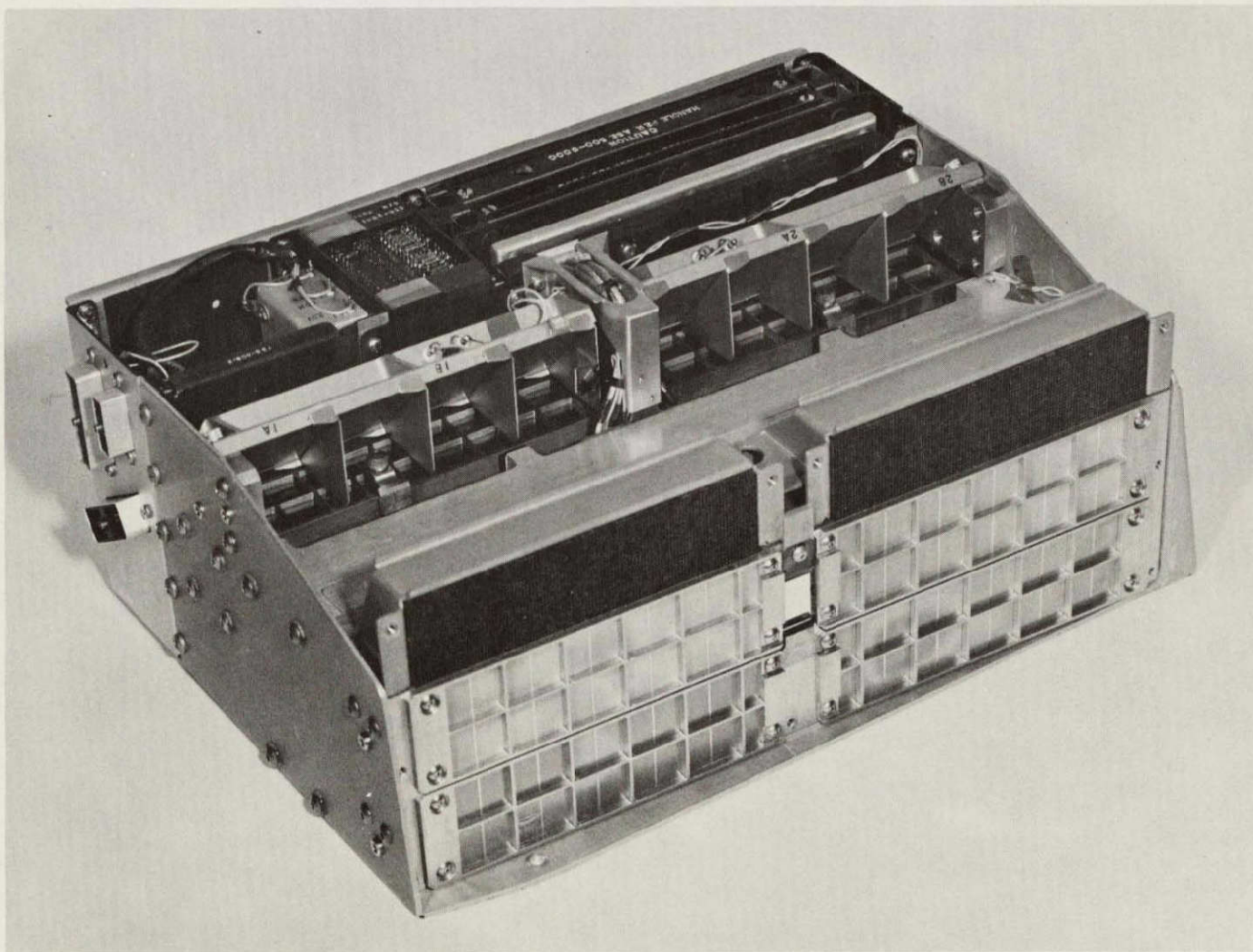


Figure 3-7. HXX Flight Unit

ES-149

gas. Refurbishment was completed in mid-May 1974 without further counter problems. Arrangements were made with the Dutch to have this unit replace the HXX flight unit in the spacecraft. This exchange was completed by the end of May. No further counter problems occurred.

### 3.7 HXX Flight Unit Refurbishment as a Spare Backup

At the time of delivery of the refurbished protoflight unit, two LAD counters, LAD #5 and LAD #6, had never been installed into an HXX. LAD #6, however, degraded during its acceptance testing. LAD #5, the previous companion of LAD #4, remained stable. AS&E proposed to replace LAD #4 with LAD #5 and deliver the flight unit to Western Test Range as a spare backup. NASA concurred and this effort was accomplished as shown in Figure 3-1. LAD #5 is the only Xenon counter of the six procured on the program that remained stable.

### 3.8 Detailed History of HXX Proportional Counters

This section provides a detailed history of all the flight quality proportional counters purchased on the ANS program. Figure 3-8 lists the sequence of key events relating to each proportional counter. Detail in this figure may be compared directly to Figure 3-1, ANS program history, to obtain additional insight into the sequence of program events.

#### 3.8.1 Background

During the HXX design phase, AS&E conducted considerable Pulse Shape Discrimination (PSD) performance testing with various gas mixtures using a test proportional counter. The Xenon-Propane gas mixture provided best overall results over the 1-40ke V range (for LAD counter) with a Xenon-Co<sub>2</sub> gas mixture second. The Bragg counter gas mixture was selected to be Argon-Co<sub>2</sub> covering 1-7keV range. As discussed in Section 3.1, the recommendation to build a full-up electrical model was put aside due to cost and schedule constraints, and the electrical model was fabricated using non-flight counters. At that time, AS&E experience in procuring flight quality counters had been very good. The initial purchase order for the two Bragg and two LAD proportional counters was placed in May 1971, with deliveries expected by the end of July 1972. However, in June 1972, the beryllium supplier in Pennsylvania was flooded by hurricane Agnes, delaying initial beryllium deliveries by a month. At this time, AS&E found the LAD proportional counter performance to be improved by having the window grid on the outside surface and this modification was implemented. Delays in obtaining acceptable machined main housings for the initial order of the two LAD and two Bragg proportional counters further delayed initial delivery to mid-September 1972.



### 3.8.2 Bragg Proportional Counters #1 and #2

Bragg #1 was received from LND in mid-September 1972, and was found to have a gain a factor of 4 high. The gain problem was finally resolved by changing the gains in the Bragg preamps and summing amplifiers. This counter, however, was returned to LND for replacement of a helicoil and refill of gas mixture to include 0.5% helium. Both Bragg #1 and Bragg #2 were delivered to AS&E on 20 October 1972. These counters completed acceptance testing in late November and both were accepted. These counters have since functioned flawlessly. The Bragg counters each had, beryllium housing, Argon-CO<sub>2</sub>-He gas mixture, 1 mil beryllium window, and internal grid support structure.

### 3.8.3 LAD Proportional Counter #1

LAD #1 was delivered to AS&E on 20 October 1972, at which time acceptance testing was started. On 7 November, during thermal vacuum testing, a shift in the center channel (1.5 out of 178) of the photopeak of Fe<sup>55</sup> was found. The counter was returned to LND to investigate a suspect slow leak. The suspect leak could not be confirmed and it was surmized that the tubulation seal must have been the area of leakage, as a new tube had to be installed to check for the leak. The counter was retubulated, returned to AS&E on 21 November, and acceptance test started anew. During the last week of November, a pronounced leak was observed and the counter was returned to LND on 4 December, where the leak was verified. The leak resulted from a crack in the epoxy, bonding the grid frame to the proportional counter body. The crack most likely occurred during leak testing at LND, where the technique used permitted a positive differential pressure on the counter, from outside to inside. The crack then worsened during acceptance

testing. This leak testing technique, had not been used on LAD #2, due to the simultaneous processing of both counters, and limited facilities. It is to be noted, that as of the end of December 1972, both Braggs and one LAD proportional counter had successfully passed acceptance tests and that one LAD had an epoxy crack.

The agreed-to solution was to replace the grid frame and window on LAD #1, and to conduct all future testing with positive differential pressure, inside to outside. Scheduling problems with machining of the new beryllium grid were reduced with the assistance of the NASA/GSFC project office, who contacted the suppliers and machine shops to stress the urgency of rapid and quality deliveries. However, due to the degradation (suspect leak) in one chamber of LAD #2, work on LAD #1 was delayed due to unsuccessful efforts to locate the suspect leak in LAD #2. As a result, additional leak testing and thermal cycling testing was added into the acceptance test cycle of LAD #1.

In early March 1973, LAD #1 developed a leak in one of its window elements. A detailed review of the problem by AS&E and LND resulted in a flight-worthy fix. This fix consisted of sealing the window element with a precisely machined beryllium plug, and forming a uniform thin epoxy layer between the plug, the window and the window frame. The detailed procedure for plug installation was worked out in advance and the actual plug installation was witnessed and approved by AS&E. LAD #1 was then thermally cycled and leak tested to confirm the acceptability of the fix. The counter was then processed in a normal manner and delivered to AS&E on 30 March 1973.

Upon receipt at AS&E, the counter was functionally checked and then tested under thermal-vacuum where a spectrum change was

observed. A review of the test results and all previous test data, resulted in AS&E changing the LAD counter gas mixture from Xenon-Propane-He to Xenon-CO<sub>2</sub>-He. It was also during this time frame that the degradation in LAD #2 had stabilized, and hence the suspect leak theory was replaced by gas contamination or breakdown of the propane. LAD #1 was returned to LND, refilled with the new gas mixture, and redelivered to AS&E by the end of April. This counter successfully passed acceptance testing, however, it did exhibit a very slight loss of resolution at high temperature only. Minute amount of residual propane was theorized and the counter was refilled with a fresh mixture of Xenon-CO<sub>2</sub>-He, to insure maximum reliability. Also, it was determined at this time, not to expose the proportional counters to temperatures in excess of 40°C (50°C previous thermal vacuum test temperature). The HXX in orbit, was projected never to exceed 30°C, and the HXX qualification test temperature was 40°C, hence reducing the counter maximum temperature exposure to 40°C was realistic. LAD #1 was retested after refill, accepted and installed into the flight unit in early June 1973.

In late July 1973, degradation of LAD #1 resolution was observed during integration testing of the flight unit. A spare proportional counter (LAD #3) had been ordered in late April 1973 for use in refurbishing the protoflight unit's LAD #2. A decision was made with NASA concurrence to replace LAD #1 with LAD #3 when available and convert LAD #1 to an Argon-CO<sub>2</sub>-He counter as a backup. It was felt that the Xenon gas was too sensitive to minute amounts of propane or possible contaminants slowly outgassing from the beryllium. The beryllium for the spare (LAD #3 counter) was cleaned using detergent type cleansing throughout its fabrication, and it had never been exposed to propane. LAD #1 was removed from the

flight unit and a residual gas analysis test was conducted at MIT with the result that LAD #1 was confirmed not to have a leak. LAD #1 was then returned to LND for conversion to Argon. The conversion process required replacement of the anode wires, rebake, refill and retest cycles. One of the replacement anode wires failed during counter testing. Following rework of the anode wire, LAD #1 developed a leak in the 1 mil beryllium window. At this point, all work on this counter stopped as it was now considered unreliable due to past rework and handling.

#### 3.8.4 LAD Proportional Counter #2

As previously discussed, LAD #2 was ordered at the same time as LAD #1. This counter was delivered to AS&E on 21 November 1972. LAD #2 was acceptance tested and passed, and was installed directly into the protoflight unit by the end of December. Degradation in gain and resolution of this counter was first observed during protoflight unit integration testing in February 1973. This degradation occurred in only one of the two proportional counter chambers. Due to the Dutch requirements for a full-up integration unit and due to the fact that LAD #1 was being reworked (new grid frame and new window), a decision was made, with NASA concurrence to complete integration testing, complete protoflight testing, and deliver this unit for spacecraft Protoflight Unit integration testing. A decision to refurbish the HXX protoflight unit was considered and final decision deferred until after delivery of the flight unit HXX. When this decision was made in March 1974, LAD #2 was replaced with LAD #7. LAD #2 had a beryllium housing, a Xenon-Propane-He gas mixture, and 1 mil beryllium window.

When LAD #2 degradation was initially observed, a slow leak in one chamber was suspect. The degradation however stabilized and in fact when the protoflight unit was returned to AS&E on March 1974,

the degradation on the bad side, had partially recovered. It was during the stabilization period from March through May 1973, that the suspect slow leak was discounted for a gas contamination theory. Either halogen type outgassing was occurring from beryllium or the organic propane was breaking down into contamination type products. It was noted that Xenon gas is considerably more sensitive than argon to halogen contamination and that the machining house for the LAD #1 and LAD #2 beryllium housings utilized halogen type cleaning agents. This was not considered conclusive because MIT had similar Xenon counters fabricated at LND at the same time, without degradation problems. (The MIT counters, however, did not contain any propane gas.)

A gas analysis on LAD #2 was conducted after removal from the protoflight unit, however, the results were non-conclusive.

### 3.8.5 LAD Proportional Counter #3

In anticipation of refurbishment of the protoflight unit, AS&E placed the purchase order for LAD #3 in April 1973. A different machine shop was selected for the beryllium machining of LAD #3. This shop happened to use detergent cleaning agents rather than halogen type cleaning agents in its processes. Hence, when gas contamination emerged as the most likely cause of the previous counter failures, the processes and gas mixture (Xenon-CO<sub>2</sub>-He) selected for LAD #3 were thought to resolve the problem. LAD #3 was received in August 1973, and then passed the most comprehensive thermal-vacuum acceptance test ever given any proportional counter at AS&E. LAD #3 was then installed in the flight unit (replacing LAD #1). On 15 September 1973, following completion of installation, a degradation in resolution in one of the two LAD #3 channels was observed. The last step in the installation process was the conformal coat and temperature cure cycle of trim

components selected to electrically align the detector assembly. The degradation was isolated to LAD #3 by a sequence of troubleshooting tests. It had previously been decided that if problems arose with this counter, then an argon gas mixture would be used in place of the Xenon gas mixture due to the Xenon being too sensitive to contamination. At this time LAD #1 had been returned to LND for conversion to argon, however, LAD #1 subsequently failed (anode wire failure and window leak). Due to the non-availability of a replacement counter, and the Dutch schedule need for the flight unit in December 1973, a decision was made with NASA concurrence, to continue the flight unit with LAD #3 (degraded on one side) and fly this unit.

#### 3.8.6 Additional Procurement of LAD's #4, #5, #6 & #7

During the week of 21 October 1973, Dr. Gursky reported from Holland that it appeared that a 15 February 1974 delivery of the HXX flight unit could be accommodated by the Dutch. As a result, AS&E recommended to NASA, the procurement of four (4) additional proportional counters of a more conservative design and selection of one of these for replacement of LAD #3 in the flight unit. NASA program management concurred with this recommendation and on 6 November 1973, a rush purchase order was placed with LND for four (4) additional counters. The counters were procured to revised specifications which incorporated all identified refinements in processes resulting from previous joint NASA/AS&E/LND meetings held relative to past difficulties. It is noted that in these past meetings, no conclusive discrepancies had been noted in the existing procedures.

The four (4) additional counters consisted of three aluminum body counters and one beryllium body counter. The aluminum body counters (LAD's #4, #5 & #6) contained a Xenon-CO<sub>2</sub>-He gas

mixture and had a 2 mil beryllium window. The beryllium body counter (LAD #7) contained an Argon-CO<sub>2</sub>-He gas mixture and had a 2 mil beryllium window supported by an internal grid.

The aluminum LAD's #4 & #5 were received in mid-December, were acceptance tested together, and both passed. LAD #4 was arbitrarily selected over LAD #5 for replacement of LAD #3 in the flight unit. Replacement was accomplished in the second week in January 1974 and all was well until the completion of the abbreviated acceptance test in mid-February, when a slight gain shift in one channel of LAD #4 was observed. Due to the 15 February spacecraft requirement, a decision was made, with NASA concurrence, to deliver the flight unit with LAD #4 and exchange it for the protoflight unit, as the flight unit was a superior unit as a scientific instrument.

In the meantime, LAD's #6 & #7 had been delivered in the first week in January and had started acceptance testing. LAD #7 passed the acceptance test and LAD #6 failed. In March, a decision was reached to refurbish the protoflight unit using LAD #7, the only LAD with argon gas mixture. Upon completion of refurbishment, the protoflight unit (now having no LAD degradation) was returned to the Netherlands and again exchanged for the flight unit. The flight unit, upon return, was refurbished as a spare backup by replacing the degraded LAD #4 with the stable LAD #5. This effort was accomplished in June 1974, and the flight spare delivered to the Western Test Range in July 1974.

Of the six LAD Xenon counters procured on this contract, all but one (LAD #5) malfunctioned. The one LAD argon counter and the two Bragg argon counters functioned flawlessly.